2013

The Design and Evaluation of a 5.8 GHz Laptop-Based Radar System

Kevin Chi-Ming Teng
Purdue University

Graduate School ETD Form 9
(Revised 12/07)

PURDUE UNIVERSITY
GRADUATE SCHOOL
Thesis/Dissertation Acceptance

This is to certify that the thesis/dissertation prepared

By KEVIN CHI-MING TENG

Entitled THE DESIGN AND EVALUATION OF A 5.8 GHZ LAPTOP-BASED RADAR SYSTEM

For the degree of Master of Science

Is approved by the final examining committee:

JOHN P. DENTON
Chair

GRANT P. RICHARDS

DAVID B. JANES

To the best of my knowledge and as understood by the student in the *Research Integrity and Copyright Disclaimer (Graduate School Form 20)*, this thesis/dissertation adheres to the provisions of Purdue University's "Policy on Integrity in Research" and the use of copyrighted material.

Approved by Major Professor(s): JOHN P. DENTON

Approved by: JAMES L. MOHLER 11/21/2013
Head of the Graduate Program Date

THE DESIGN AND EVALUATION OF A 5.8 GHZ LAPTOP-BASED RADAR SYSTEM

A Thesis

Submitted to the Faculty

of

Purdue University

by

Kevin Chi-Ming Teng

In Partial Fulfillment of the

Requirements for the Degree

of

Master of Science

December 2013

Purdue University

West Lafayette, Indiana

ACKNOWLEDGEMENTS

This work would not be completed without the help from many others. First I would like to thank my advisor Dr. Denton for his encouragement, inspiration and his help throughout my entire undergraduate and graduate studies. I also like to thank my friends who help me along the way on this project, especially Ho-I Cho, Tung-Chueh Lo, Yu-Fan Wang, and Hsiao-Hsuan Juan who participated in the experiments and gave me support during difficult times. Lastly, and most importantly, I wish to thank my mother Hua-Kuei Hsu for supporting me financially and mentally. Without her, I would not have the opportunity to study in the United States and accomplished the things I've done in the past ten years.

TABLE OF CONTENTS

Page

Page

LIST OF TABLES

Table Page

LIST OF FIGURE

Figure Page

Figure Page

Figure Page

ABSTRACT

Teng, Kevin C. M.S., Purdue University, December 2013. The Design and Evaluation of a 5.8 GHz Laptop-Based Radar System. Major Professor: John Denton.

This project involves design and analysis of a 5.8 GHz laptop-based radar system. The radar system measures Doppler, ranging and forming Synthetic Aperture Radar (SAR) images utilizing Matlab software provided from MIT Open Courseware and performs data acquisition and signal processing. The main purpose of this work is to bring new perspective to the existing radar project by increasing the ISM band frequency from 2.4 GHz to 5.8 GHz and to carry out a series of experiments on the implementation of the radar kit. Demonstrating the radar at higher operating frequency is capable of providing accurate data results in Doppler, ranging and SAR images.

CHAPTER 1. INTRODUCTION

1.1 Introduction

Radar is used in many fields. In aerospace, it is used as an aircraft detection system. Similarly, on the seas it is used to detect the speed and distance of ships. Radar is also employed to guide missiles. Currently, this technology has been employed in other areas, like the detection and movement of weather formations, motor vehicles and terrain. In addition, the costs and complexities of radar depend upon the number of functions the system is required to fulfill and how it is being used in the specific areas. Radar has a variety of applications such as surveillance, remote sensing, imaging and measurement of altitude. Each application uses various principles of radar operation.

This project involves the design, fabrication and testing of a 5.8 GHz laptop-based radar system that is able to operate between Continuous Wave (CW) mode and Frequency Modulated Continuous Wave mode (FMCW) to measure Doppler, ranging and form SAR images. The radar frequency at 5.8 GHz is expected to produce accurate results and images due to the decrease in wavelength of electromagnetic radiation and less 5.8 GHz signal interference in the surroundings.

The radar system is expected to operate in ISM band of 5.8 GHz with approximately +13 dBm of transmitted power. Two antennas will be built and used as transmitter and

receiver for the radar, respectively. This work will involve carrying out a series of experiments on the implementation of the radar system. The Matlab code provided by MIT's open courseware site will be used for data acquisition and signal processing during every stage of the experiment. The experimental data will include Doppler versus time intensity (DTI), ranging versus time intensity (RTI) and SAR images. The test measurements data will be collected for each experiment by using audio recording software to monitor the process.

The system’s overall blocks include antennas, modulator, voltage-controlled oscillator (VCO), power amplifiers, splitter, mixer, and video amplifier. The entire system is powered using a 24V battery with voltage regulators.

CHAPTER 2. LITERATURE REVIEW

2.1 Introduction

Radar technology has been present for the last 85 years, and, if one has experienced a reflection of sound, in a cave or a canyon, then the person has experienced the functionality of radar in its most basic form. Shouting from a close distance towards a valley or a mountain produces sound reflections known as echoes. Mathematically, the time required for the sound to go out and return as an echo can be employed to make an estimate on the distance of the reflecting object if the speed of sound in the medium (e.g., air) is known.

Radar functions in this same manner and is most commonly employed to obtain the location of a moving object through the use of radio frequency (RF) waves rather than sound. In engineering, radar is regarded as a system that is used to detect an object by employing radio waves to identify its range, direction, distance and altitude. The name itself is acronym of **Ra**dio **D**etection **a**nd **R**anging, in which radar is used to detect an object's presence and determine its distance and bearing with the help of radio frequency waves (Peebles, 1998). This chapter provides an overview of basic radar principles, radar components and radar limitations.

2.2 Basic Radar Principles

The principles of radar are based on radiated electromagnetic energy properties. The movement of electromagnetic energy through space takes place in straight line and with a constant speed approximated by the speed of light. Atmospheric effects cause the propagation of these waves to differ slightly. When a surface that is electrically conductive is struck by an electromagnetic wave, some part of the energy is reflected back to the source, while the remaining part of the non-absorbed energy is radiated in various directions (Figure2.1). Energy that is reflected in the direction of the source is considered an indication of an obstacle in the propagation direction of the radar transmitter.

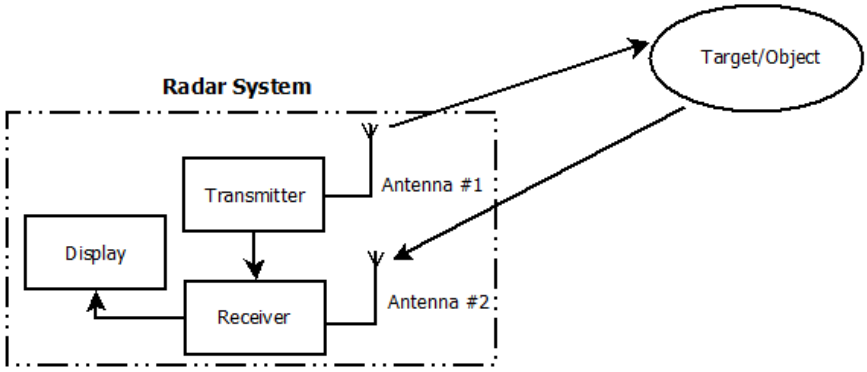

Figure 2.1 Basic form of radar system

A simple radar system is shown in Figure 2.1. It consists of a transmitter unit; two antennas, which are used for emitting electromagnetic radiation waves and receiving echo signals, and a receiver, which is used for detecting energy.

To understand how a radar system operates, it is essential to understand the basic principles. Radar system transmits a RF signal through space that is intercepted by an object, and the signal is reflected off the object back to the radar. The reflection of the

signal will be in many directions and some goes directly back to the radar system. The radar system then analyzes the differences between the original transmitted signal and the reflected signal to provide useful information such as distance (time), size (intensity), velocity (phase shift), and direction (elevation, azimuth) of an object with respect to the radar system.

The function of the antenna is to collect all the returned energy in the direction towards the receiver or duplexer, an improved radar system is shown in Figure 2.2. This radar system has a single antenna that operates as both a receiver and a transmitter is referred to as monostatic radar. This is the most common form of radar.

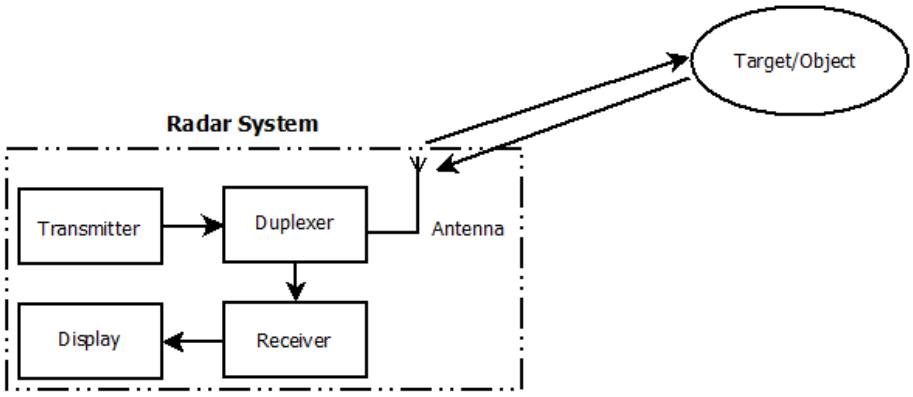

Figure 2.2 Basic form of radar system with duplexer

A duplexer is essential in the design of a radar system. Its functions include the following:

- Isolation of the transmitter and receiver during transmission and reception.
- Protection of the receiver from the transmitter's high power.
- Facilitation of a single antenna for receiver and transmitter.

In addition, the distance from the transmitter and the object can be obtained from the time it takes for the electromagnetic signal to travel to the object and return, which is referred to as radar ranging. Radar ranging is an application of a radar system that is

capable of measuring the range of an object from the radar's location by transmitting a pulse and receiving its echo. The range is measured from the time difference (or delay) between departure and arrival of the pulse, this ranging method is known as "Pulse Delay Ranging". Another ranging method is Doppler based ranging, where the change in frequency and wavelength of a wave when traveling is called Doppler Effect or Doppler shift (Nessmith & Trebits, 2003).

2.3 History of Radar

Radar is considered one of the most essential discoveries that emerged during the Second World War. Development of radar systems, like many other scientific developments, occurred out of necessity. The idea behind radar can be traced back to classic experiments of the 19th century conducted on electromagnetic radiation. Michael Faraday, an English physicist, carried out a demonstration to show that electrical current had the ability to produce a magnetic field and the energy from this field is able to return to the circuit upon stopping the current. Electromagnetic general equations were formulated by James Maxwell in 1864. These equations were used to demonstrate that "light and radio waves are actually electromagnetic governed by the same fundamental laws but having different frequencies" (United States Government, 2001, p. 2).

"Maxwell proved mathematically that any electrical disturbance could produce an effect at a considerable distance from the point of origin" (United States Government, 2001, p. 2). Maxwell's discovery showed that electromagnetic energy moves outwards from the source in the form of waves that travel at the speed of light. However, at the time of Maxwell's discovery, there was no means of propagating or detecting any form of

electromagnetic waves. Maxwell's theory was eventually tested in 1886 by a German physicist, Heinrich Hertz (Kingsley & Quegan, 1999).

Through Hertz's work it was established that electromagnetic waves move in straight lines and are reflected by a metallic object in the path. It was discovered that these waves share the same properties as light waves and a mirror. Discovery of radar came closer in 1904, when a German engineer, Christian Hulsmeyer, obtained a patent for a system which was able to detect ships remotely. This system was first used by the German navy but was unable to create much interest due to its limited range.

In 1922, Guglielmo Marconi had interest in Hertz's work and repeated his experiments. Marconi proposed what he came to term; marine radar. Dr. Albert Taylor was the first person to observe a radar effect in 1922. In his discovery, he noticed that a vessel that passed between a receiver and a radio transmitter reflected a wave back to the transmitter. The U.S. Naval Research Laboratory (NRL) conducted further research in 1930, but with aircraft flown through a beam transmitted by an antenna (United States Government, 2001).

The essence of radar and its use in tracking aircrafts and ships were finally recognized after engineers and scientists understood how a single antenna was used for transmitting and receiving transmissions. Because of the prevailing military and political situations that were taking place at the time, major countries, including the US, Soviet Union, Great Britain, Japan and Germany, started carrying out radar experiments. During the 1930s, several countries made efforts to use radio waves to detect aircraft. Radar was first used as warning system for approaching aircraft. It proved to be a valuable defensive system, something that the British and the Germans found essential.

Despite its origins as a defensive system, radar gained traction as an offensive weapon as the war intensified. By mid-1941, radar had already been employed to help track aircraft in azimuth as well as elevation. It was later used to track targets, which it did automatically when an object was in range. At the time, all radar systems worked in the VHF band (30 - 300MHz). These are regarded as low-frequency radar signals and are therefore subject to a number of limitations. However, despite the low-frequency drawbacks in the early days, the VHF band is still recognized as the frontier of radar technology and still in use of today (United States Government, 2001).

Radar technology continued improving. In 1939, British physicists created a cavity magnetron oscillator which operated at frequencies higher than those of VHF. The discovery of the magnetron oscillator allowed the use of radar systems employing microwave technology. This technology is credited by many engineers and scholars as the progenitor of modern radar systems. Advancements in radar technology slowed down after World War II in the absence of major conflict (Curry, 2012).

The 1950s marked the arrival of new, better radar systems and its use in other areas. Despite its military applications, radar has spilled into many essential civilian applications such as marine navigation. The principles that were used decades before are still practical today. The main difference between radar systems then and now lies within the design and development of these systems.

2.4 Radar Operation

Generally, there are two basic radar displays used to represent the position of a target and its motion on a Plan Position Indicator (PPI) radar navigation. “The relative motion display portrays the motion of a target relative to the motion of the observing ship.

The true motion display portrays the actual or true motions of the target and the observing ship. Depending on the desired PPI display, navigational radars are classified as either relative motion radars or true motion radars" (United States Government, 2001, p. 35).

Despite these classifications, true motion radar can be accomplished with relative motion displays by using range scale settings that are longer. It is essential to note that some systems "classified as relative motion radars are fitted with adapters" (United States Government, 2001, p. 35). which enable true motion displays. Such radars lack certain features, like high-persistence CRT screening, that are associated with true motion radars.

While these concepts are mostly associated with all forms of radars, it is necessary to understand the operation, functionality and behavior of the radars. For instance, weather radars are designed to operate in accordance with its function (i.e., detection of weather conditions in a particular area). However, as stated earlier, all radar operates using the same basic principles. When a signal is transmitted, it is reflected by an object (clouds, for a weather radar) and then received by a receiver. This process of having a signal transmitted and received from a radar kit is a fundamental process and there are several major components that will be discussed in the next section.

2.5 Components of Radar

Basically, radar has three components: the transmitter, the antenna and the receiver. See Figure 2.3 for overall block diagram. Understanding these components on an individual level is essential. Each of the components is discussed below.

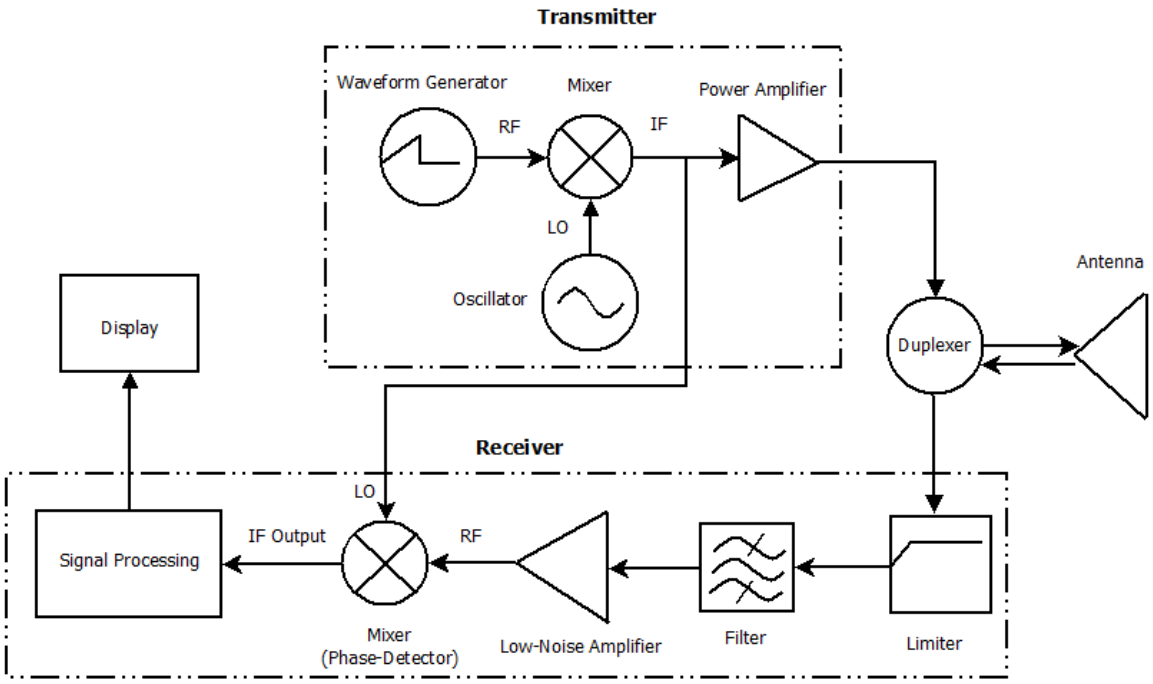

Figure 2.3 Overall block diagram of a radar system

2.5.1 Antenna

A radar antenna is the interface between the radar system and all radio waves in free space. The antenna is included in a radar system for a single purpose, to act as a transducer of RF signals to free space propagation. It guides propagated RF waves during transmission to free space and does the opposite when reception occurs. When waves are being transmitted, the radiated energy is concentrated into a beam that points in the desired direction, which is called directivity. During reception, the antenna is used to collect all the energy that is contained in the returning signal and deliver it to the receiver (Varshney, 2002).

There are two main types of antennas that are used in radar: Horn (cone) and parabolic dish. Radar generally uses a horn antenna to radiate the RF energy. Horn antennas have directional radiation pattern and the gain often increases as the operating

frequency increases. The horn's flared directions and length are used to determine the radiation directivity, which energizes the radiator as well as the termination of antenna impedance. There are three types of horn antenna, E-plane, H-plane and pyramidal. The main difference between the types is the where the radiation is flared to E-plane, H-plane or both. Figure 2.4 shows three different types of horn antenna. In theory, horn antennas have very little loss, which means the directivity of the antenna is proportional to the gain.

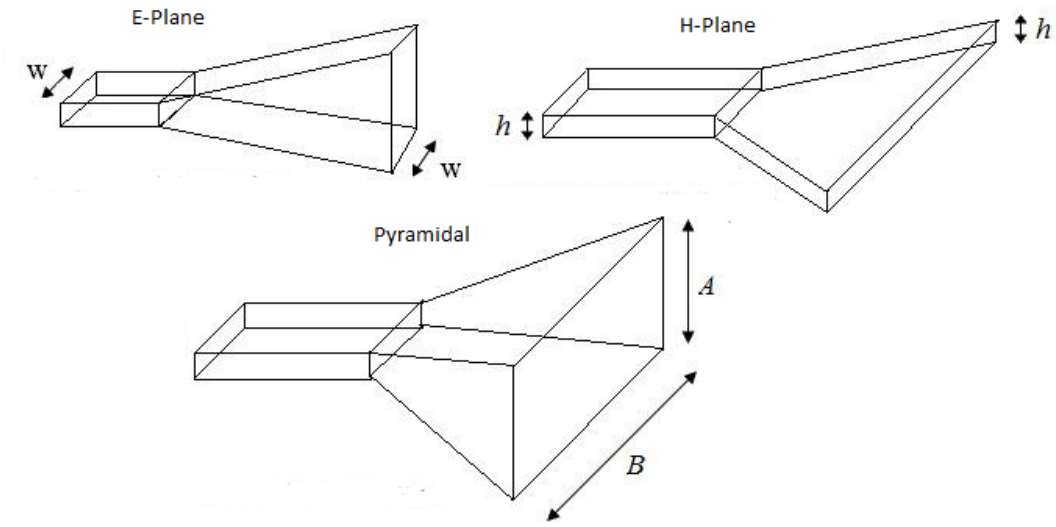

Figure 2.4 Types of horn antenna (Antenna Theory, Horn Antenna)

Another type of antenna used in the radar system is the parabolic reflector (dish). This antenna has properties that are extremely useful to concentrate the RF energy, such as during the reception and for transmission or when radar is being used to create a constant wave front (Varshney, 2002). A source of radiation placed at the focus of a parabolic reflector is illustrated in Figure 2.5. The transmission of energy takes place in all directions, which strikes the parabolic reflector creating a uniform front of RF energy focused in the same direction. Reflection of energy takes place perpendicularly to the axis. Because of the parabolic reflector has narrow vertical plane and wider horizontal plane, it

has the ability to produce a wide beam in its vertical plane and narrow beam in its horizontal plane.

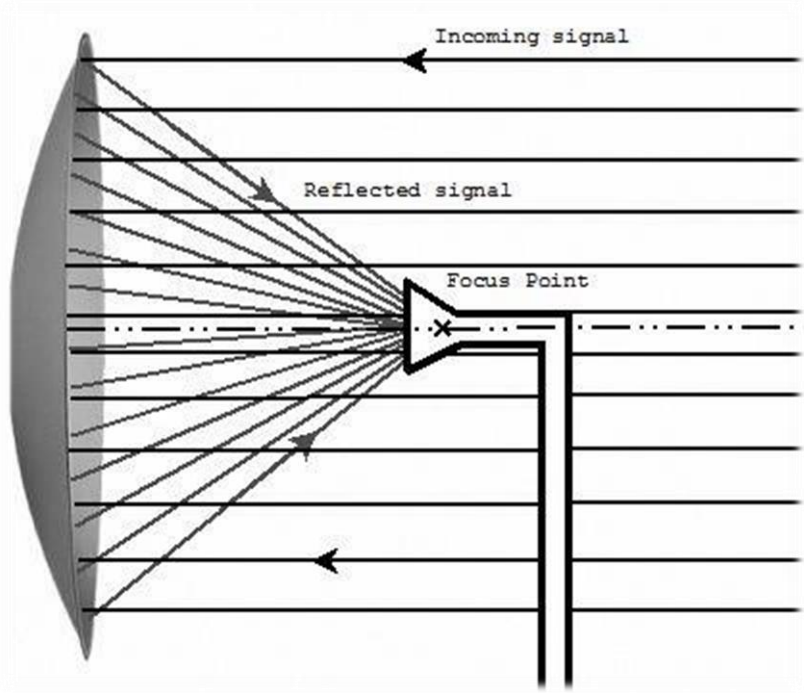

Figure 2.5 Parabolic reflector

Advantages of using parabolic antenna in radar system are its high antenna gain, directivity, and high sensitivity due to the narrow beam angle. The downsides of using a parabolic antenna are the complexity of the design, weight and low efficiency as compared other types of antenna.

The measure of how well of an antenna is directing the microwave energy through free space is known as the 'antenna gain'. The gain of the antenna 'G' can be determined as follows:

$$G = \eta * \left(\frac{\pi * D}{\lambda}\right)^2 = \eta * \frac{4 * \pi * A}{\lambda^2} \qquad (Eq.\ 2.1)$$

Where "η is the aperture efficiency and typically range from 0.6 to 0.8" (Devine, 2000, p. 79). D is the antenna's diameter, A is the antenna area, and microwave wavelength λ. The ability of an antenna to concentrate the transmitted energy in a particular direction when compared to total power radiated isotropically is referred to as the directional power (Figure 2.6).

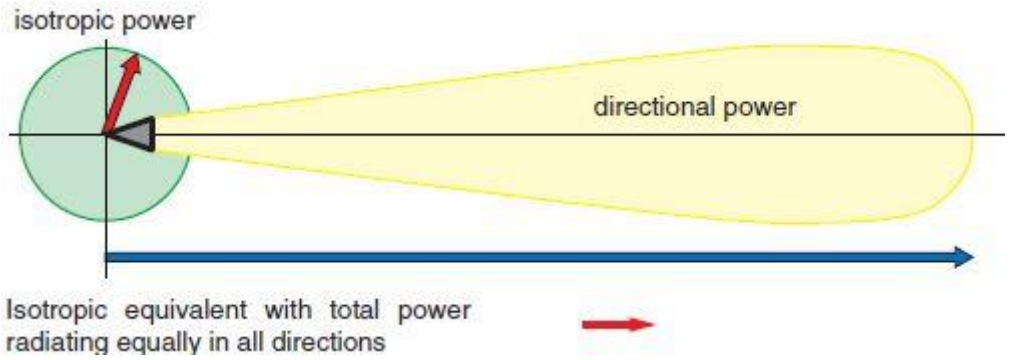

Figure 2.6 Illustration of antenna gain and directional power (Devine, 2000)

From equation 2.1, "directivity improves in proportion to the antenna area" (Devine, 2000, p. 79), in which an antenna for a given size, its beam angle will be much narrower at higher frequencies due to shorter microwave wavelength. For a standard horn antenna, the beam angle φ can be expressed as follow:

$$\varphi = 70° * \frac{\lambda}{D} \qquad (Eq.\ 2.2)$$

Where λ and D are the same as from equation 2.1.

2.5.2 Transmitter

In the design of radar, the transmitter is regarded as the main power, cost and weight budget consumer. It is also the radar system's prime thermal load. The transmitter should be designed in such a way that it operates at the desired frequency bandwidth with adequate peak power, which is needed to create the required radar range. Generally,

transmitters have three primary components: mixers, waveform generator (oscillator) and the power amplifier (Figure 2.7).

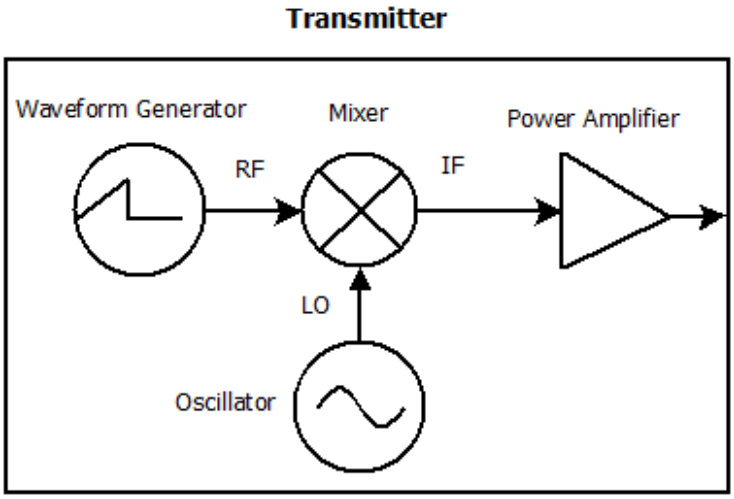

Figure 2.7 Transmitter block diagram

A digital waveform generator is used to generate transmission waveforms, typically in a baseband frequency range. The conversion of this waveform to the RF frequency range and is performed by employing an up-conversion mixer with either a variable or a fixed oscillator. The power amplifier is to provide amplification to the transmitted signal (Varshney, 2002).

2.5.3 Mixer

The purpose of a mixer is to transform incoming signals from the waveform generator into another range of frequency signals at the output. Typically, there are two types of signal conversion inside a mixer, up-conversion and down-conversion. Mixers are capable of converting between the intermediate frequency (IF) signals and RF signals depending on the radar system's configuration. In Figure 2.8, the mixer's conversion process is shown. The conversion by the mixer is accomplished by combining either IF or RF signals with local oscillator (LO) signal. The LO signal is a known source signal. The

output signals of a mixer consist of harmonics, and the sum or difference between IF and RF signals during the process of up-conversion or down-conversion.

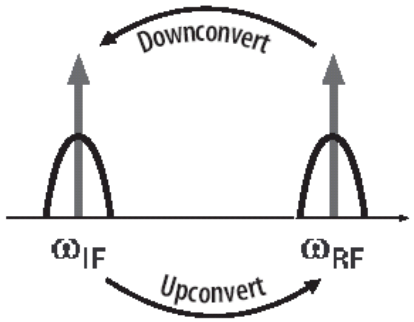

Figure 2.8 Mixer's up-conversion and down-conversion process (Varshney, 2002).

Mixer with dc coupled ports can be function as a phase detector to compare the phase shift variations of the signals applied on LO and RF ports. However, there are some non-ideal characteristics when using a mixer as a phase detector, such as dc offsets. These problems can be minimized depending on the use of the applications in the systems. The basic concept of phase detectors is to generate a dc output signal, proportional to the output phase difference between two signals at the same frequency and constant amplitude signals to a mixer (Kurtz, 1978). Most of the phase detectors utilize four-diodes in the design, which form a double balanced mixer (Figure 2.9).

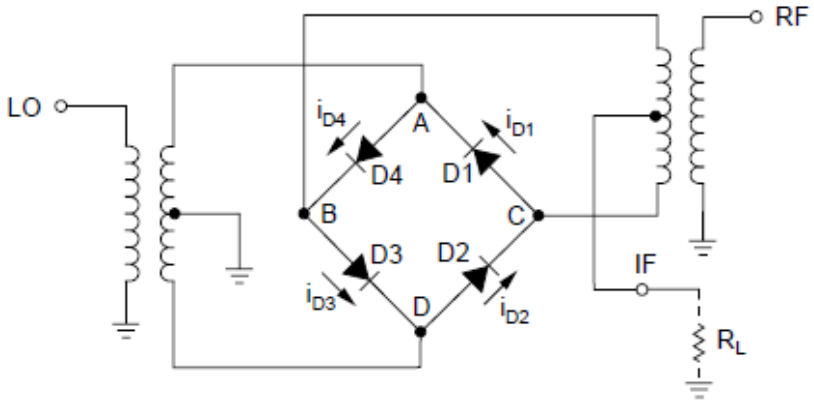

Figure 2.9 Double balanced four-diode mixer schematic (Kurtz, 1978).

In Figure 2.9, LO and RF are the input ports of the mixer. The signal at the LO ports causes the current flow through diodes in pairs: D1, D2 and D3, D4. Since construction of the mixer is double balanced, means that when the diode pairs alternate conduction, causing the voltage at point B and C to be essentially zero volts because of the voltage divider of the diodes pair. The rate of switching is identical to the frequency input at LO (Kurtz, 1978). Thus, the voltage at output IF port is determined by:

- "The level and polarity of instantaneous voltage at the RF transformer's secondary winding" (Kurtz, 1978, para. 4).
- "Which terminal of the secondary is at ground potential at that instant" (Kurtz, 1978, para. 4).

The output signal at the IF port produces the sum and difference of the frequencies signal input to the RF and LO port. Since the RF and LO have the identical input frequency signal, meaning the difference is zero Hz or a DC voltage and the sum of frequency is twice of the input frequency. The dc voltage presented at the IF port is considered the most important signal in radar system. By observing this signal under oscilloscope, a full wave rectifier waveform can be seen. Example of a phase detect output waveform is in Figure 2.10.

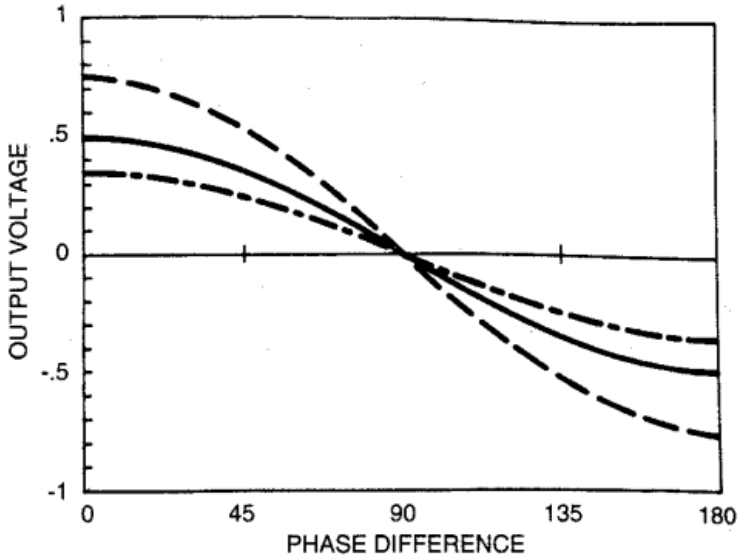

Figure 2.10 IF output voltage vs. phase difference between LO and RF signals. (M/A-COM, 2001)

2.5.4 Frequency Synthesizers and Oscillators

Frequency synthesizers or oscillators are important to create the baseband RF signals for radar operations. “oscillators represent the basic microwave energy sources for an microwave system such as radars” (Varshney, 2002, p. 5). In a voltage-controlled oscillator (VCO), the frequency of the oscillations is controlled through input of a DC voltage with the use of varactor diode that works as the major element of tuning to vary the oscillation frequency. The voltage applied to the diode is used for the purpose of tuning of the oscillator frequency throughout the frequency band of the oscillator. The frequencies of such oscillators are stabilized with the use of phase locked loop (PLL) circuits. PLLs feedback the output signal to the input signal correcting for any error between the input and output frequencies. Thus PLLs are beneficial in recovering the frequencies of the oscillators to deliver frequencies that are stable and controlled. A PLL

essentially performs as a mechanism for feedback control of the VCO giving control over the different phases of the VCOs (Levanon & Mozeson, 2004).

2.5.5 Power Amplifier

Power amplifiers are used for converting RF of lower power to higher power for the transmission of signals. The term power amplifier is used as it creates an amount of power needed for the transmission of signals. Generally, the desired level of output power requires consideration of the amplification method. Some of the traditional examples of power amplifiers include grid controlled tubes, magnetrons, klystrons, travelling-wave tubes (TWTs), and crossed field amplifiers (CFAs). These are basically tube amplifiers that have proved to highly effective as power amplifiers but at a lower duty cycle. The powers that these different power amplifiers can provide vary from each other. For example, the power that the klystron amplifier can provide has been found to be in the range of over a megawatt to hundreds of megawatts. TWT's operation is similar to klystron but with extremely broad frequency bandwidth. CFAs are capable of providing large amount of power with high efficiency of about 70 percent. "Power level of many megawatts peak and tens of kilowatts average are currently being obtained from productions of CFAs" (Gilmour, 2011, p. 543). Thus with different power capabilities, these amplifiers make the transmission of the signals more powerful and effective for radar systems (Varshney, 2002).

2.5.6 Low-Noise Amplifier (LNA)

Low-noise amplifiers are used to enhance the power of the signals with the addition of little noise as possible such that the signals stay as noise free as possible. Thus weak signals are basically amplified with this amplifier. LNAs are typically used as

preamps for the power amp in a transmitter and signal amplifiers for low power signals in the receiver. The input noise figure represents the amount of noise added to signal when amplifying the power of the signals. LNAs have been effectively used in radars.

2.5.7 Duplexer

The use of a single antenna to take care of both reception and transmission operation (like in monostatic radar systems) requires the inclusion of a duplexer. The duplexer routes the radar system from receive mode to transmit mode and vice versa. To ensure this component operates properly, four requirements must be met. These are as follows:

- In time of transmission, the switch needs to connect the antenna to the radar transmitter and, at the same time, disconnect it from the radar receiver
- Isolation of the receiver from the transmitter during high-power transmission. This is required to avoid damaging sensitive receiver components
- After transmission is complete, the switch needs to disconnect the transmitter and, at the same time, connect the antenna and the receiver.
- Extremely rapid switch action is required when an object being targeted is close to the radar. Little insertion loss during transmission and reception is required.

Duplexer sometimes is referred to circulator. A circulator with three ports, known as a three-port ferrite connector circulator or a Y-junction circulator, is the most commonly used. This circulator employs spinel ferrites, which operate in the presence of

a magnetic bias field to provide an effect that is non-reciprocal. This concept is represented in Figure 2.11.

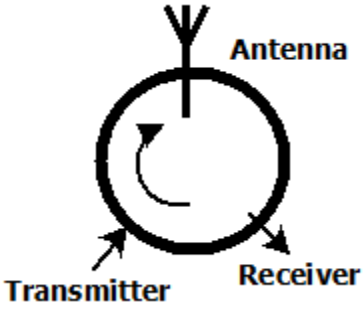

Figure 2.11 A schematic of a circulator

When a signal originates from a transmitter port, it emerges to the antenna port with minimal insertion loss. In a typical situation, the insertion loss values are between 0.1 and 0.5 dB. In addition, it is possible to experience some form of leakage in the reverse direction, which appears at the receiver port, which originated from the transmitter port (Curry, 2012). Such leakage, also known as isolation, is typically 20 to 25dB. Similarly, signals received from the antenna travel with minimal insertion loss to the receiver port and due to the high isolation, little of signal travel towards the transmitter.

2.5.8 Transmit/Receive Switch

The transmit/receive switch is used to communicate with the antenna, setting it to transmit signals and to receive them. In some cases, a transmit/receive switch is employed in place of the duplexer. The switch comes in many different designs, all with identical functionality. The two functions of a transmit/receive switch are:

- Attach the antenna to the transmitter or receiver at the required time. (Kingsley & Quegan, 1999).

- Protecting the receiver from the full force that comes with the transmitted pulse. (Kingsley & Quegan, 1999).

The transmit/receive switch is essential for radar systems. A returning target signal enters the radar's receiver through this switch. It also isolates the high-power transmitter from the front end of the receiver. A circulator is the preferred method of routing the signals to/from the radar antenna.

2.5.9 Radio Frequency Subsystems

The radio frequency subsystem is used to take signals from the transmitter and propagate them to free space when transmission is taking place. This subsystem is also used to take signals from free space and pass them to the receiver when reception is taking place. This subsystem consists of an antenna feed, a duplexer, an antenna and a number of filters (Figure 2.12). In many cases, various devices are required to convert the wave-guide propagation to a coaxial cable propagation (Varshney, 2002).

Filtering is required for attenuation of signals that fall out of the frequency band, such as images and interference from other devices that are highly powered during reception. A band pass filter is used to pass the desired band frequencies and is also known as preselect. A duplexer can be used to provide some form of isolation mechanism, which is required between the receiver and the transmitter during high-energy pulse transmission (Varshney, 2002). The antenna feed is used to collect energy received from the radar antenna and transmit energy from the radar antenna. The antenna is considered the final element in the radio frequency subsystem for transmission. For reception, the antenna is the first element.

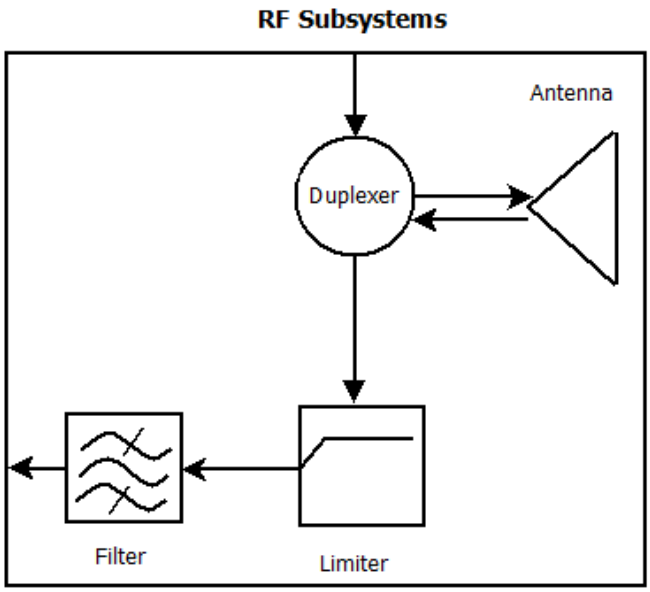

Figure 2.12 Radio Frequency Subsystems

2.5.10 Receiver

The receiver is required to separate desired signals from undesired signals as well as to amplify the desired signals for processing. It also must to detect wanted echo signals if noise, interference or clutters are present. “Receiver design depends on the design of the transmitted waveform” (Varshney, 2002, p. 7). Other aspects that are considered when designing this component are the target’s nature, noise characteristics, and interference.

Receivers are used to maximize the returned echo signal to noise ratio (SNR). The components of a receiver subsystem are the low-noise amplifier (LNA) and a mixer, which is used as a phase detector. The front end of the receiver consists of limiter, which is put in place to prevent inadvertent damage caused by reflected transmitter power or a high-power signal from other channels. In many cases, engineers of this subsystem convert signals from analog to digital at the receiver signal path end. This is essential in

case digital signal processing is required (Curry, 2012). See Figure 2.13 for the receiver block diagram.

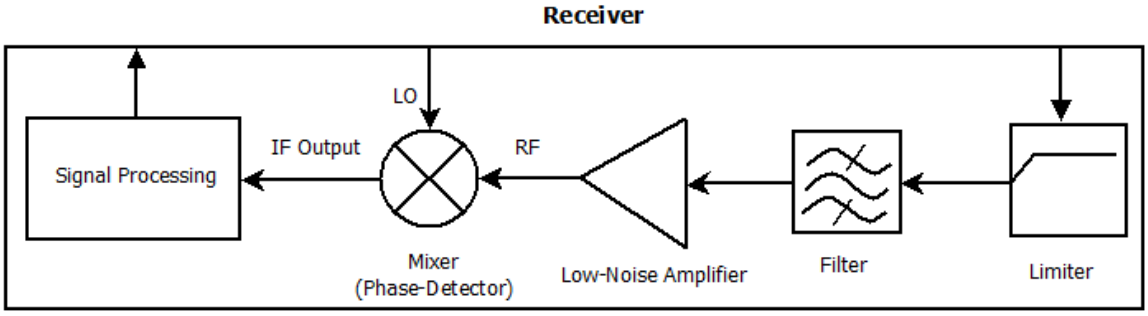

Figure 2.13 Receiver block diagram

There are other subsystems: the power system, the antenna positioning system, the signal processing system, the data processing system and the control subsystem. Understanding how the different components work together helps understanding how each component fits and contributes to the whole system. For instance, when transmission is taking place, waveforms are produced by the transmitter and are passed to the antenna, where the radio waves are transmitted into a propagation medium. The waveform reflects back to the radar after it has reached the target. At this time, the radar is set to a reception mode.

2.6 The Science of Radar

As noted earlier, radar operation uses principles that are simplistic in nature. Operation of radar involves electromagnetic waves such as radio waves, which are sent out using a transmitter at a speed that is near to or equal to the speed of light. However, this will not be recognized as a complete cycle until the waves have bounced back to the receiver from a target. Unlike sound waves, RF waves carry energy in a vacuum. This is

the primary reason why electromagnetic waves are employed in deep space, where satellite communication is required (Peebles, 1998).

The basic components for fully functioning radar are a transmitter, an antenna, a switch, a receiver and a display, which is used to produce information obtained from the radar system. To understand the science of radar requires an understanding of how all the different radar components interact with each other. Everything begins with the transmitter, which is used to send high-frequency pulses using the antenna (Bacon, 1965). After the transmission takes place, the receiver, the control switch and the antenna are automatically set ready to receive the waves that bounce back to the radar in the form of reflected transmissions.

After these signals have been received, the control switch automatically switches back to the transmitter. The switching between the receiver and the transmitter can occur approximately a thousand times per second. The returning signal provides useful information, which is used to calculate the distance of either a ship or an aircraft. The same concept is harnessed when radar is used in weather forecasting. The returning signal is analyzed for time duration, strength and frequency (or phase).

The information obtained from these analyses is used to determine other parameters, like an object's speed, direction and distance. It is also possible to generate an image of the object using this information. In most cases, the speed of the object is determined by analyzing the frequency of the returning signal. This analysis is referred to as the Doppler Effect - the faster the targeted object, the larger the change in the frequency of the returned signal. After hitting the surface, electromagnetic waves are

partly reflected off of the surface and partly refracted into the surface the degree to which these waves are reflected or refracted is dependent on the surface's properties.

In case the waves hit a surface that is not flat, the likelihood that many waves are going to be reflected is higher. However, these waves are not all going to be reflected in the same direction (Bacon, 1965). This means extremely few waves that originated from the radar will bounce back to the source. This concept has been used by different countries to design aircraft that will retard waves reflected back to its original direction. A good example of this is the F-117 stealth fighter, employed by the US, was designed to absorb most of the incoming waves by having the energy bounce against the F-117's surface and the energy is lost as the remaining waves are reflected to directions different from that of the radar (United States Government, 2001).

2.6.1 Doppler

In 1842, Christian Doppler, an Austrian physicist, discovered what many people have come to know as the Doppler Effect. The Doppler Effect is a scientific theory stating that sound waves change in pitch when a shift in frequency occurs due to the velocity of the object emitting the sound. A good example of Doppler Effect is the siren produced by ambulance. The ambulance siren begins with a high-pitched sound when it is approaching but changes to a lower pitch when traveling away. By using Doppler Effect theory, it is possible to calculate the speed of the ambulance by using the shifts in the frequency produced by the siren (Peebles, 1998).

This theory is implemented frequently in the weather applications of radar. It is used to determine precipitation speed as it moves through the atmosphere, both towards the radar and away from it (Australian Government, 2013). Considering that precipitation

moves with the wind when it is falling, it is easy to determine the velocity of the wind by employing Doppler Effect theory. More details on the Doppler measurements are in upcoming sections.

2.7 Types of Radar

2.7.1 Continuous Wave (CW) Radar

There are two basic types of radar, continuous wave (CW) radar and pulse radar. CW radars transmit a continues RF signal to the target and echoes are reflected back continuously maintaining a constant return signal energy. The frequency of the signal from CW radars can be either unmodulated or modulated. A disadvantage of unmodulated CW radars is the inability to measure range of a stationary target; because of the frequency of return echoes is exactly the same as the signal transmitted to the target. However, unmodulated CW radars can measure the speed an moving target illustrated in Figure 2.14. "When the frequency of the return signal from a moving target is changed depending on the speed and direction of the target" (Devine, 2000, p. 33), this is known as Doppler Effect as mentioned in section 2.6.1.

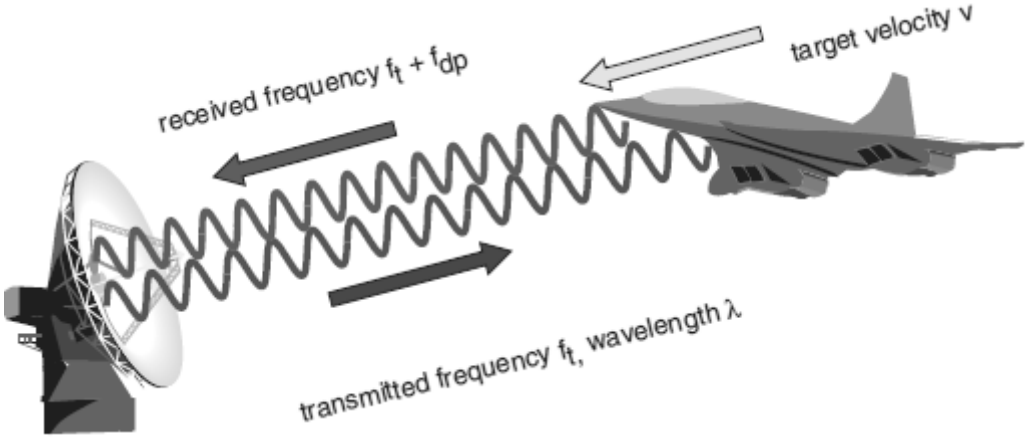

Figure 2.14 CW radar uses Doppler shift to measure speed (Devine, 2000)

Modulated CW radar is known as Frequency Modulated Continuous Wave (FMCW) radar. The FMCW radar is able to measure the range of a stationary target by transmitting a modulated frequency. A modulated frequency signal is essentially a time reference mark to measure the delay in the return echo from the target. The time reference can be measured when the frequency of the transmitted signal is in a linear-ramping form or sometime referred to as "chirp" signal similar to Figure 2.15.

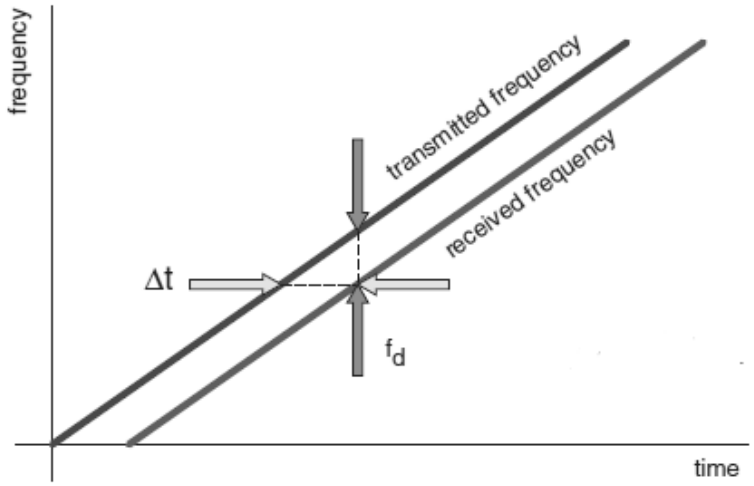

Figure 2.15 Principle of FMCW radar (Devine, 2000)

In Figure 2.15, Δt is measured from the difference between the transmitted and received frequency signal in the range from the target R, and $c \approx 3x10^8 \frac{m}{s}$ is the speed of light, then the Δt can be obtained as:

$$\Delta t = \frac{2 * R}{c} \qquad (Eq.\ 2.3)$$

Generally, there are three types of modulating signals used in FMCW radar including sine wave, triangular wave, and saw tooth wave. The most common signals used is the saw tooth wave.

2.7.2 Pulse Radar

In radar systems, pulse radar is widely used to measure range from a target. Pulse radar simply transmits a pulse toward a target and waits for the echo signal to be reflected back before transmitting a new pulse. The duration time of the pulse can vary from a millisecond to a nanosecond depending on the system. Each pulse forms a short wave packet and the number of signal periods in the pulse is determined by the carrier frequency used in the system. The time between each transmitted pulses is referred to as the pulse repetition time (PRT), the pulse width (PW) is the duration of the pulse, and the rest time (RT) is the measured time from the end of the first pulse to the beginning of the second pulse. Figure 2.16 shows a transmitted pulse radar signal.

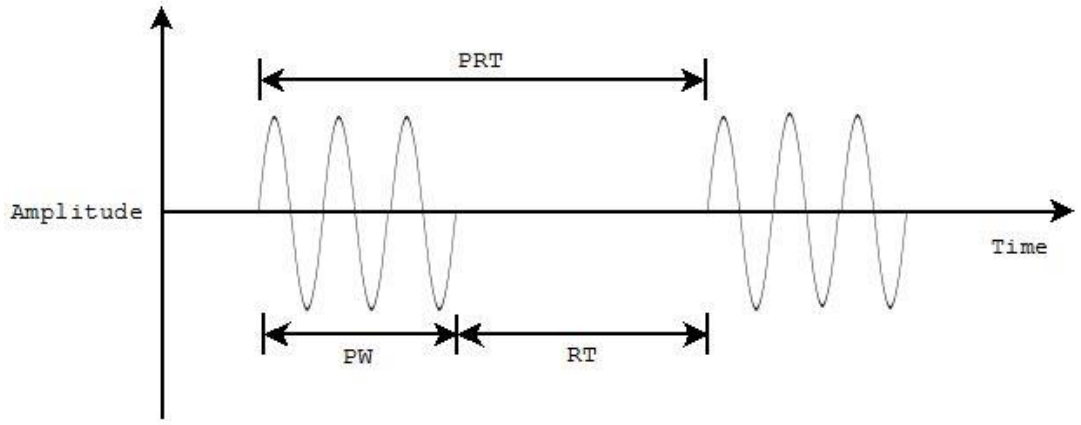

Figure 2.16 Pulse radar signal

2.7.2.1 Ambiguous Range

A problem that arises from the typical pulsed radar is how to discern between unambiguous range and the real detection range of the target. For a pulsed radar system, the unambiguous range is directly related to the pulse repetition frequency (PRF) where:

$$PRF = \frac{1}{PRT} \qquad (Eq.\ 2.4)$$

An example of ambiguous range is shown in Figure 2.17. There are two transmit pulses, TX1 and TX2, separated between a timeframe in PRT. “When the TX1 pulse sent out, RX1 becomes the echo from TX1 reflected by a target at range A. Immediately after TX2 pulse sent out, RX2 becomes undermined. RX2 could either be the echo signal from TX2 reflected by a target at range B or from TX1 reflected by a target at range C” (Renato, 2002, para. 2).

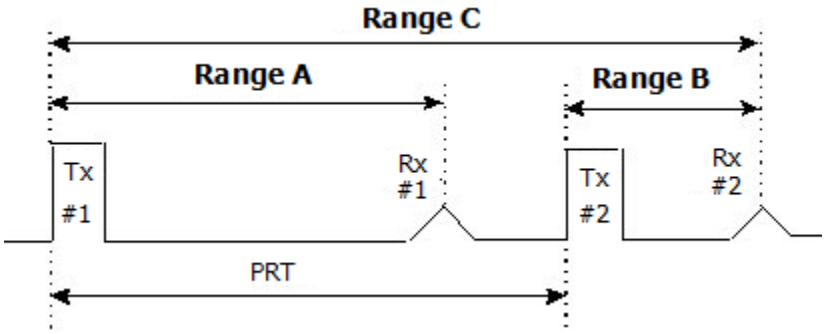

Figure 2.17 Example of an Ambiguous range (Renato, 2002)

In order to avoid the ambiguities that can occur, the radar is required to provide sufficient time for the transmitting signal to reach its target and reflect back again before the next signal occurs. The maximum non-ambiguous range equation can be expressed as:

$$R = \frac{PRT * c}{2} \qquad (Eq.\ 2.5)$$

2.8 Radar Implementation

2.8.1 Radar Power Density

For deriving radar range equations, it is assumed to be dealing with electromagnetic waves under ideal conditions since it corresponds to the physical dependencies of the power of radar. It assumes that there is no dispersion. High frequency radio waves are transmitted by an isotropic radiator. The isotropic radiator radiates the emissions of electromagnetic waves evenly across all directions. The waves propagate uniformly in all

the directions around the radar with the same power and density in the form of a sphere. As the power density forms a sphere, the area of sphere is taken as:

$$Area = 4 * \pi * R^2 \qquad (Eq.\ 2.6)$$

Since the power density is in the form of a sphere, the S_u non-directional power density equation can be obtained from the radar system, where P_S is the transmitted power and R is the range of the antenna (aim):

$$S_u = \frac{P_S}{4 * \pi * R^2} \qquad (Eq.\ 2.7)$$

In equation 2.7, it is assumed that spherical segment distributes all radiation into one direction at constant transmit power, however, when the transmit power is redistributed, the gain of the antenna G, will need be taken into consideration. The S_g directional power density of the radar can be expressed as:

$$S_g = S_u * G \qquad (Eq.\ 2.8)$$

2.8.2 Radar Range

The radar range equation represents the relationship that the propagation of RF waves has with the signals of the received reflected echo. Targets can be measured by radar systems through the distances of range. The simplest form of radar range equation is composed by timing the delay between the signal to the target and its return as reflected echo. This equation is expressed as:

$$\mathrm{R} = \frac{\mathrm{c} * \Delta\ \mathrm{t}}{2} \qquad (Eq.\ 2.9)$$

Where c is the speed of light and $\Delta \mathrm{t}$ is the round trip time delay.

When considering all other quantities that have influences on wave propagation of the radar signal, the radar range equation becomes more sophisticated in equation 2.10

whereas the power returning to the receiving antenna is noted as P_E, transmitted power P_S, the slant range R, antenna gain G, microwave wavelengths λ, and the reflecting characteristics of aim (radar cross-section σ) (Wolff, 2009). The radar range equation is expressed as:

$$R = \left(\frac{P_S * G^2 * \lambda^2 * \sigma}{P_E * (4\pi)^3}\right)^{\frac{1}{4}} \quad (Eq.\ 2.10)$$

$$\lambda = \frac{c}{f} \quad (Eq.\ 2.11)$$

The microwave wavelength (λ) is measured in meters, where c is the speed of light, and f is the frequency of the radar system.

2.8.3 Radar Target

The measurement of a target's size or extent can be determined from the radar's cross section (RCS). RCS is the measurement of how well a target can be detected from the radar system. Generally, a larger RCS value means that the target is easier to be detected but there are few factors that could have impact on how much electromagnetic energy reflected back to the radar:

- Target's material type.
- Target size and shape.
- Incident angle, angles where the radar beams reflected the signal on to the target.
- Reflected angle, angle where the signal is reflected from the target to the radar.
- Polarization of the transmitted signal from the antenna.

The RCS measurement of a target is to measure the ratio between backscatter density S_r, from the radar to the target (range) r, and the power density intercepted by the

target S_t. Figure 2.18 illustrates the backscatter from common shapes. From equation 2.12, power density is distributed on the shape of a sphere; therefore, the general RCS σ equation is defined as:

$$\sigma = \frac{4 * \pi * r^2 * S_r}{S_t} \qquad (Eq.\ 2.12)$$

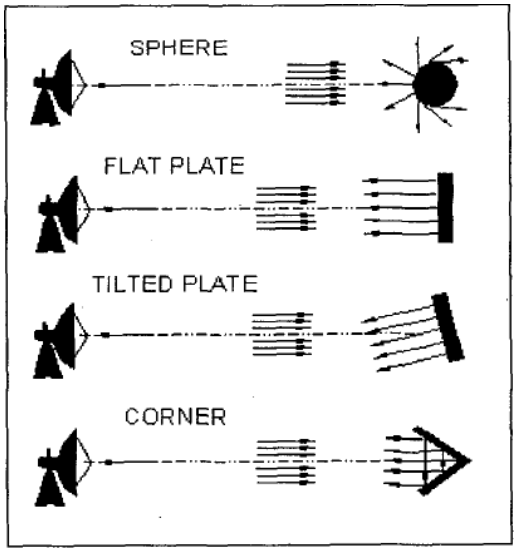

Figure 2.18 Backscatter from objects from different shapes of object (Nicolaescu & Oroian, 2001)

2.8.4 Doppler Effect

In relation to radar, the Doppler Effect is used to measure of speed, Moving Target Indication (MTI), and the determination of tangential distances through radar systems in air or space. It reflects the change in the frequency when a source of signal moves closer or away from the receiver. The general form of Doppler frequency f_D can be obtained from the given wavelength λ (m) and velocity of the object v (m/s) (Wolff, 1996):

$$f_D = \frac{2 * v}{\lambda} \qquad (Eq.\ 2.13)$$

There is another form of Doppler frequency equation, which is only valid when the target is moving at the radial speed, meaning the target is moving away or toward the radar at an angle, such as airplanes. "The angle between the direction of the transmitted/reflected signal and the direction of the target" (Wolff, 1996, para. 5) is known as θ. Figure 2.19 illustrates this concept and Doppler equation becomes:

$$f_D = \frac{2 * v}{\lambda} * \cos\theta \qquad (Eq.\ 2.14)$$

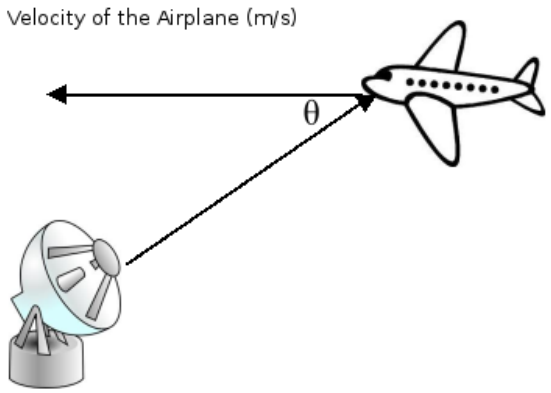

Figure 2.19 Doppler Effect of a moving target at an angle

Doppler Effect occurs once when the signal is transmitted from the radar, and again when it gets reflected. In the radar system, the "Doppler frequency will be divided by the actual transmitted frequency to eliminate the influence of different transmitter's frequencies" (Wolff, 1996, para. 8). This means the Doppler frequency measures only the radial speed of the target.

2.9 Radar Frequencies

The electromagnetic wave spectrum has frequencies of up to 10^{24} Hz. This range is extremely high and is subdivided into a number of sub ranges. Frequency division in different ranges is formed using either historical or international standards. These

frequencies bands and in Table 2.1 and have been adopted by the Institute of Electrical and Electronics Engineers (IEEE) and International Telecommunication Union (ITU).

Table 2.1 *Radar Frequencies (AIAA, 2012).*

EU/NATO/US ECM Bands	IEEE Band	Frequency	Usage
A	HF	3 - 30 MHz	Surveillance on long range
B	VHF	30 – 330 MHz	Surveillance on long range
C	UHF	300 MHz – 3 GHz	Surveillance on long range
D	L	1 -2 GHz	Traffic control, long range surveillance
E, F	S	2 -4 GHz	Long range weather, moderate range surveillance, terminal traffic control
G	C	4-8 GHz	Airborne weather, long range tracking
H,I	X	8 -12 GHz	Missile guide, short range tracking, marine radar, mapping, airborne interception
J	Ku	12 – 18 GHz	Satellite altimetry
K	K	18 -27 GHz	Absorption of water
K	Ka	27 – 40 GHz	Resolution mapping that are very high and airport surveillance
L,M	mm	40 – 100+ GHz	Mostly for experiments

Table 2.1, shows the various frequency bands that radar operates. “The higher a radar frequency, the more likely it is going to be affected by weather conditions such as clouds or rain” (Wolff, 2009, p. 10). However, the higher transmission frequencies produce higher resolution information. Since its development, radar systems have employed many different frequency ranges.

2.9.1 A and B Band (HF and VHF radar)

These bands are typically in the range from 30-300 MHz and have a lengthy history, considering that these frequency bands were mostly used during the Second World War and are considered as the frontier of radio technology at the time. In current developments, these frequency bands are used in warning radar systems and have adopted the term "Over the Horizon Radars". By employing lower frequencies; radar users have been able to obtain transmitters of higher power. Electromagnetic wave attenuation is much lower than at higher frequencies. However, the use is limited since using lower frequencies will require the installation of an antenna that has a large physical size to determine the accuracy and resolution of the angles. The bandwidth of radar using these frequencies is limited since these frequencies are also used by broadcasting and communication services (Bacon, 1965).

2.9.2 C Band (UHF radar)

A number of radar sets have been developed to work in this frequency band, 300 MHz – 1 GHz. This is considered to be good for radar operations and is used to track satellites and ballistic missiles. Radars that operate in this frequency range are also used as system warning and target acquisition such as in surveillance for air defense systems. There are a number of weather radar systems (e.g., wind profilers) that also employ this frequency range (Wolff, 2009).

This range of frequencies allows the inclusion of **U**ltra-**W**ide**b**and (UWB) radar technology, which enables radar systems to use the frequencies from A to C bands. "UWB radars transmit low pulses in all frequencies simultaneously to be used for

technically material examination such as **G**round **P**enetrating **R**adar (GPR)" (Wolff, 2009, p. 10), which is used in archaeological explorations.

2.9.3 D Band (L band radar)

The D band frequencies are range from 1 – 2 GHz and is used with radar systems that operate over long distances, such as air surveillance radar systems. These radar systems transmit high power pulses, a broad bandwidth and intrapulse modulation. Considering the Earth's curvature, this band can only be used at a limited target that is flying at a lower attitude. Such targets are likely to disappear at higher speeds when in the radar horizon. "When used in air traffic management, radar systems like Air Route Surveillance operate efficiently in this frequency" (Wolff, 2009, p. 10).

2.9.4 G Band (C Band radar)

"The G-band frequencies are used by mobile military for battlefield surveillance, ground surveillance and control of missiles" (Wolff, 2009, p. 10). These are radar sets that have short or medium ranges. The antenna size of these radars provides excellent accuracy and resolution. To ensure accuracy of information being sent over these radars, the antenna feeds are equipped with some form of circular polarization. Such a frequency band is used in most weather radar types when the location of precipitation is required.

2.10 Radar Images

Radar images are oftentimes weather images, which are map views of reflected particles for areas that surround a radar system. Considering precipitation intensity, radar images are produced in different colors and tend to appear on the map. Each color that appears on the radar image display corresponds to a different level of energy and thus has a separate pulse reflected from precipitation. This concept is represented by Figure 2.20.

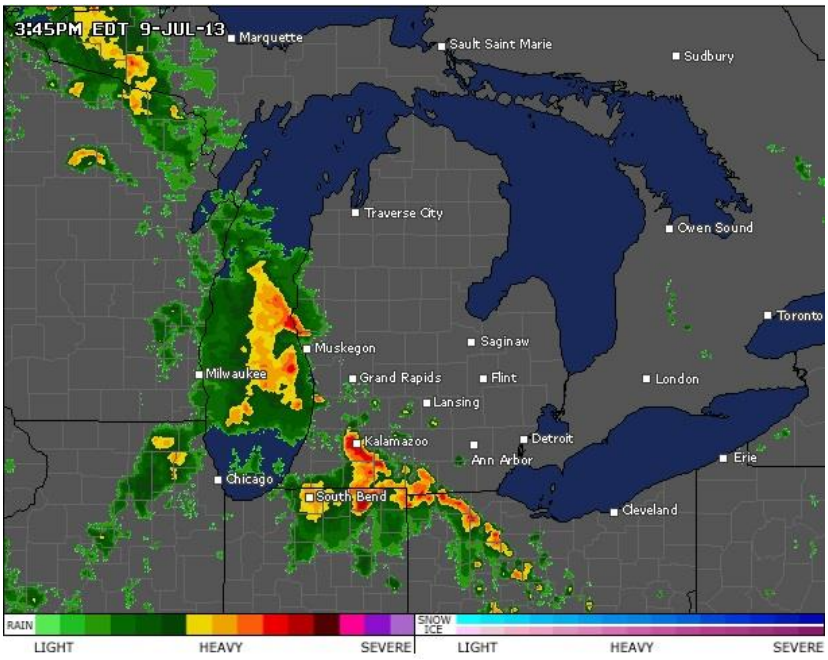

Figure 2.20 Weather radar image (Accuracy Weather, Weather Radar)

The pulse strength returning to the radar is dependent on particle size, the number of present particles and state. It is also essential to note that these particles and properties rely on assumptions which reflect the precipitation particles that exist in the atmosphere.

2.11 Radar Limitation

Formation of radar images does not accurately reflect the nature of the atmosphere, and not everything that appears on a radar image is useful information. In weather forecasting, for instance, radar sometimes detects precipitation in the atmosphere which does not have the ability to reach the ground. This is the reason why the weather radar sometimes shows rain when it is not raining. This form of error is known as virga. When radar is near the coast and has beams that are broad enough, it can reflect off the sea, returning a strong signal in the process. This reflectivity is known as “sea clutter” (United States Government, 2001).

When some wavelengths are used, the beam of the radar might not be fully reflected when the beam is passed through heavy hail and rain. This is likely to reduce or obscure the intensity of the echo further outside the radar (United States Government, 2001). In mountainous areas or areas with many trees, the path of the radar beam is blocked. It is also possible for the whole radar beam to be blocked, which significantly reduces the intensity of the echo. This type of error is known as "ground clutter" and can be caused by buildings as well.

It is also possible for weather radar to detect a bird, plane or a swarm of insects. This error is mostly associated with Doppler radar because of its higher sensitivity, when moving away from the radar, the returning waves become weaker. This error occurs since long distance causes radar beams to broaden, lessening the returning wave's intensity with time. The weather radar is also affected by the Earth's curvature. This concept is shown in the Figure 2.21.

Figure 2.21 Earth's curvature effect on weather radar

From Figure 2.21, it is evident that the Earth's curvature causes the weather radar to miss some of the rain, causing errors in the information produced by the radar receiver.

2.12 Radar Applications

Since the advancement of radar technology, different types of radar have emerged. At first, military services were the only ones who used these systems. However, others have come to appreciate the technology and, in the process, come up with different types. The most important of these are discussed in this section.

2.12.1 Military Radar

The military radar systems are divided into land-based, airborne and shipborne categories. Therefore, to define and describe this radar will require defining the three sub classes. Land-based radar systems are used to cover all 2D and 3D systems that are fixed, mobile or transportable, and are used in the military's air defense missions ranges (Global Security, 2012). This radar system includes air defense radar systems, missile control, battlefield radars and surveillance radars. The battlefield radars are used for tracking, locating weapons and controlling fire.

Airborne radar consists of three subcategories: surveillance radar, fire control radar and spaceborne radar. Surveillance radar is designed to act as an early warning system. This radar system is used to survey the land and seas. It is fixed on aircraft or vehicles that are remotely piloted. Fire control radar, which includes airborne radar systems that are used for weapons required for fire control, such as missiles and guns. This radar is also used for aiming weapons (James, 1980).

Another radar system that falls into this category is the spaceborne radar, which is used in space for surveillance and reconnaissance missions. The US Department of Defense has expressed interest in this type of radar. Military Air Traffic Control (ATC) and ranging and instrumentation radars fall into both the shipborne and land-based radar

categories. These radar systems were first employed as instruments that assisted aircraft during landing and supported tests that required testing ranges (Bacon, 1965).

Shipborne radar is a form of radar that is located on the surface of ships and is used to search the air and any land close to the sea. It includes systems such as the naval fire control radars, which are used partly as radar and partly as a fire control and weapon system.

2.12.2 Simple Pulse Radar

Simple pulse radar uses a waveform that consists of repeated, short-duration pulses. Examples of simple pulse radar are the marine surveillance radar, long-range air radar, weather radar and surveillance radar. Most of these radars employ the received signal shift Doppler frequency to detect a moving object such as an aircraft. These radars are efficient because it has the ability to reject large and unwanted waves coming back from the object, which is typically solid and stationary or clutter that lacks Doppler shift (Kingsley & Quegan, 1999).

2.12.3 Moving Radar Indication Radar (MTI)

This is a type of radar that employs Doppler frequency sensing in which MTI radar is able to differentiate returning waves that have bounced off of a moving object from those that have bounced off of a stationary object. Because of this property, this type of radar can easily reject the waveforms that come from a stationary objects and clutter. The waveform of a MTI is a train of pulses, which have the low Pulse Repetition Rate (PRR) that are used to avoid ambiguous ranges (Global Security, 2012). This means that the range used by this type of radar at a low PRR will always be good, although the measurement of speed is not accurate when this radar is used at high PRRs. Most aircraft

search systems and other ground-based surveillance systems have employed some form of MTI.

2.12.4 Pulse Doppler Radar

This type of radar functions with the Doppler frequency shift of returning the waveform. It is completely different from the simple pulse and MTI radar, which try to avoid the Doppler frequency shift. The Doppler frequency shift as employed by a pulse Doppler radar enables it to differentiate between a waveform that has bounced off a moving object and one that has bounced from a stationary object or a clutter (Nessmith & Trebits, 2003). Another difference between this type of radar and simple pulse radar is its operations are usually carried in PRR that is much higher than that of simple pulse radar.

A pulse Doppler radar that operates in high PPR operates at 100 kHz, whereas simple pulse radar operates at 300 Hz (United States Government, 2001). It is the difference between these PRRs that produces different behaviors. For instance, MTI radar employs low PRR to acquire a measurement range that is ambiguous. This causes the measurement of the object's radial velocity, which is almost the same as the one which has been derived from a Doppler shift, to highly be ambiguous. The problem with this type of radar is that it can easily miss some targets.

Doppler pulse radars operating at high PRR do not have this problem. On the other hand, high PRR causes range measurements that are highly ambiguous. The true range of waveforms used by Doppler pulse radar is resolved by transmission of multiple waveforms, which is done by different PRRs. This type of radar is also employed by the Navy, US Cost Guard (USCG), Air Force, Army and National Aeronautics and Space Administration (NASA) (United States Government, 2001).

2.12.5 Syntheric Aperture Radar (SAR)

Synthetic aperture radar is a particular form of data imaging radar. This system makes use of the platform of the radar and the processing of signal generated images that are of high resolution. In this system, the resolution along the tracks of the radar beams are enhanced with the use of Doppler frequency analysis of signals that are obtained from radar coherently traveling along the track. The primary concept of the synthetic aperture radar is the ability to capture the phase histories responses at each position of the target and to form into one high-resolution image (Zyl, 2011).

The operation of the synthetic aperture radar can be represented through the following Figure 2.22.

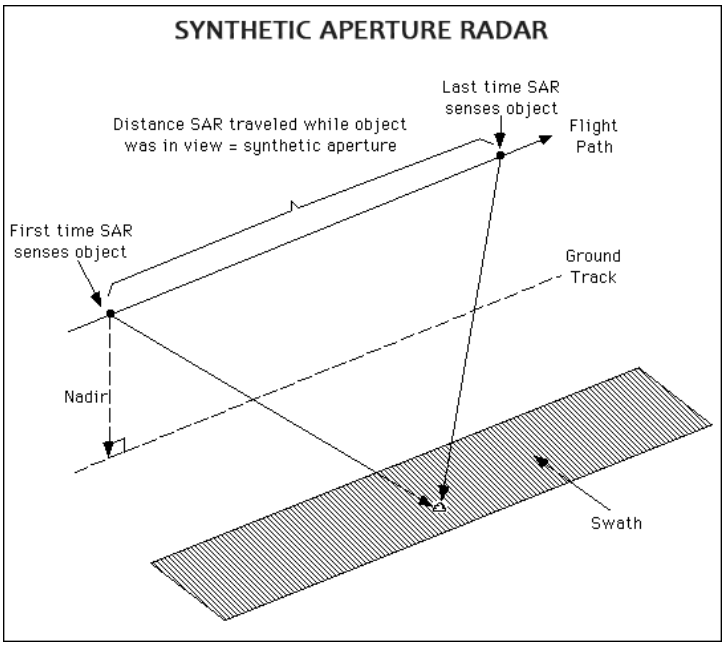

Figure 2.22 Synthetic Aperture Radar (EOSNAP, 2009).

The angular measurement of azimuth is required in this system. Depending on the measurement of the traces along the azimuth angle, the clarity of the resolution is

obtained. The narrower the width, the finer the resolution. The width of the footprint can be determined by the following equation:

$$p_{ra} = \frac{R\lambda}{D} \qquad (Eq.\ 2.15)$$

Where, p_{ra} represents the resolution obtained from the real aperture of the antenna, D, R represents the series between the midpoint of the trail and the antenna, and λ is the wavelength of the frequency of the signal that has been transmitted (Noorizadeh, 2010).

Synthetic aperture radar systems make use of advanced processes of digital signaling in order to take advantage of the movements that are ahead of the platform. This allows synthesizing a large aperture for the antenna thereby increasing the resolution of the range. However the antenna apertures do not increase in sizes that can be considered as unrealistic, thus benefitting the process of imagery through the use of synthetic aperture radars (Noorizadeh, 2010). Synthetic aperture radars can be used on oceans for tracking illegal activities, accidental oil spills, for wave forecasting, and monitoring of the levels of ice. On the land, the system can be used for passing through cloud cover and determining the uses of the land for agriculture and forestry, for detection of the geological and geomorphological features of a land to understand its suitability for use, for reference of other imageries on satellites to make them highly precise, as well as for realizing the aftermaths of floods in order to determine the measures necessary to be considered for recovery of the regions (Loekken, 2013).

2.12.6 Phase Array Radar

Phased array radar represents a directive antenna that is either formed of individual radiation antennas, or formed by elements that generate radiation. The relative phases of each element are capable of variation, hence allowing steering of the radar beams. Applications of this radar is most common, where the beams need to be shifted from one location to another (Skolnik, 2006). The use of phased array can be made in radar applications for airborne fighter or attack radar applications. This is particularly possible through phased array radar that can be electronically steered (Skolnik, 2003).

The concept behind phased array radar is that it makes use of the signal phases through its electronic controls. The phases are obtained at specific sections of the array leading to generation of constructive interference in a path that is preferred for the positioning of the beams. Mechanical positioning is not required in the process. Depending on each individual pulse, the radar beam can be steered, the time interval of such steering generally being 1ms. The steering can be obtained in any desirable direction and in different angles. The flexibility of the beam steering is unlike other mechanical radars thus making the phased array radars unique (National Research Council, 2008).

2.12.7 Tracking Radar

This is a type of radar that is engaged to continuously follow a single object in an angle and range in order for it to determine the path and trajectory of the object as well as predict the future position of the object. Tracking radar is used to provide target locations continuously. Typical tracking radar has the ability to measure the location of a target at a rate of about ten times per second. The ranging instrument radar belongs to this category. Military tracking radar uses sophisticated signal processing to estimate the size of the

target and identify other characteristics before enemy is able to activate weapons system (Global Security, 2012). When tracking radars are used in military operations it is called fire control radars.

2.12.8 3-D Radar

3-D radar is used for air surveillance to measure the location of a target in two dimensions, azimuth and range. The angle of elevation, which is used to derive the altitude of a target, is easier to determine. An antenna is implemented in 3D radar to mechanically and electronically allow the radar to rotate on a vertical axis so that it may acquire the target's azimuth angle. There are other radars with a capability of measuring the properties of a target in 3D, but 3D radars are the most commonly used. These radars are capable of measuring the elevation and azimuth angles. 3D radars are employed by major defense departments in the US (Global Security, 2012).

CHAPTER 3. METHODOLOGY

3.1 Introduction

The 5.8 GHz laptop radar system is capable of measuring Doppler shift, ranging, and perform simple SAR imaging of objects. There are two operating modes for this radar: Continuous Wave (CW) or the Frequency Modulated Continuous Wave (FMCW). In CW mode, the radar is used to measure Doppler shift (speed) and in FMCW mode, the radar used to perform range measurement and SAR images. In the following sections, the basic concept of CW and FMCW radar will be explained, followed by the methodology used in this project including the overall block diagram, circuit schematic, parts used, data acquisition and test results.

3.1.1 Continuous Wave (CW) Radar

The basic principle and use of continuous wave radar is simple and does not require signal modulation. When the radar signal is unmodulated, the system is capable of detecting the Doppler-frequency shift that occurs in the signal returning from a moving target. The amount of change in frequency, a Doppler shift can be measured from equation 3.1, where $\Delta\lambda$ is the wavelength shift, λ_0 is the wavelength of the source not moving, v is the velocity of source and c is the speed of light.

$$\frac{\Delta\lambda}{\lambda_0} = \frac{v}{c} \qquad (Eq.\ 3.1)$$

By rearranging equation 3.1, the velocity of the moving target can be calculated in equation 3.2:

$$v = c * \frac{\Delta\lambda}{\lambda_0} \qquad (Eq.\ 3.2)$$

In the CW radar system, two antennas are often used. One is the transmitter antenna and the other is receiver antenna. The purpose of using two antennas in the design is to prevent transmitter signal noise leaking to the receiver to affect the sensitivity and range performance of the radar system (Charvat, & Kempel, 2008). Although the target's velocity can be measured with CW radar, the range is not provided due to the lack of timing mark in the waveform that gets transmitted to the target (Chang, 2004, p.216).

Several advantages and disadvantages of CW radar system are:

The advantages of CW radar include (Golio, 2003, p.12.1):

- Its simplicity of concept and use
- Spectral spread of transmitter is low
- Peak power is similar to average power

Disadvantages of CW radar include (Golio, 2003, pp.12.1-12.2):

- Need to provide isolation of antenna
- Not able to determine the range of the object
- Does not detect stationary or slow-moving objects

3.1.2 Frequency Modulated Continuous Wave (FMCW) Radar

In a frequency modulated continuous wave (FMCW) radar, the transmission of an electromagnetic signal is continuous. The frequency of the transmitted signal is changed

linearly with respect to time. With a continuous change in the frequency of the signal transmitted, the amount of frequency difference between the transmitted and received signal is determined by the time it took the signal travel to the object and back.

An example of a modulated signal is shown in Figure 3.1. The signal is frequency modulated from 5.8 GHz to 5.9 GHz. This frequency bandwidth is noted as "B". The amount of time for the signal up-ramp sweep from 5.8 GHz to 5.9 GHz is noted as "T". At T0, the transmitter sends out a 5.8 GHz signal to the object. The transmitted signal hits the object and bounces back to the receiver at T1, while the transmitter sends out a 5.85 GHz signal. At T1, the receiver is mixing two signals consisting of a 5.8 GHz return signal (f_R) and a 5.85 GHz transmitted signal (f_T). The output of the mixing two signals produces the sum and difference frequencies: f_T+f_R and f_T-f_R. By using a low-pass filter to filter out the undesired term f_T+f_R, the frequency of f_T-f_R is the beat frequency (f_B) (Krishnan, 2000).

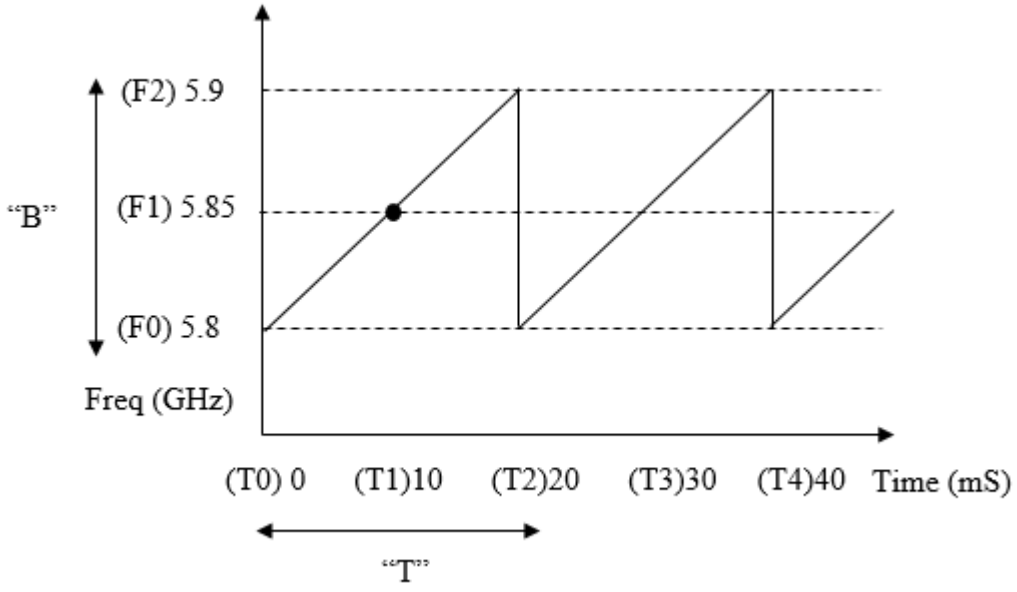

Figure 3.1 Example of a frequency modulated signal

Since the change of frequency “B” and the change of time “T” is known. The rate of change of frequency and time can be calculated as:

$$\alpha = \frac{B}{T} \qquad (Eq.\ 3.3)$$

Using the equation 2.3 from section 2.7.1 to calculate the time difference between the transmitted and received frequency signal, the beat frequency (f_B) is expressed as follow:

$$\begin{aligned} f_B &= f_T - f_R \\ &= \alpha * \Delta t \\ &= \frac{B}{T} * \frac{2 * R}{c} \\ &= \frac{2 * R * B}{c * T} \end{aligned} \qquad (Eq.\ 3.4)$$

By knowing radar system’s frequency bandwidth (B), up-ramp sweep time (T) and beat frequency (f_B), the distance (R) from the radar to the object using the FMCW method can be calculated using equation 3.5. Typically, most FMCW radars are capable of storing the beat frequency internally and perform Fast Fourier Transform (FFT) analysis externally to interpret beat frequency and display the output results in the radar range.

$$R = \frac{f_B * c * T}{2 * B} \qquad (Eq.\ 3.5)$$

Applications of FMCW Radar are effective for the measurement of distances particularly where high accuracy and repeated measurements are necessary with reliability. For example, tank level gauging is one area where this radar is applicable as

measurements of high resolution without any physical contact. FMCW Radar is also used in oil and liquefied natural gas (LNG) tankers and storage tanks, allowing measurements of volumes of products in aircrafts, as well as for industrial purposes where dimensions of products in automated systems can be verified using FMCW Radar (Siversia, 2011). Some of the advantages of FMCW Radar include (Siversia, 2011):

- High resolution distance measurement
- Functions effectively in varied weather conditions
- Easy penetration through varied materials
- Better detection of target/object in motion

Some of the disadvantages of FMCW Radar include (Siversia, 2011):

- Expensive
- More complex and requires advanced data acquisition
- Subject to licensing and regulations (due to larger frequency bandwidth)

The working of SAR is different in the way that the movement of the radar is used to 'synthesize' image of a target or object over a distance known as the cross-range. The actual distance from the radar to the object is known as the down-range (Figure 3.2). The cross-range resolution for SAR images can be calculated in equation 3.6, where λ is the wavelength of the radar frequency, R is the distance to the target, and D is the antenna's aperture created by moving the radar.

$$\Delta cr = \frac{\lambda \mathrm{R}}{D} \qquad (Eq.\ 3.6)$$

The down-range resolution of SAR can be implemented using equation 3.7, where c is the speed of light, and B is the bandwidth of the modulated signal.

$$\Delta r = \frac{c}{2B} \qquad (Eq.\ 3.7)$$

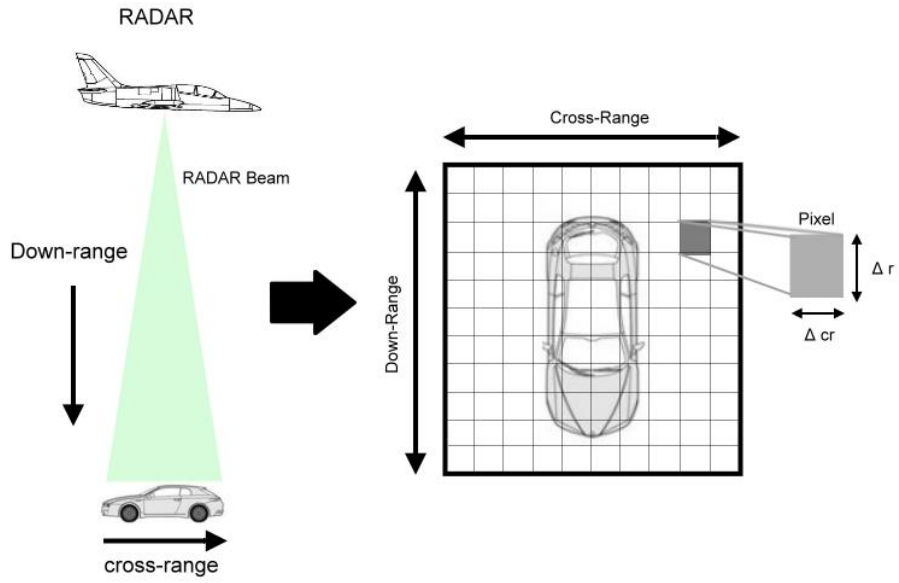

Figure 3.2 SAR image showing down-range and cross-range resolution

The principle of SAR combines the characteristics of Doppler and ranging measurement. The radar transmitted a signal at each moving position to the object and received its echo. The data received consist of Doppler frequency variation for each point of the object, using these Doppler frequency variations, the object's reflection signal strength can be determined by the radar. In order to find the location of an object on the territory of the SAR, an estimation of the azimuth position needs to be determined. This is achieved through the use of FMCW mode, measuring the delays between transmitted and receive signal.

There are two most common SAR data gathering modes (Figure 3.3): spotlight mode and strip-map (scan) mode. The major difference between the two types is the transmitting signal of a continuous basis or at frequent intervals and time periods. Spotlight mode is transmitting the signal at specific intervals to detect object. The

purpose of using spotlight mode is to image a specific target, which has the ability to produce a higher resolution of image. Strip-map (scan) mode is a continuous operation along a straight line which is excellent for ground surveillance and weather image capture use.

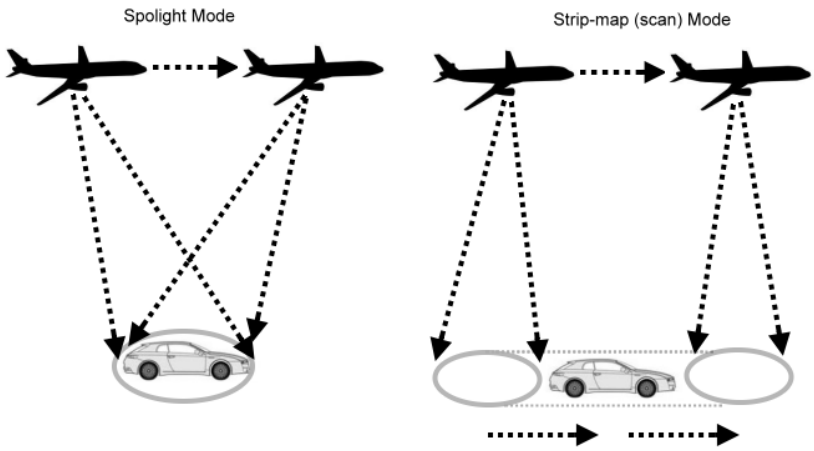

Figure 3.3 SAR data gathering modes

With development of new technologies and advancements, the use of SAR has increased and there are several applications of the concept. Applications of SAR have been found in reconnaissance, surveillance, and targeting, particularly in need in the military, with high resolution being offered for identification of terrain images and manmade targets. Other uses of SAR include verification of treaty and nonproliferation, interferometry (3-D SAR), navigation and guidance and indication of moving targets (Lopez, 2012).

3.1.3 Overall Project Description

The radar system is designed to operate in ISM band of 5.8 GHz with approximately 13dBm of transmitted power. The entire system is powered using a 24V battery with voltage regulators in Figure 3.4.

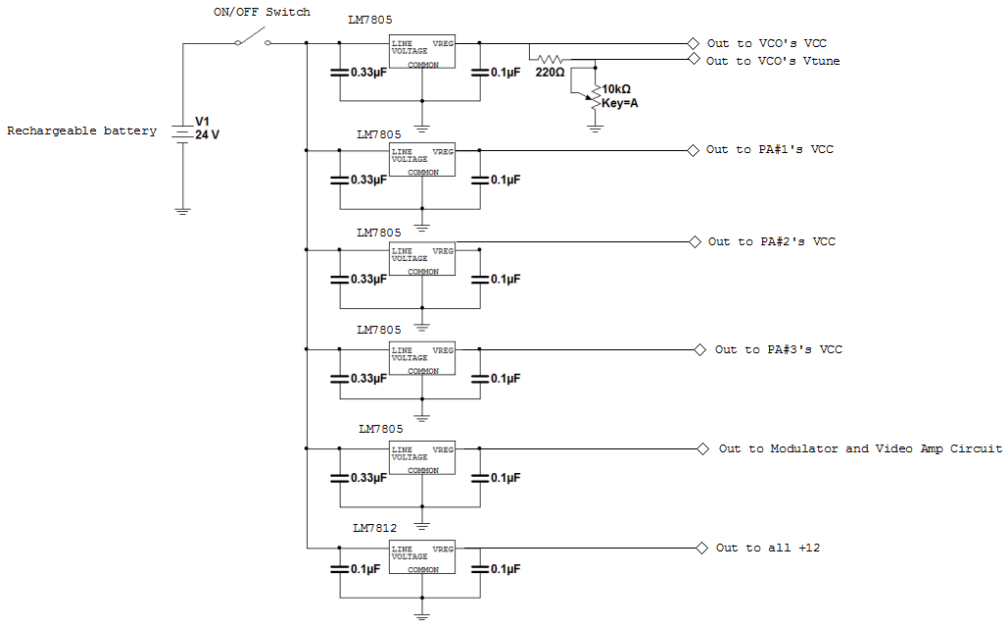

Figure 3.4 Radar's power supply schematic

For CW operation mode, the radar system consists of VCO, amplifiers, splitter, antennas, mixer and video amplifiers circuit (Figure 3.5).

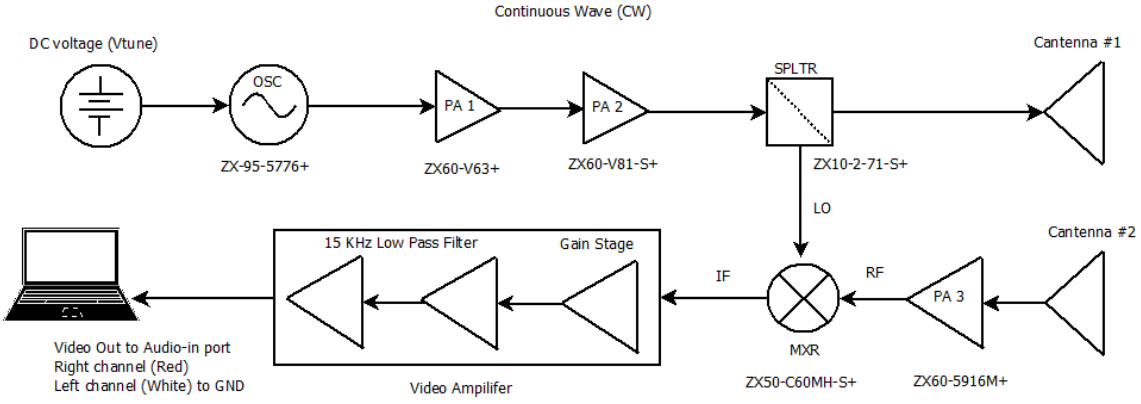

Figure 3.5 Radar system in CW mode

In the transmit chain, the VCO operates from a constant DC voltage (Vtune) from the input to generate a signal at 5.8 GHz to feed through two amplifiers and to the splitter. The splitter separates the incoming signal out to two output ports. One output goes directly to the transmitter antenna, and the other goes to the LO port of the mixer. In the

receive chain, the receiver antenna's signal is fed through an amplifier and to the RF port of the mixer. The IF signal of the mixer is expected to be a constant DC voltage for a fixed target. The mixer's output signal on the IF port is fed to a video amplifier circuit. Finally, the signal at the output of the video amplifier is connected to a PC's audio-in port to record .wav file. The data acquisition of the .wav file is analyzed in the Matlab software to determine the Doppler shift and velocity on a Doppler-Time-Intensity (DTI) plot.

For FMCW radar operation, it is much similar to CW mode but the input signal (Vtune) to the VCO is a modulated chirp signal from a modulator circuit to replace the constant DC Vtune. The modulator circuit also generates a pulse at the output to indicate the start of the chirp signal to the VCO, referred to as the "pulse inhibit switch". This pulse inhibit signal is connected to the left channel of the audio-in port to indicate the time of start and stop of the chirp signal with respect to the raw radar data collected on the right channel. The left channel signal is recorded continuously for range measurement and for SAW imaging requires to toggle the left channel signal to indicate the position of the radar. Matlab will analyze the recorded .wav file for range and SAW data and output Range-Time-Indicator (RTI) plot for range and a cross-range (ft.) versus down-range (ft.) SAR image. See Figure 3.6 for the FMCW overall block diagram and Figure 3.7 for modulator and video amplifier circuits.

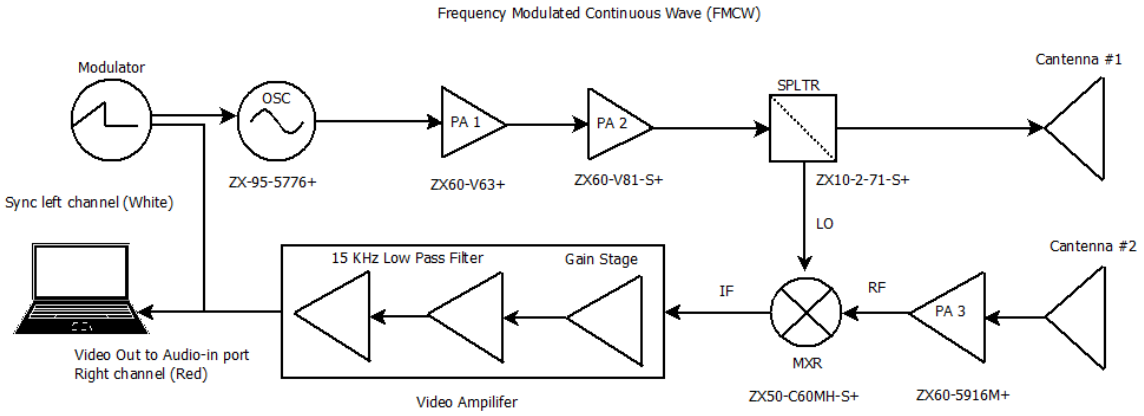

Figure 3.6 Radar system in FMCW mode

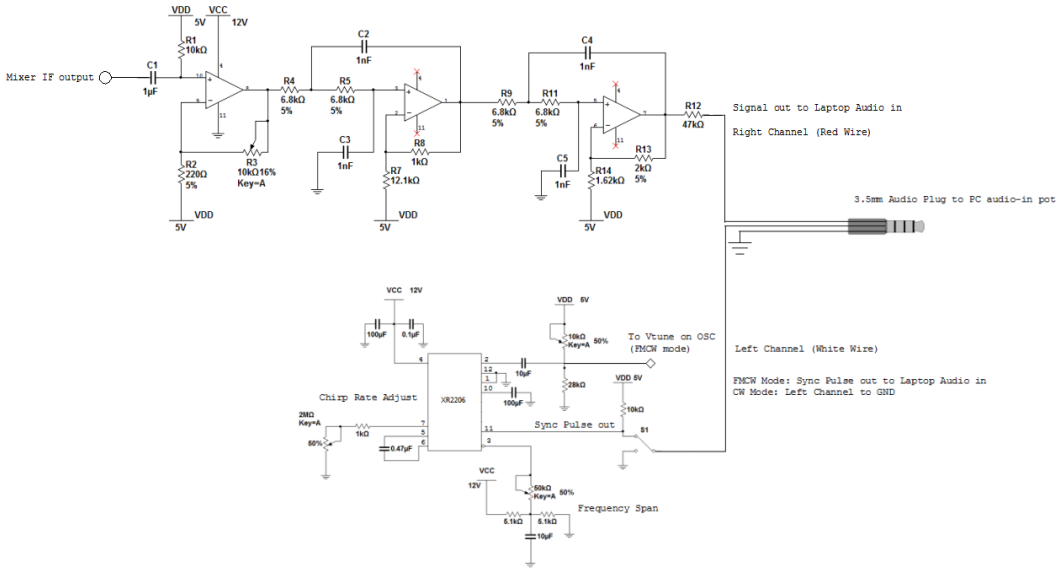

Figure 3.7 Circuit schematic for modulator and video amplifier

3.2 Block Test Results

3.2.1 Cantenna

The type antenna chosen for the transmitter and receiver of the radar system is an aperture antenna called a cantenna. Cantenna is a directional antenna and it offers two major advantages. The first advantage of a directional antenna is the ability to radiate greater power in one direction, which is good for the radar pointing in one direction at an object or target. The second advantage is the simplicity of the design. The cantenna can

be built with materials found in most hardware shops. The final selection of the can for the radar system measured at 85mm length and 55mm in diameter. The connector used for the cantenna is the SMA connector SMA864L model from JYEBAO. The contact pin (Beryllium copper) on the SMA connector was trimmed down to 10mm and the insulator at 7mm. The connector was placed at approximately 16mm from the bottom of the can. See figure 3.8 for the cantenna construction and Figure 3.9 the finished cantenna design.

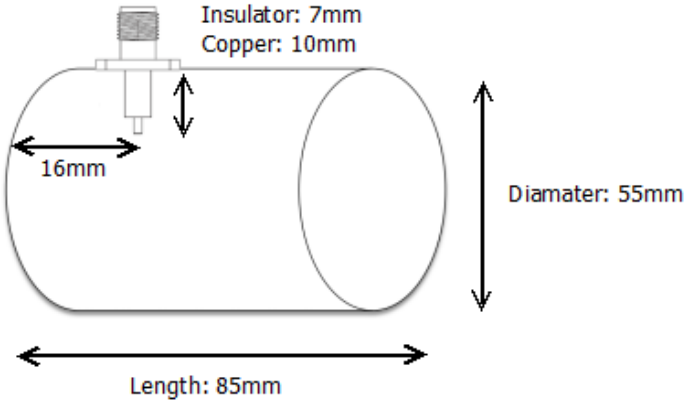

Figure 3.8 Cantenna construction measurements

Figure 3.9 Finished cantenna design

3.2.1.1 Cantenna Test Procedure and Results

The antenna testing requires one and two port testing. One port (S11) testing is to measure the return loss and the operating frequency of the antenna on a calibrated Vector

Network Analyzer (VNA). This measurement requires that the VNA transmit a small amount of power to the antenna and measures how much power reflects back to the VNA. Another one port measurement on the VNA is the Smith chart. The Smith chart is a graphical way of viewing the antenna's input impedance to determine the presence of a mismatch to 50Ω. The last S11 measurement is the Voltage Standing Wave Ratio (VSWR). VSWR is a function of the magnitude of the reflection coefficient, and it's a quick way of estimating how much power is reflected by the antenna. An ideal antenna design has VSWR equal to 1:1. See Figure 3.10 for S11 test setup on VNA.

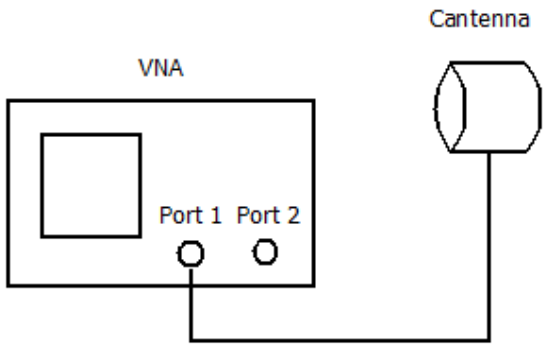

Figure 3.10 S11 antenna testing on VNA

Two-port (S21) antenna testing represents the power received at antenna 2 relative to the power input to antenna 1. For this test setup, a known Log Periodic antenna (EM-6952) will be connected to port 1 and the cantenna to port 2. See Figure 3.11 for the S21 setup. The distance between the known antenna and the Log Periodic antenna must be greater than Far-Field distance (R) in order to make the correct measurement on the VNA. The calculated R for this cantenna is 0.28 meters. Measurement distance for this test is one meter. When measuring S21, the polarization of the antenna will have a huge impact on the output reading because polarization is the orientation of the electric field.

Therefore, rotate the can-antenna around to either 90° or 180° to get the best output results, which indicates matching the polarization of the two antennas.

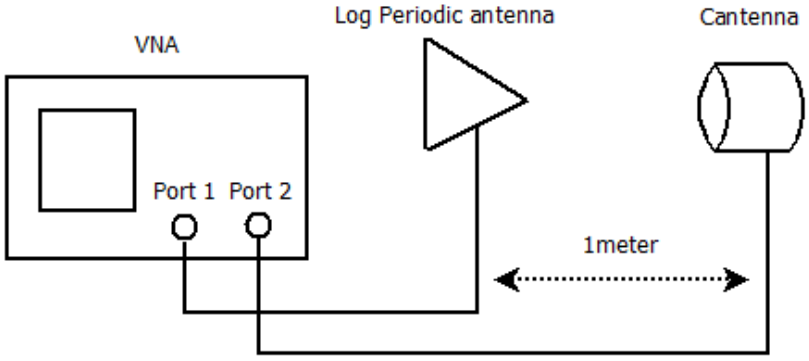

Figure 3.11 S21 Antenna setup on VNA

Using the antenna test procedure, S11 measurement was performed on two cantennas. At the operating frequency 5.8 GHz, cantenna #1 is measured at S11= -30dBm (Figure 3.12) and cantenna#2 is at S11= -37dBm (Figure 3.13).

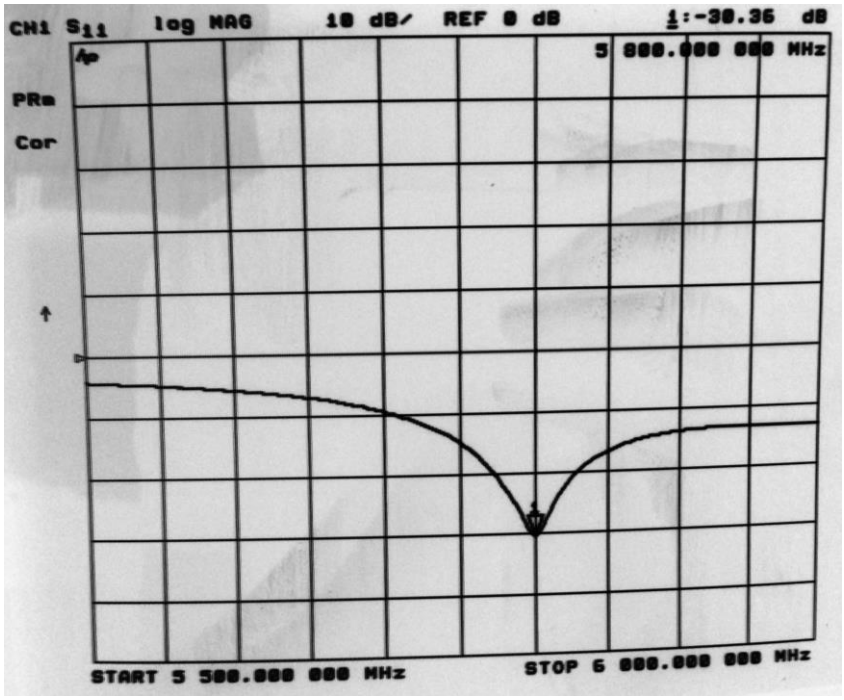

Figure 3.12 S11 measurement of cantenna #1

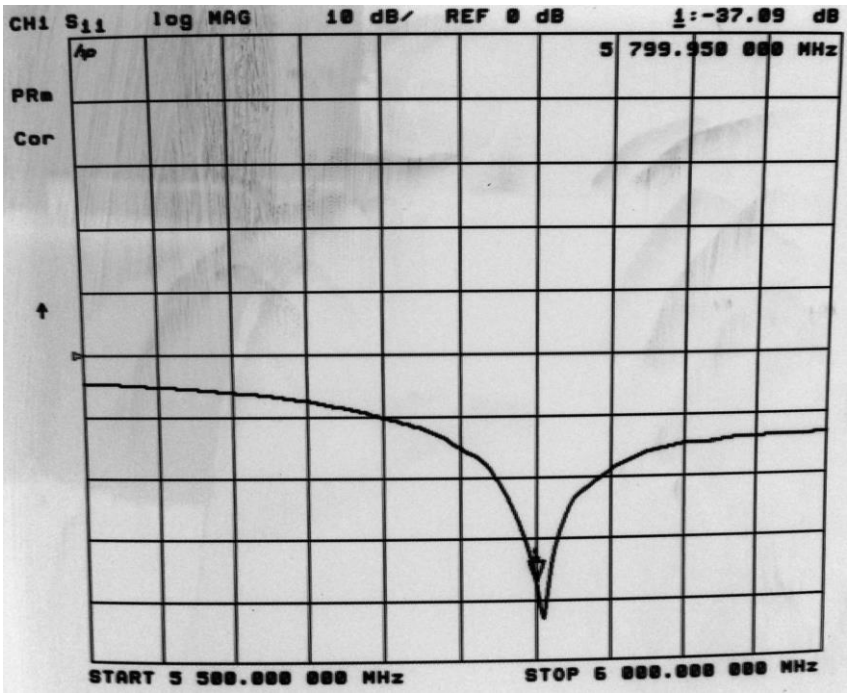

Figure 3.13 S21 measurement of cantenna #2

For the VSWR and input impedance of the both cantennas, Table 3.1 shows the results. S21 measurement of both cantenna is performed using a known log periodic antenna providing a gain of 6.5dB at 5.8 GHz. The distance between cantenna and Log Periodic antenna is exactly one meter away. See Figure 3.14 for S21 measurement setup. The output value was recorded in Table 3.2 and Figure 3.15.

Table 3.1 *VSWR and input impedance for both cantenna*

	Cantenna #1	**Cantenna #2**
VSWR	1.06	1.03
Input Impedance (Ω)	51.5	51.5

Figure 3.14 Cantenna S21 measurement setup with log periodic antenna

Table 3.2 *S21 measurement of both cantenna*

	Cantenna #1	**Cantenna #2**
S21 (dBm)	-23.2	-21.2

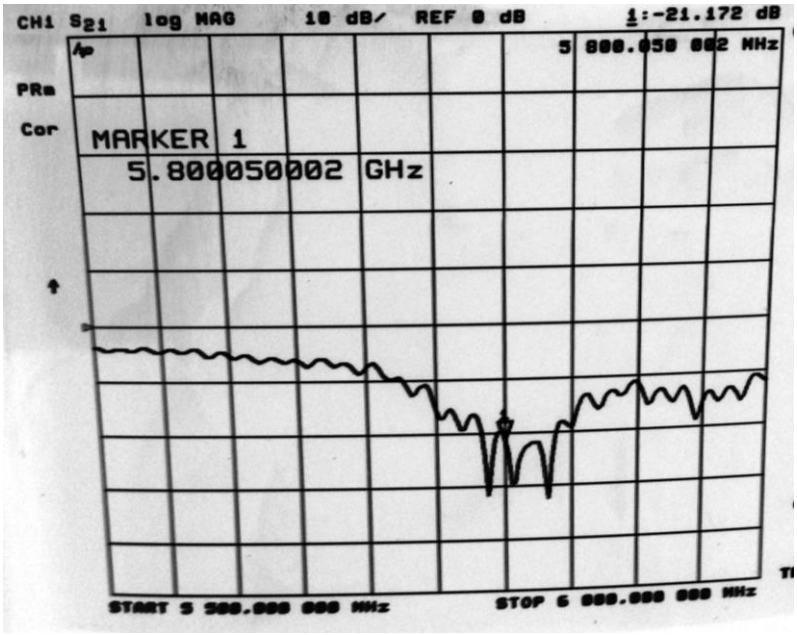

Figure 3.15 S21 measurement of cantenna #2

Using the Friis' Transmission equation 3.4, the actual gain of each cantenna can be calculated.

$$S21(dB) = G1\ (dBi) + G2\ (dBi) + 10 * \log((\frac{\lambda}{4 * \pi * \mathrm{R}})^2) \qquad (Eq.\ 3.4)$$

Where, $S21\ (dB)$ = Cantenna #1 from Table 3.2 = -23.2 dB

Or $S21\ (dB)$ = Cantenna #2 from Table 3.2 = -21.2 dB

$G1\ (dBi)$ = Known Antenna gain = 6.5 dB

$G2\ (dBi)$ = Calculated gain of the cantenna

$\lambda = \frac{(Free\ Space = 3*10\text{^}8)}{(Frequency = 5.8*10\text{^}9)}$

R = 1 meter

Solve for $G2\ (dBi)$ for cantenna #1 = -23.2 – 6.5 + 47.7 = 18 dBi

Solve for $G2\ (dBi)$ for cantenna #2 = -21.2 – 6.5 + 47.7 = 20 dBi

After confirming both cantennas are working properly with a known antenna pointing directly each other (zero degree). Both cantennas were then rotated left and right to six different positions with respect to the log periodic antenna and record the gain (Table 3.3 and Table 3.4). By plotting gain values and degree of rotations, antennas radiation pattern for both cantenna can be observed in Figure 3.16 and Figure 3.17.

Table 3.3 *Cantenna #1 gain output at different positions*

Cantenna #1		
Degree	**dBm**	**Gain (dBi)**
-90	-25.2	16.2
-45	-25.4	15.8
-15	-23.7	17.5
0	-23.2	18.8
15	-24.9	16.3
45	-25.5	15.7
90	-27.2	14.2

Table 3.4 *Cantenna #2 gain output at different positions*

Cantenna #2		
Degree	**dBm**	**Gain (dBi)**
-90	-30.6	11.2
-45	-25.7	16.2
-15	-23.4	17.8
0	-21.2	20.1
15	-24.4	16.8
45	-26.4	14.8
90	-29.1	12.2

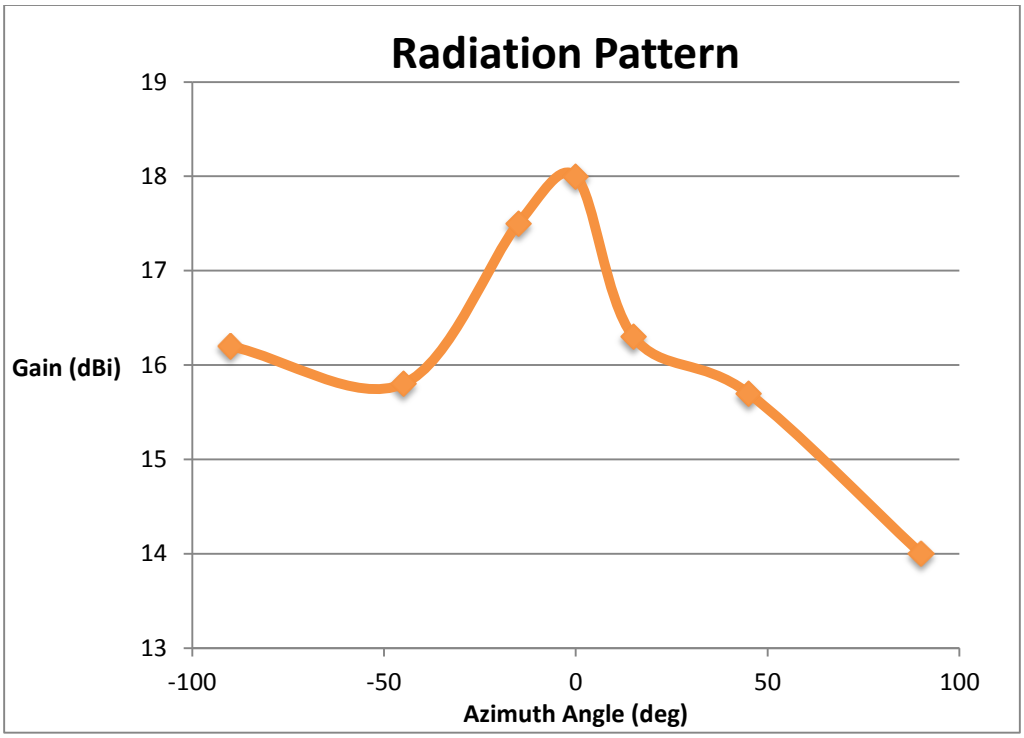

Figure 3.16 Radiation pattern for cantenna #1

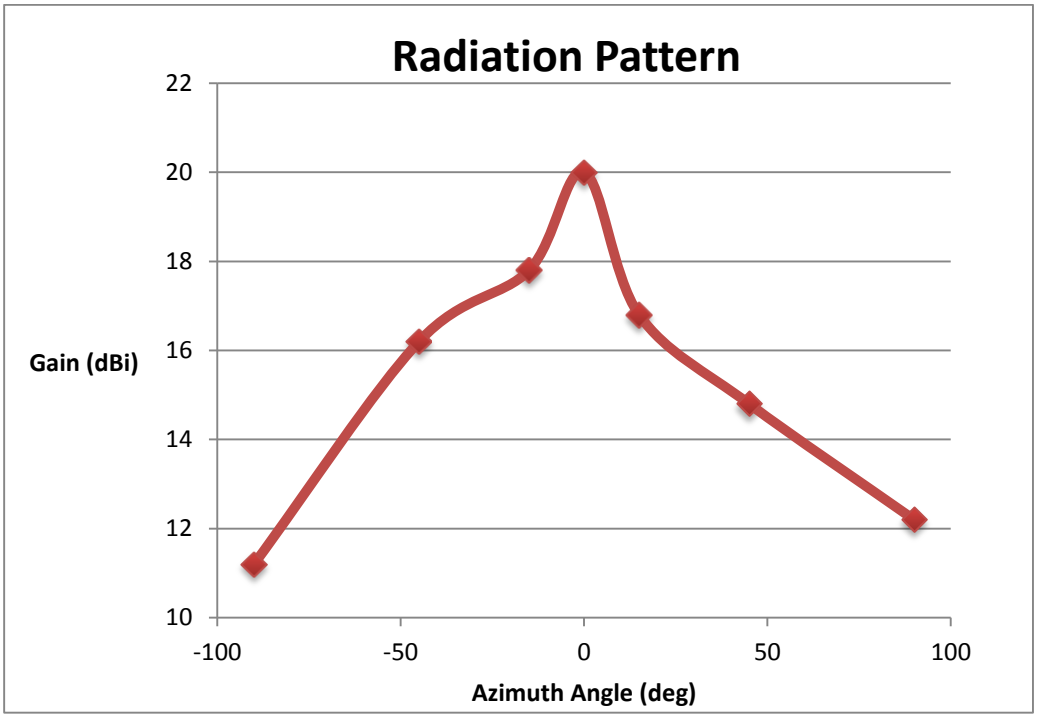

Figure 3.17 Radiation pattern for cantenna #2

Another measurement performed on both cantennas was the isolation. Antenna to antenna isolation is to measure the signal leakage between two antennas when the antennas are side by side as will be used on the radar set (Figure 3.18). This test was setup using a vector network analyzer to perform both S12 and S21 measurement by connecting cantenna #1 to port 1 and cantenna #2 to port 2 on the VNA. Both cantennas are separated from one inch to seven inches and the data is in Table 3.5.

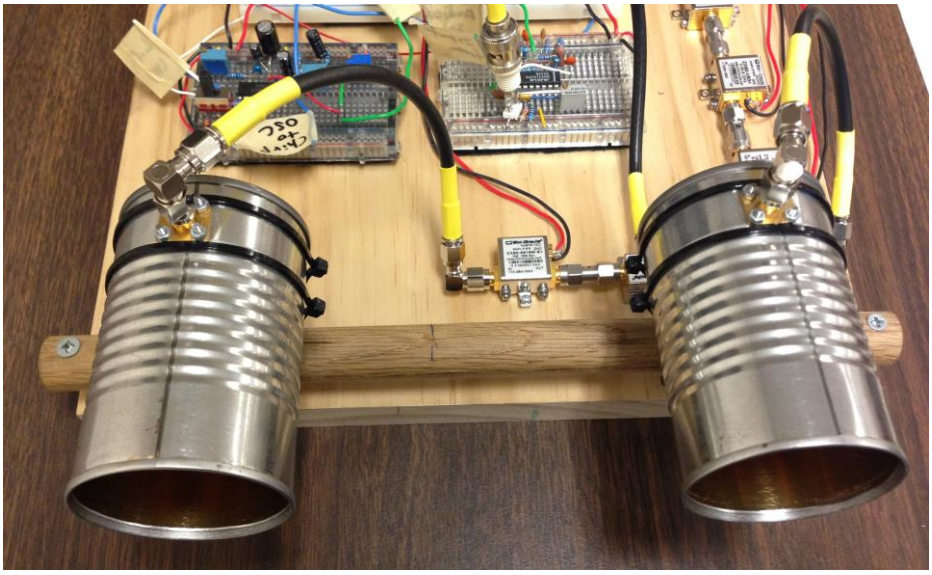

Figure 3.18 Cantenna side by side in the radar system

Table 3.5 *Cantennas isolation*

Distance (inches)	Isolation: REV S12 (dBm)	Isolation: FWD S21 (dBm)
1	-26.5	-36.9
2	-29.8	-29.1
3	-31.4	-30.6
4	-34.1	-33.3
5	-35.9	-35.2
6	-37.5	-38.1
7	-38.4	-39.4

After the series of antenna tests including the return loss, impedance, VSWR and isolation, both cantenna's performance is proven functional at operating frequency of 5.8 GHz. Two cantenna are able to provide large gain at different azimuth angle, matched input impedance 50 ohms with high isolation.

3.2.2 Voltage Controlled Oscillator

The first sub-block of the radar system is the voltage-controlled oscillator. The VCO frequency is designed to be controlled by a voltage input (most of the time called "tuning voltage"). The frequency of the oscillation and output power level is proportionally affected by changes in the applied DC supply voltage (pushing) and the changing load (pulling). The VCO will require a tuning-voltage input and a 5Vdc supply voltage. The expected output frequency from the VCO is 5.8 GHz.

The VCO chosen is the ZX-95-5776+ model from Mini-Circuits. This VCO is operating at +5Vdc power source and has the ability to operate at frequencies between 5726 MHz to 5826 MHz, tuning voltage range from 0 to 5Vdc and typical output power at +1.5dBm. According to the tuning curve in Figure 3.19, the output frequency response and tuning voltage of the VCO have a fairly linear relationship. The tuning sensitivity range for this VCO have a sine-wave variation from 59 to 78 (MHz/V) meaning each voltage tuning step will have at 59 MHz to 78MHz of frequency variation. The ideal tuning voltage at 3.2Vdc will output the frequency at about 5.8 GHz, and power at about +2.23dBm.

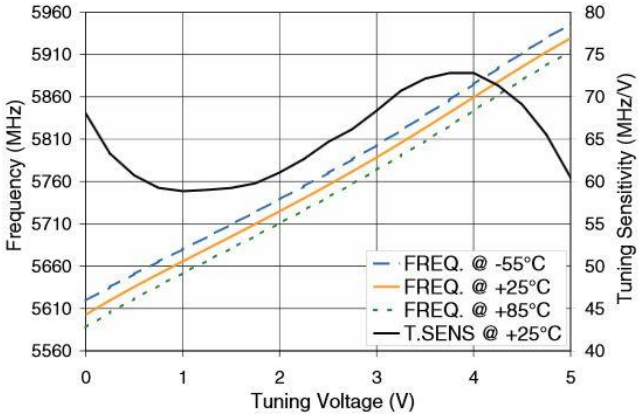

Figure 3.19 Tuning voltage vs. Frequency (MHz) (courtesy of mini-circuits)

3.2.2.1 Voltage Control Oscillator Test procedures and Results

The VCO was tested using a spectrum analyzer to ensure the component works within the specifications. The input parameters to the VCO are listed in Table 3.6. The VCO's output power at 5.8 GHz measured at 1.26 dBm with Vtune voltage of 3.39V, See Table 3.7 and Figure 3.20 for the data. The VCO was adjusted between 5.7 GHz and 5.8 GHz to determine Vtune voltages for the modulator circuit setup parameters. (Table 3.8)

Table 3.6 *Setup parameters to the VCO*

Parameters	**Value/Type**
Supply Voltage (volts):	5
Supply Current (mA):	33
DC Offset (Vtune):	0 to 5
Input Impedance Port (ohms):	50
Transmission Medium:	Input Female SMA connector

Table 3.7 *VCO's measured values*

Parameters	**Expected value**	**Measured Value**	**% Error**
Vtune (Vdc)	3.2	3.39	5.9
Output Power (dBm)	2.23	1.26	30.6
Output Frequency (MHz)	5800	5800	0

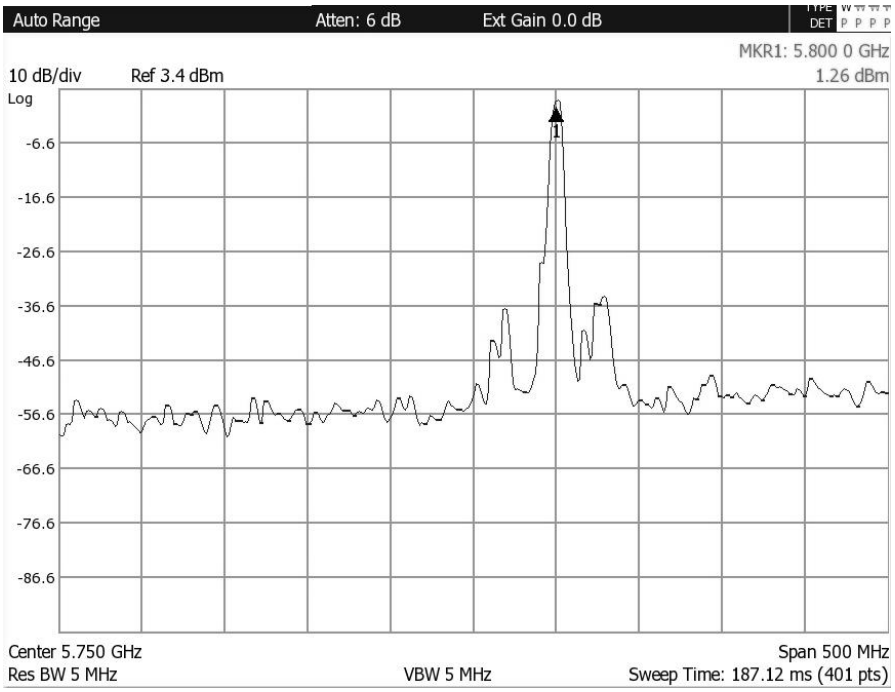

Figure 3.20 VCO's output power at 5.8 GHz.

Table 3.8 *VCO's output frequency and Vtune at 5.8 GHz bandwidth*

Parameters	**Measured Value**	
Vtune (Vdc)	3.04	4.84
Output Frequency (MHz)	5771	5902
Frequency Bandwidth (MHz)	131	

3.2.3 Amplifiers (Transmit Chain)

A 5.8 GHz signal from the VCO will be input to the amplifiers to increase the power level at the output. Due to the high power dissipation of the amplifier, a larger gain amplifier was not selected. Instead, cascade amplifiers will be used in the design to lower the power dissipation on each amplifier. The first amplifier chosen was the ZX60-V63+ from Mini-Circuits, it is a wideband frequency range amplifier and is capable of providing about 14dB gain at 5.8 GHz (Figure 3.21).

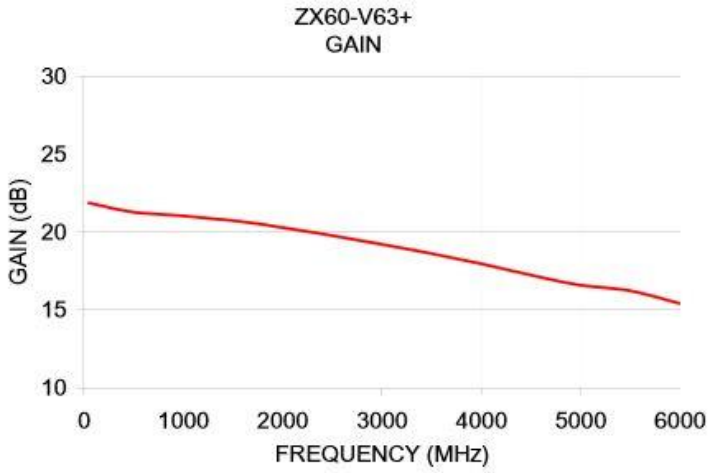

Figure 3.21 ZX60-V63+ amplifiers output power performance
(Courtesy of mini-circuits)

The second amplifier chosen was the ZX60-V81-S+ model from Mini-Circuits. This amplifier is able to provide 6.5dB gain at 5.8 GHz (Figure 3.22). The output power at 1dB compression point for this amplifier at 5.8 GHz is approximately 17dBm (Figure 3.23). Both amplifiers are power from +5Vdc source.

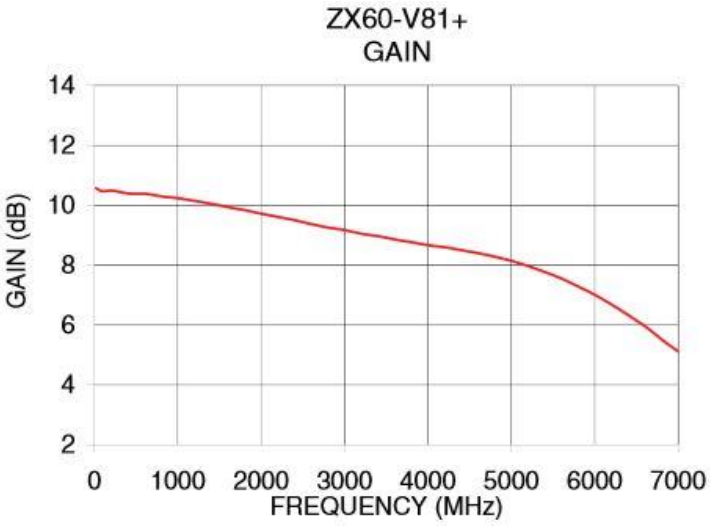

Figure 3.22 ZX60-V81-S+ amplifier output power performance
(Courtesy of mini-circuits)

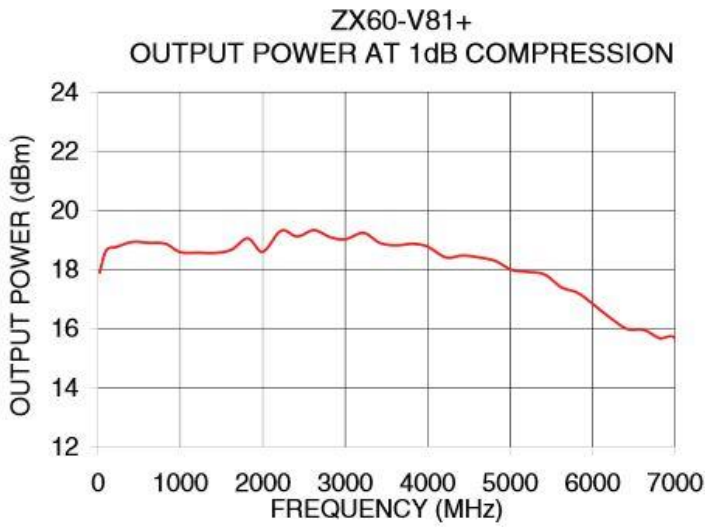

Figure 3.23 ZX60-V81-S+ amplifiers output power at 1dB compression (Courtesy of mini-circuits)

3.2.3.1 Amplifiers Test Procedures and Results

The actual performance of both amplifiers was tested using the VCO as signal source to measure the output power of each amplifier using spectrum analyzer. The output power at 5.8 GHz after first amplifier is measured to be 13.46dBm (Figure 3.24), so the actual gain of the amplifier is 12.2dB when accounting for the VCO output power of 1.26dBm. The output power of the second amplifier is measured at 18.53dBm yielding a gain of 5.07dB (Figure 3.25). See Table 3.9 for complete data. Since the output power level for second amplifier is at 18.53dBm, which means that the amplifier is operating in compression. An amplifier operating in compression will generate additional noise and harmonics. The harmonics will not be a problem at 1.6 GHz but the added noise could add error to the radar results, however, as will be seen this did not occur.

Table 3.9 *Amplifiers (transmit chain) output performance*

Amplifiers (Transmit Chain)	Expected Gain (dB)	Measured Gain (dB)	% Error
Amplifier #1 ZX60-V63+	14	12.2	33.9
Amplifier #2 ZX60-V81-S+	6.5	5.07	28.0

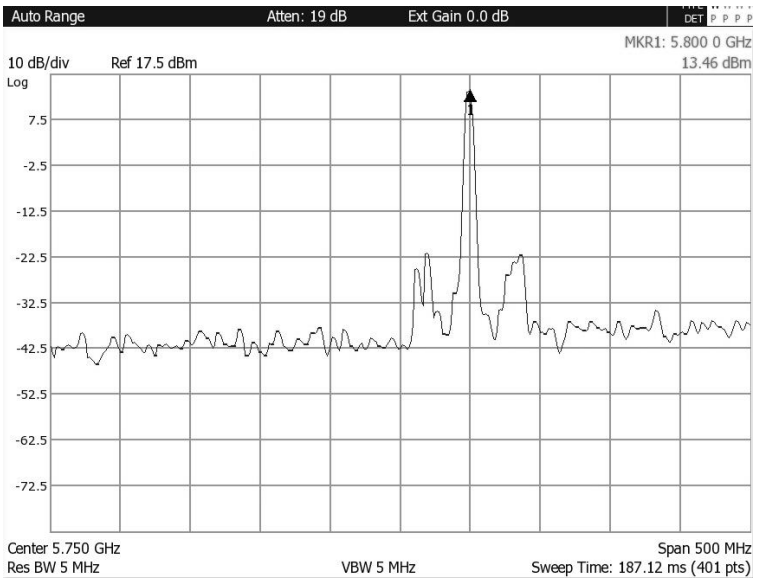

Figure 3.24 Output power level at 5.8 GHz after first power amplifier

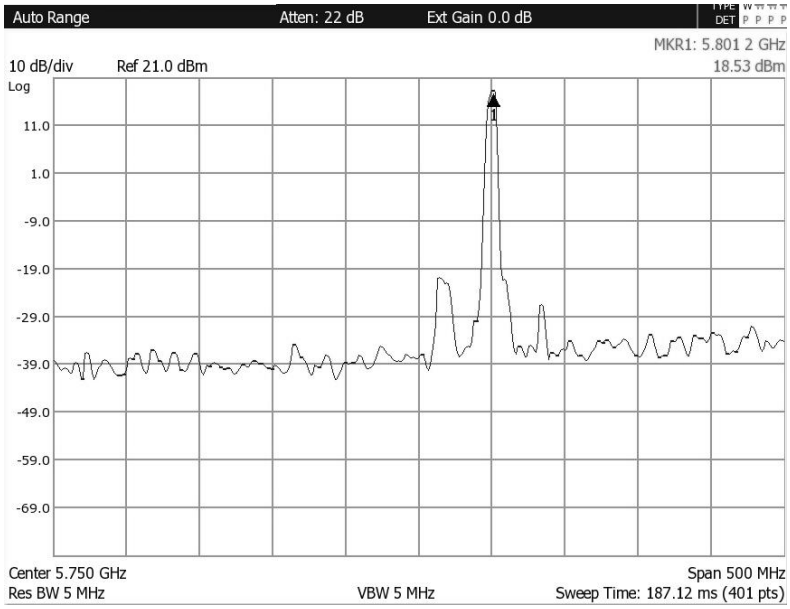

Figure 3.25 Output power level at 5.8 GHz after second power amplifier

3.2.4 Power Splitter

The power splitter used in the design is the ZX10-2-71+ from Mini-Circuits. The purpose of this power splitter is to separate the incoming signal from the second power amplifier to output port 1 and 2 on the power splitter. According to the datasheet in Figure 3.26, the total loss through the splitter at 5.8 GHz is approximately 3.05dBm for port 1 and 3.18dBm for port 2.

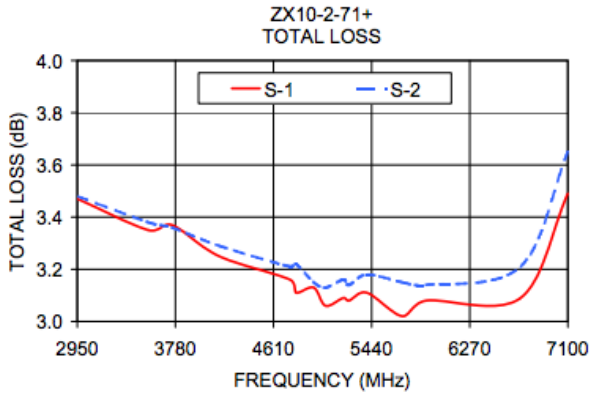

Figure 3.26 Power splitter's total loss on each output port (Courtesy of mini-circuits)

3.2.4.1 Power Splitter Test procedure and Results

The power splitter was tested with VCO and amplifiers attached to measure the output power on each port. Input signal to the power splitter is from the power amplifier (18.53dBm), output port 1 of the splitter is measured at 14dBm (Figure 3.27) and port 2 at 13.88dBm (Figure 3.28). The power loss on both output ports are much higher than expected listed in Table 3.10.

Table 3.10 *Total loss of the power splitter on each output port*

Total Loss of the power splitter	**Expected (dB)**	**Measured (dB)**	**% Error**
Port 1	3.05	4.53	40.6
Port 2	3.18	4.65	40.3

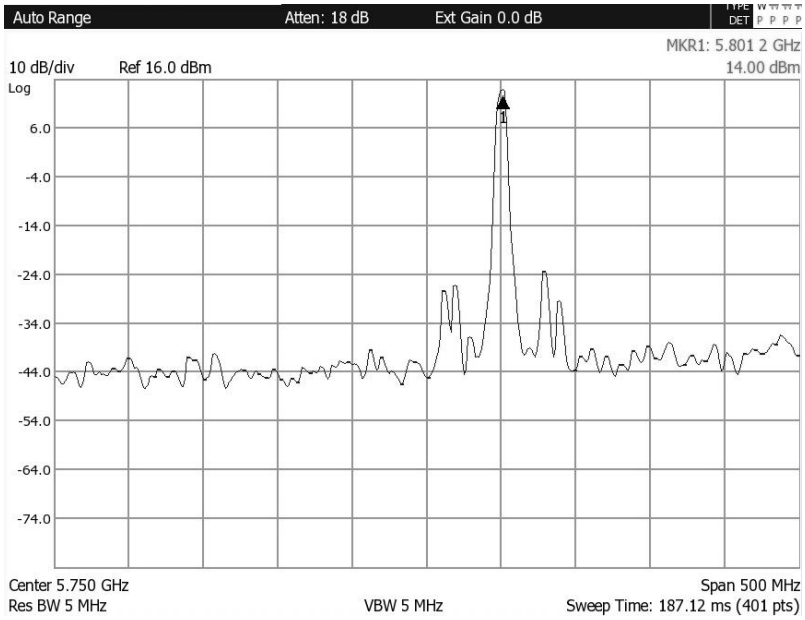

Figure 3.27 Splitter output port 1 to transmitter antenna

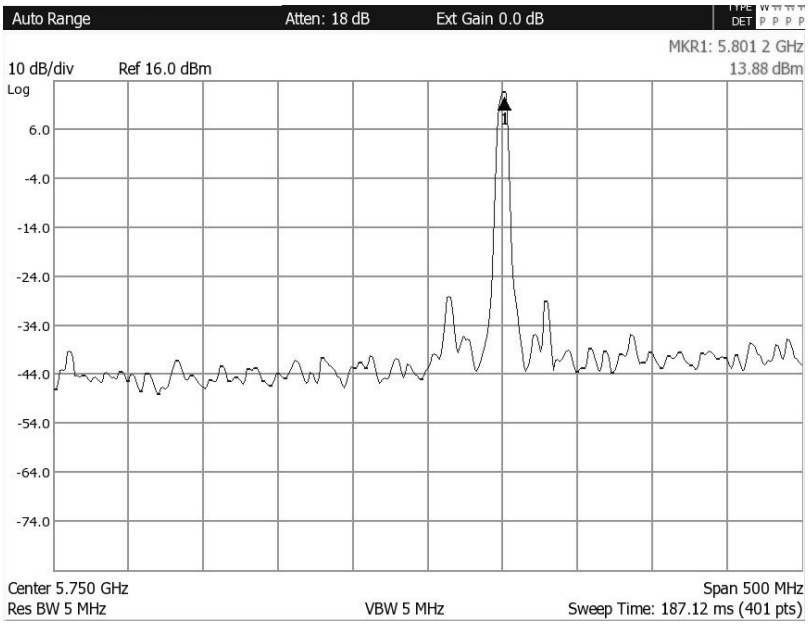

Figure 3.28 Splitter output port 2 to the mixer

3.2.5 Amplifier (Receive Chain)

In the receive chain, a power amplifier is placed after the receiver cantenna. The power amplified chosen was the ZX60-5916M-S+ model from Mini-Circuits. This

amplifier is able to provide approximately 14.5dB at 5.8 GHz using +5Vdc supply source. See Figure 3.29 for expected amplifier output power performance.

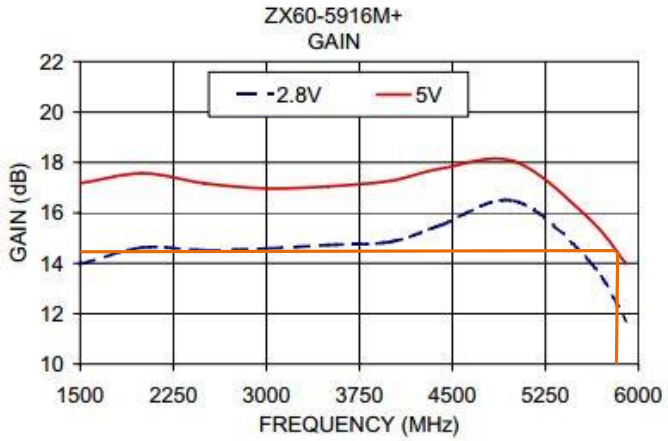

Figure 3.29 ZX60-5916M-S+ amplifier output power performance
(Courtesy of mini-circuits)

3.2.5.1 Amplifier Test Procedure and Results

The amplifier is tested using VCO as signal source and measuring the output power level of the amplifier on the spectrum analyzer (Figure 3.30). The actual gain of the amplifier is calculated in Table 3.11 by subtracting the VCO's output power 1.26dBm from amplifier measured power.

Table 3.11 *Amplifier (receive chain) output performance*

Amplifier (Receive Chain)	**Expected Gain (dB)**	**Measured Gain (dBm)**	**% Error**
Amplifier ZX60-5916M-S+	14.5	13.04	28.6

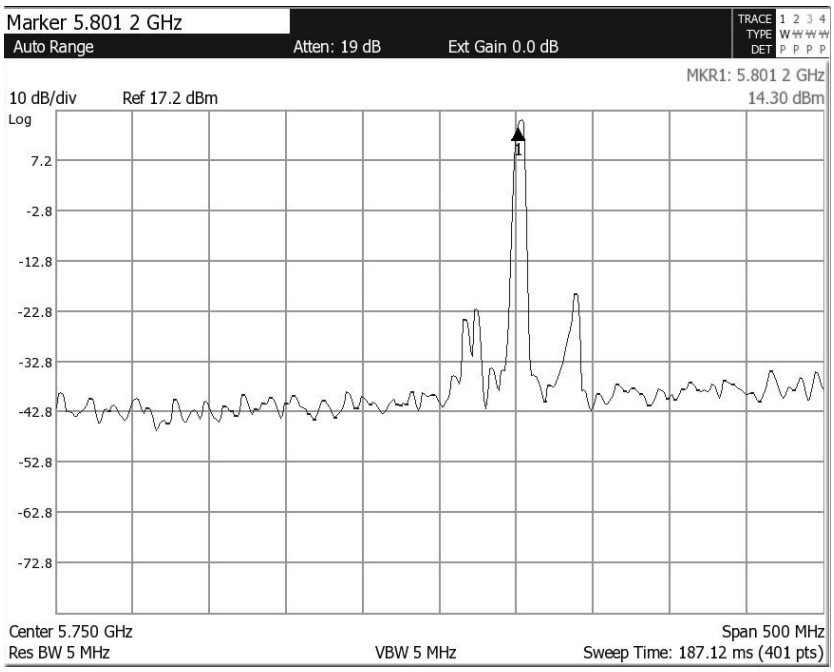

Figure 3.30 Amplifier's (ZX60-5916M-S+) output power level

3.2.6 Mixer

The mixer in this radar system is to function as a phase detector. The phase detector is used to detect the phase difference between LO and RF port. Since the frequency signals on the LO and RF port are almost identical at 5.8 GHz, the phase difference is zero, which results in a constant DC voltage at the output of the mixer. The mixer module used in the design was ZX05-C60MH+ from Mini-Circuits level 13 (LO power +13dBm) with wide range operating frequency from 1600 MHz to 6000 MHz The conversion loss of this mixer is approximately 6.5dB at 5.8 GHz when +13dBm signal power is at the LO port (Figure 3.31).

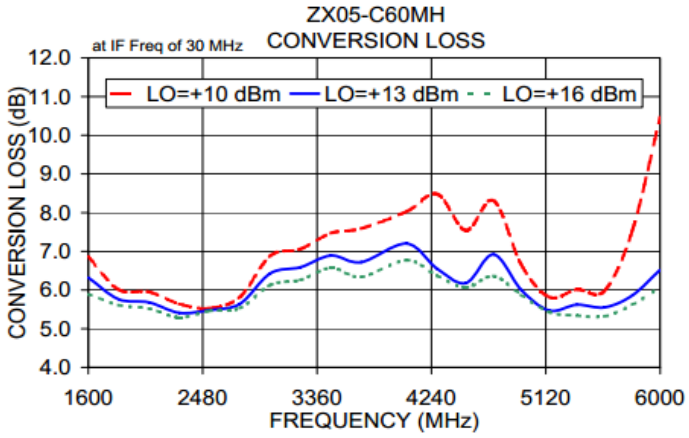

Figure 3.31 Mixer's (ZX05-C60MH+) conversion loss (Courtesy of mini-circuits)

3.2.6.1 Mixer Test Procedures and Results

The mixer is tested under the conditions that it will be used in the system, meaning measuring the variation of the IF output DC voltage level by applying the same signal frequency at RF and LO ports. Due to the lack of the signal generator equipment capable of operating at high frequency, the mixer was tested in the completed radar system, using the signal sources of the RF and LO. The IF output was measured as a voltage on the oscilloscope. By placing an object in front of radar system from one inch to seven inches, the DC voltage variation at the IF port was measured (Table 3.12). The output voltage level varied as the object moved away from the radar, this is due to the change in phase shift between the signal applied at the LO port and the signal received at the RF port.

Table 3.12 *Mixer's DC voltage level variation at IF port*

Distance of the object in front of radar	Voltage at IF port (mV)
1 inch	-48.17
2 inches	-23.02
3 inches	-3.56
4 inches	-5.01
5 inches	-35.17
6 inches	-41.33
7 inches	-18.81
Half-meter	-33.26

The mixer test result shows that the mixer operates properly as a phase detector. The output of the mixer shows the DC voltage variation with object in front of the radar at different distances; this is due to the phase shift between two input signals that has the identical frequency.

3.2.7 Modulator Circuit

The modulator circuit uses a XR2206 IC to generate a chirp signal to the VCO's Vtune to provide modulation for the FMCW radar. By using the VCO's output test results in Table 3.8, the up-ramp sweep of the modulator signal is adjusted to 3.04V to 4.84V in 20mS time interval to sweep the ISM band frequency range from 5771MHz to 5902MHz. The output signal of the IC is on pin 2 with pull-up voltage divider to provide DC offset voltage. The sync plus output is on pin 11 to provide a square wave output waveform for left channel for FMCW radar mode. See Figure 3.32 for modulator circuit schematic.

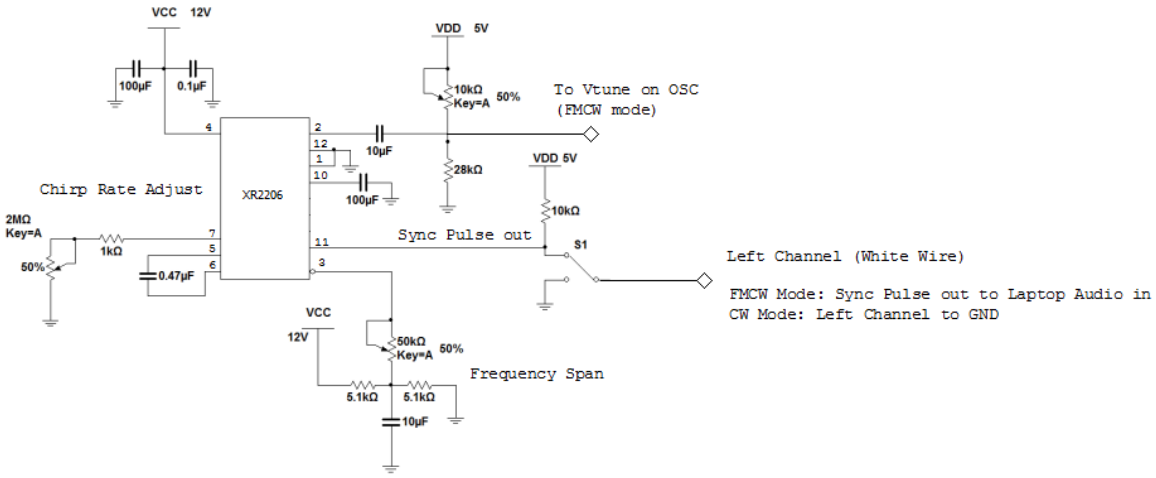

Figure 3.32 Modulator circuit schematic

3.2.7.1 Modulator Circuit Test Procedure and Results

The modulated circuit was tested using an oscilloscope to measure the triangle wave's up-ramp voltage at 3.04V to 4.84V in 20mS interval at frequency of 25Hz. (Figure 3.33, Figure 3.34 and Figure 3.35). Figure 3.36 shows the output triangle wave and sync pulse waveform. The rising edge of square wave indicates the start and stop of the modulation signal within 20ms interval.

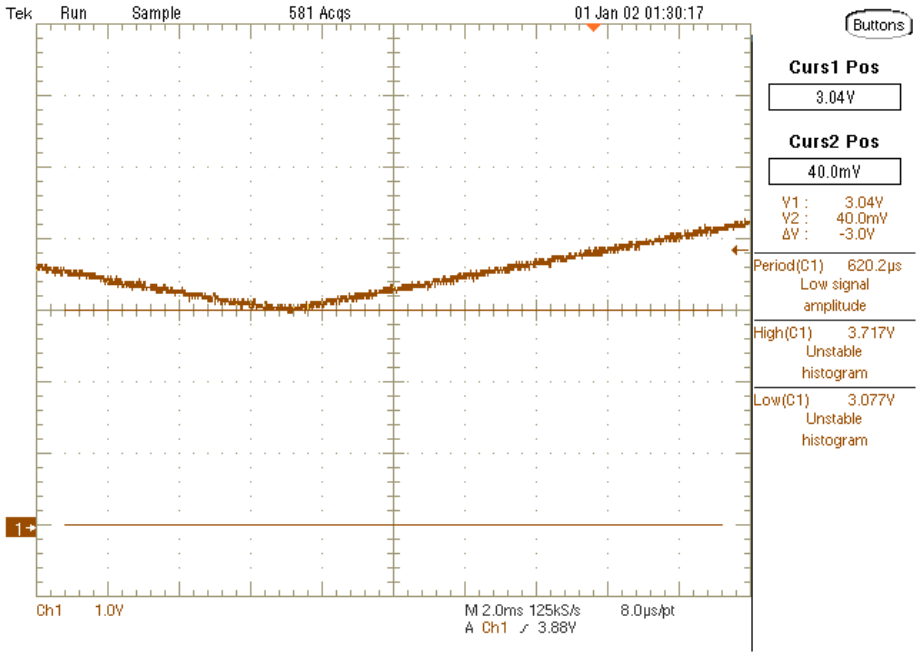

Figure 3.33 Modulator's ramp voltage starts at 3.04 V

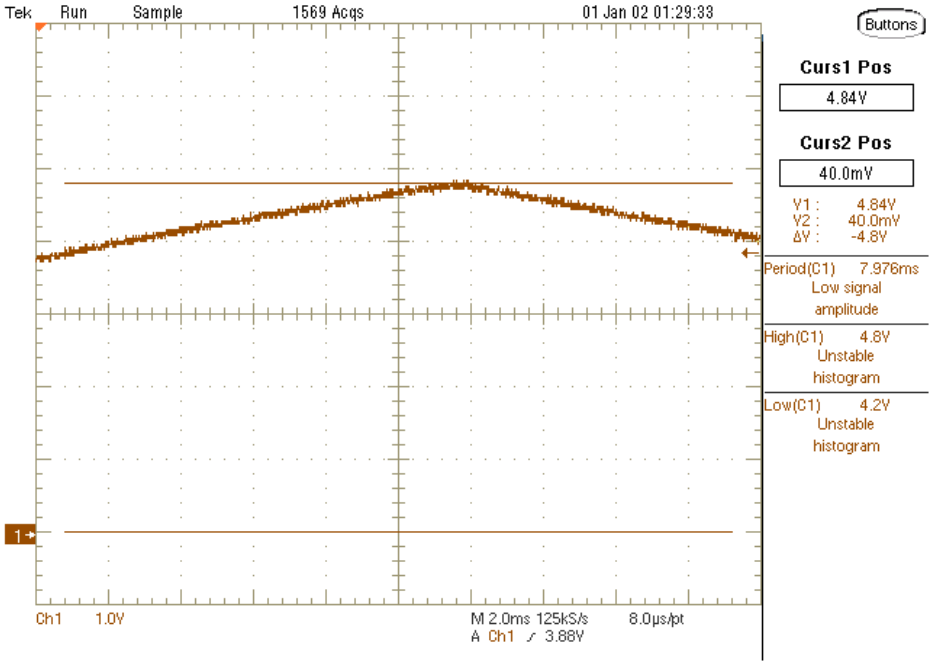

Figure 3.34 Modulator's ramp voltage stops at 4.84V

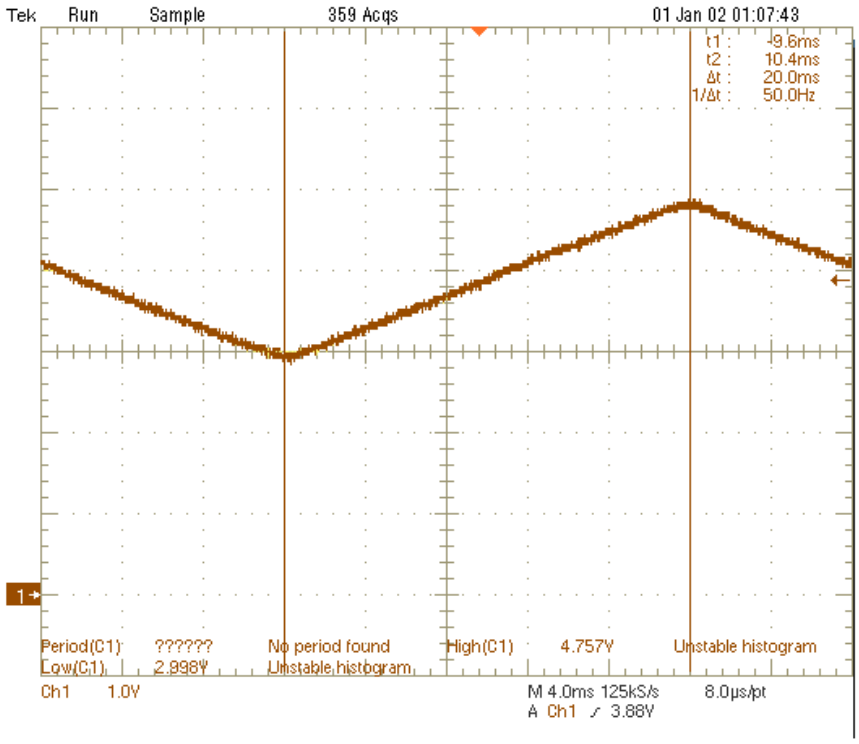

Figure 3.35 Chirp signal up-ramp in 20mS interval

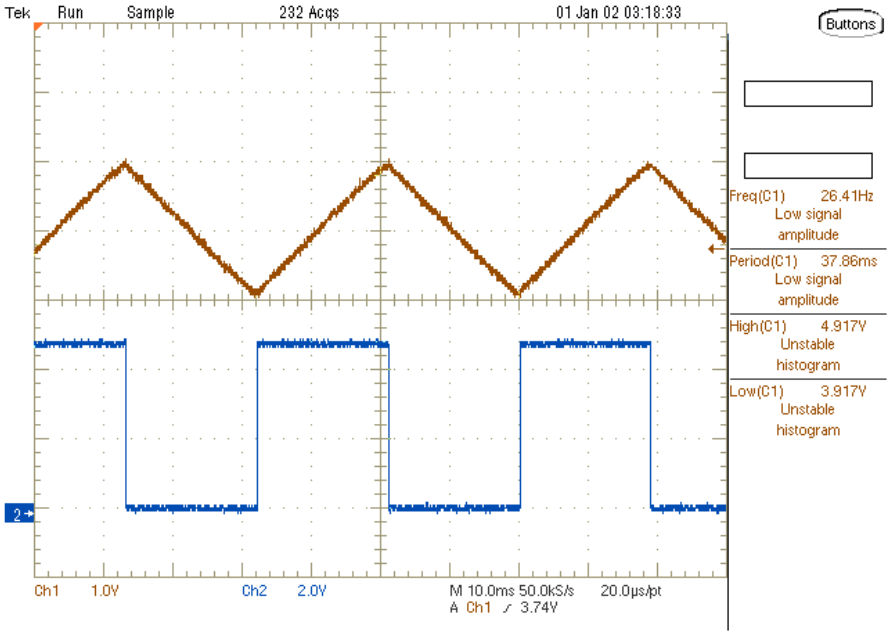

Figure 3.36 Triangle waveform output with square wave sync pulse

3.2.8 Video Amplifier Circuit

The variation of the DC voltage output from the mixer's IF port requires a video amplifier circuit using an Op-Amp MAX414 (Figure 3.37) to provide gain. After the gain stage, the signal is fed through a 15 KHz Sallen-Key low-pass filter circuit to avoid aliasing to the PC's audio input port (right channel).

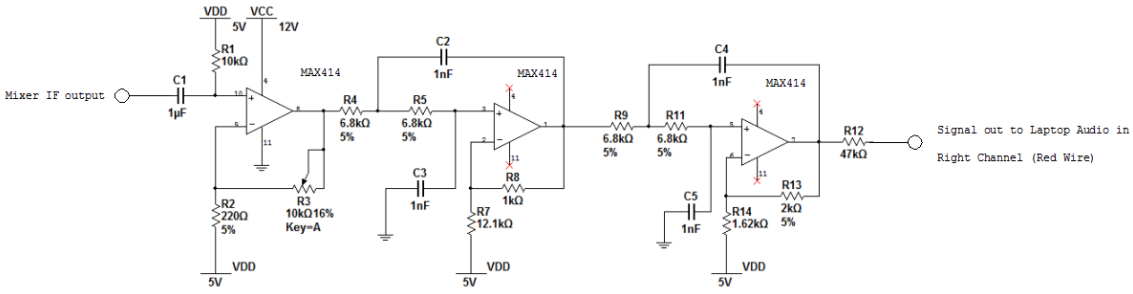

Figure 3.37 MAX414 video amplifier circuit schematic

3.2.8.1 Video Amplifier Circuit Test Procedure and Results

The gain stage of the amplifier was tested using a 15 KHz sine-wave signal 1Vpp signal source from the function generator as input source to the amplifier and measured the output signal on oscilloscope. Adjust the 10kΩ potentiometer until the output signal is at the maximum without clipping (Figure 3.38). The gain was measured to be 7.84.

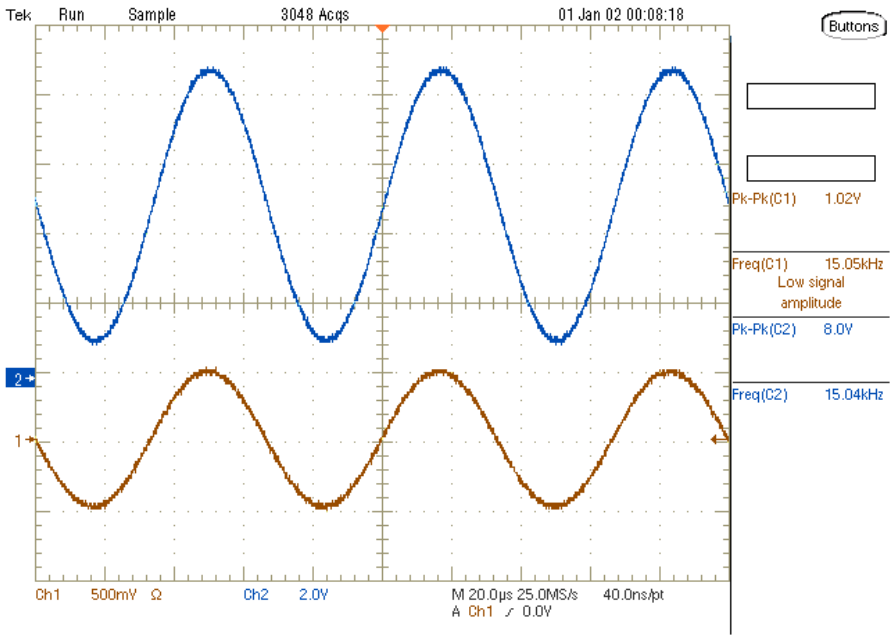

Figure 3.38 MAX414 amplifier's gain stage

The 15 KHz low-pass filter circuit was tested separately using the function generator as input source as well. The 15 KHz input signal was adjusted to 8Vpp and measured the output signal on the oscilloscope at 5.04Vpp. The following calculation confirms that the output signal's attenuation is greater than 3dB at 15 KHz. Figure 3.39 shows the gain stage with the filter output.

$$G(dB) = 20 * \log\left(\frac{output}{input}\right) = 20 * \log\left(\frac{5.04}{8}\right) = \text{- } 4.01 \text{ dB}$$

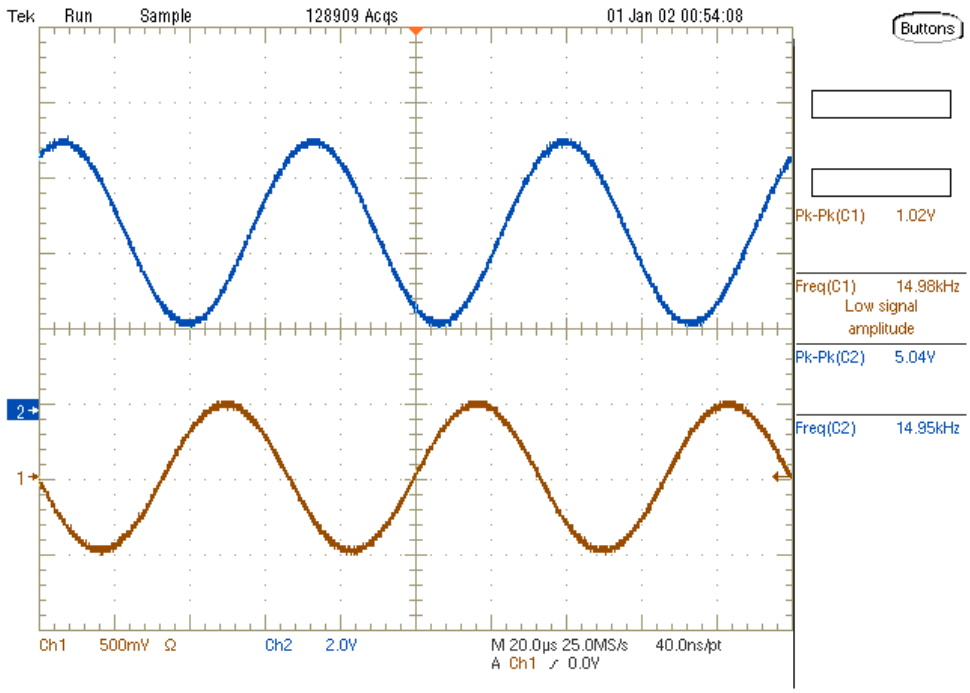

Figure 3.39 MAX414 gain stage with low-pass filter

3.2.9 Software (Matlab) Implementation

For each recorded .wav file, the data is processed and analyzed through Matlab software code provided from MIT OpenCourseWare (Appendix A, B and C). For Doppler shift, Matlab reads the raw data file and returns the sample rate (FS) in hertz, number of bits per sample (NBITS) and store the data in a string (Y) range from -1 to +1. Using the stored data, Matlab performs an inverse fast Fourier transform (IFFT) computational algorithm to convert the data from frequency to time representation of the signal. The velocity is determined by the rate of change in frequency wavelength over a 25mS pulse time period continuously. Using the calculated velocity and time, the results are plotted on a Doppler versus Time Intensity (DTI) showing velocity in meters per second and time in seconds with corresponding intensity level.

Similar for ranging, Matlab reads the raw data file into a string and parses the data at the rising edges of sync pulse on left channel 20mS at a time and perform inverse fast Fourier transform to convert from frequency to time domain. The frequency of the radar system is specified in the Matlab program to determine the transmit bandwidth and instantaneous transmit frequency for range resolution and the distance. Since the FMCW radar is transmitting the modulated signal continuously, meaning the signal reflections off the target is also continuously even when the object is stationary. To increase the accuracy of the range measurement of a moving target, Matlab performs a two pulse canceler algorithm to remove the signals that are identical for each signal received back from the target. The output results are plotted on a Range vs. Time Intensity (RTI) plot showing the objects moving in distance (meters) and time (seconds).

Forming SAR images in Matlab required additional algorithm computation. The SAR radar requires range profiles for each increment along a linear path. In this case, the cross range is set to three meters with two inches increment at a time. The left channel's sync pulse is used to indicate the new position of the image capture by the radar. Matlab first pairs up the raw data set with the sync pulse's rising edges and removes the data when sync pulse is toggled to low. By taking the remaining data, Matlab pre-transforms the data to the spatial frequency domain using 2D fast Fourier transform algorithm followed by a matched filter to filter out the signals that are identical due to the overlapping and then removes the signals that has less reflections off the target.

The raw data left in the system is used to perform a Stole Interpolation algorithm to compute the range and resolution migration and back propagation in the spatial frequency domain. The final process is to transform the reconstructed image from a Stole

Interpolation back to spatial domain using 2D inverse fast Fourier transform algorithm. The output results are plotted on a Cross range (ft.) verses Downrange (ft.) SAR images showing the reflections off the target with the corresponding intensity level and range.

3.3 Initial Radar Testing

The initial radar testing consists of cantennas spacing, Doppler, and ranging. The purpose of this test is to make sure the system is functioning properly and to use the most optimal cantenna spacing for the system.

3.3.1 Antenna Spacing

The spacing of the two cantennas were adjusted from one inch to seven inches to determine the most suitable spacing with no object in front of the radar (small signal) versus an object of the radar (large signal). Table 3.13 and Table 3.14, show the test results at the output of the receiver cantenna when there are no object in front and an object in front (half meter) of the system. By plotting two data sets in Figure 3.40, showing two, four and seven inches are the optimal spacing. Another consideration taken into account of antenna spacing is the antenna isolation in Table 3.5. At two inches apart, antennas isolation is lower could cause more interference and noise. At seven inches, the distance apart could have effect on the reconstructed signal, such as in SAR. The most suitable cantenna spacing is four inches apart with high isolation at -30dBm and maximum signal to noise ratio.

Table 3.13 *Receiver cantenna's power level with no object in front*

System with no object in front	
Distance between two cantenna (inches)	**Received Power (dBm)**
1	-12.54
2	-15.13
3	-20.22
4	-22.85
5	-24.83
6	-26.48
7	-28.70

Table 3.14 *Receiver cantenna's power level with object in front*

Antenna with object in front (half meter)	
Distance between two cantenna (inches)	**Received Power (dBm)**
1	-15.84
2	-12.27
3	-21.30
4	-18.87
5	-21.57
6	-30.83
7	-24.46

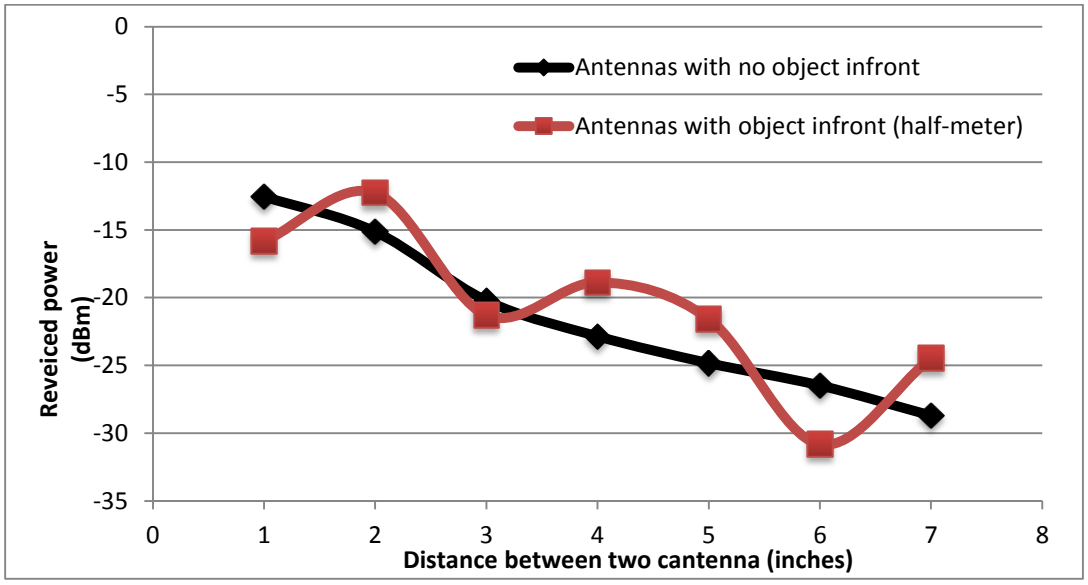

Figure 3.40 Distances between two cantenna vs. received power level

3.3.2 Doppler Initial Testing

The initial Doppler testing is to test the system performance in CW mode by connecting the VCO's Vtune pin to a constant voltage source and left channel on the 3.5mm audio cable to ground to allow the data to be recorded only to the right channel. The audio recording software used for this project is Audacity with sampling rate of 44.1 KHz (default) for every .wav file. The testing procedure is to place the radar system on the test bench, power on the system, begin record the audio and waving in front of the system by hand at different speed to record the Doppler Effect. The recorded .wav in Figure 3.41 shows the hand waving at different repetition rate in Audacity. In Figure 3.42, shows the DTI output plot with level of intensity.

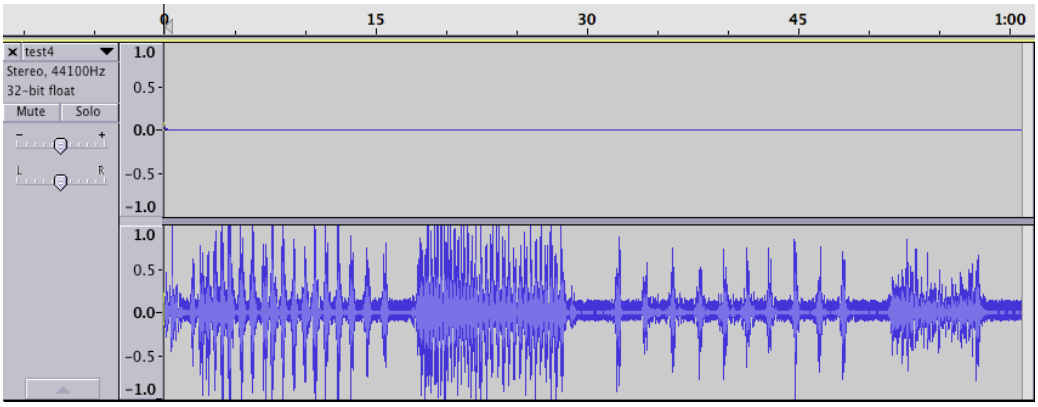

Figure 3.41 Recorded audio file with hand waving in Audacity

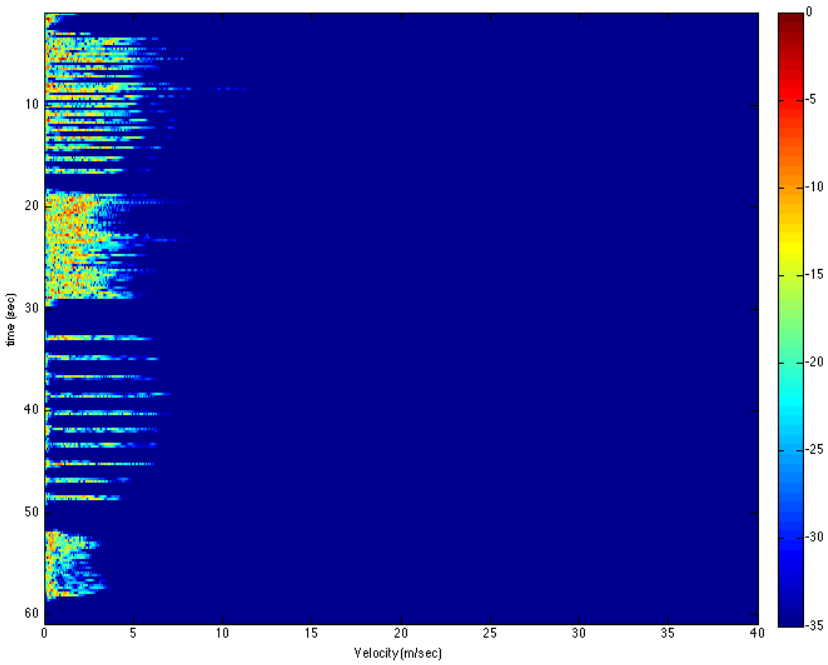

Figure 3.42 MATLAB's DTI output plot for Doppler

3.3.3 Range Initial Testing

The range test setup is to connect VCO's Vtune to the modulator's circuit output to activate the system to FMCW mode and left channel of the audio signal to the sync pulse. The test procedure is conducted by measuring a person walking away and toward the radar system from one to seven meters several times. In Figure 3.43 shows the recorded left and right channel audio signal on Audacity and Figure 3.44 shows an output RTI plot to measure the distance (range) in meters with respect to time and intensity level.

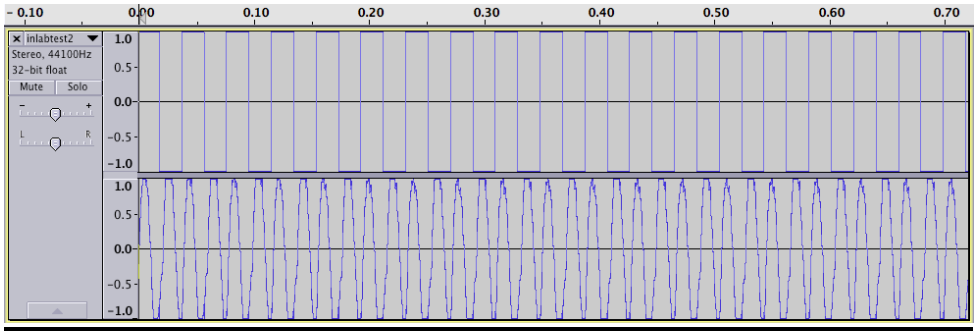

Figure 3.43 Recorded audio file with left and right channel in Audacity

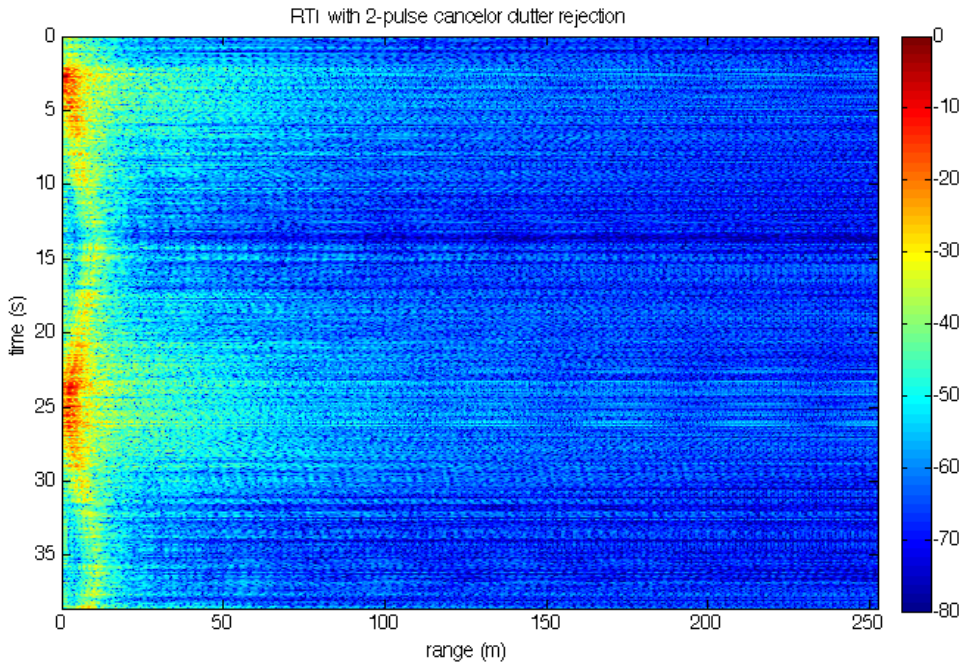

Figure 3.44 MATLAB's RTI output plot for ranging

Both of these tests indicate that the radar system has basic function and operation. Detailed testing is performed in the next chapter.

CHAPTER 4. SYSTEM RESULTS

4.1 Introduction

The radar system final test experiment are including Doppler, ranging and SAR imaging. The experiments is performed at outdoor open area to improve the accuracy of the radar system. Each measurements are repeated three times to obtain the average measured values and compare with the expected. The final assembled 5.8 GHz radar system is shown in Figure 4.1.

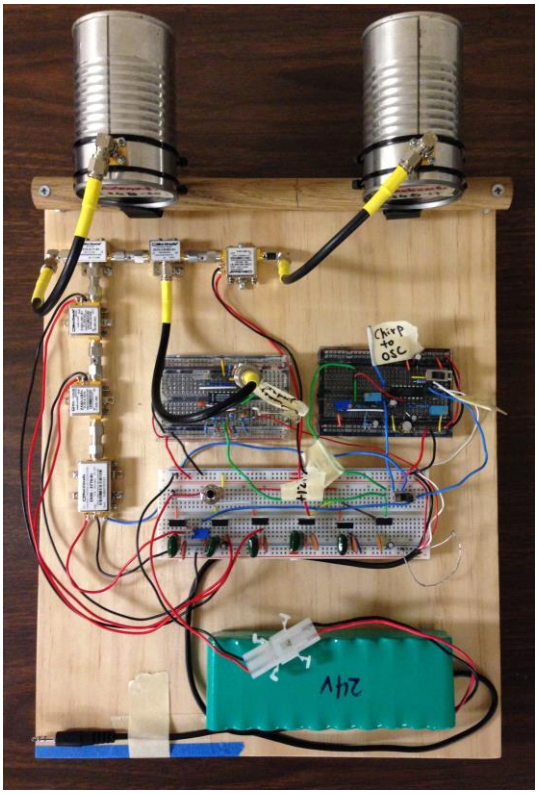

Figure 4.1 The final assembled 5.8 GHz radar system

4.2 Doppler Test Procedure

The Doppler test is essentially the measurement of velocity versus time of a moving object. For this experiment, an open area with a moving vehicle will be the experiment setup to measure the Doppler Effect. The moving vehicle will drive pass the radar system three times at different speeds to record data. The vehicle is required to maintain a constant speed when approaching the radar at 15mph, 30mph and 45mph. The vehicle type in this experiment is a sedan, therefore, the height of the radar system is placed 18 inches above the ground at an angle of 45 degrees approximately the same height to the vehicle's front bumper in Figure 4.2.

The vehicle's actual speed error is minimized by using an OBD (On-board diagnostics) II heads up display in the vehicle. The ODB II heads up display unit is connected to vehicle's on-board computer to provide the actual speed reading of the vehicle in Figure 4.3. For each speed, a computer will be used to record the Doppler radar audio file and use MATLAB file to produce a DTI plot. By measuring the same speed of the vehicle three times, the average measured speed of the vehicle will be obtained to compare with the actual speed of the vehicle.

Figure 4.2 Doppler measurement setup

Figure 4.3 ODB II heads up display

4.2.1 Doppler Test Results

The speed of the vehicle is measured three times for each speed increment of 15, 30 and 45 mph to obtain the average speed in Table 4.1, 4.2, and 4.3. The MATLAB's output DTI plot is measured the speed in meters per second (m/s) which is converted to mph to compare with actual speed of the vehicle (Figure 4.5, 4.6, 4.7).

Table 4.1 *Doppler test measurement at 15mph*

Attempt	Actual speed (mph)	Measured speed (m/s)	Calculated speed (mph)	Average speed (mph)	% Error
1	15	6.85	15.33	15.29	1.95
2	15	6.65	14.87		
3	15	7.01	15.68		

Table 4.2 *Doppler test measurement at 30mph*

Attempt	Actual speed (mph)	Measured speed (m/s)	Calculated speed (mph)	Average speed (mph)	% Error
1	30	12.85	28.74	28.68	4.41
2	30	12.60	28.19		
3	30	13.01	29.10		

Table 4.3 *Doppler test measurement at 45mph*

Attempt	Actual speed (mph)	Measured speed (m/s)	Calculated speed (mph)	Average speed (mph)	% Error
1	45	19.22	42.99	42.80	4.89
2	45	18.91	42.30		
3	45	19.27	43.11		

The interpretation of the DTI for this Doppler measurement is in Figure 4.4. At first instance, radar's transmitted signal hits the vehicle and bounced back to the radar system as the vehicle begins to enter cantenna's beamwidth. The speed of the car is determined at the start of the car as that is the maximum change; as the car enters the

beam, a difference from ‘zero’ to the car speed is determined. The reflections observed after the car entry measure the change in the ‘side’ of the vehicle which is not its actual speed. As the vehicle driving passes the radar faster and faster, the length of the vehicle decreases on the DTI plot due to less signal reflection off the vehicle at higher speed. These observations can be seen in Figure 4.5, 4.6, and 4.7.

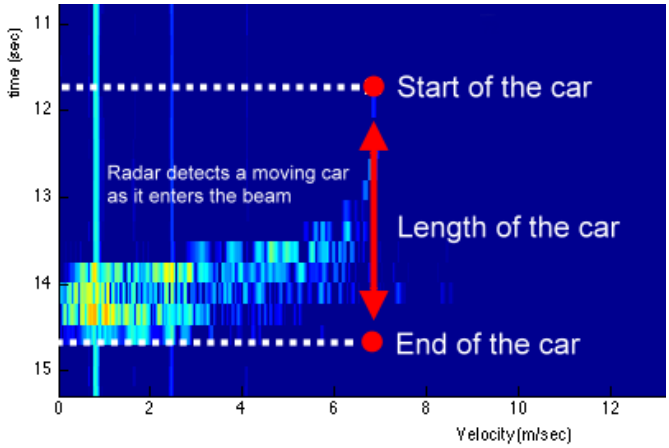

Figure 4.4 DTI plot interpretation

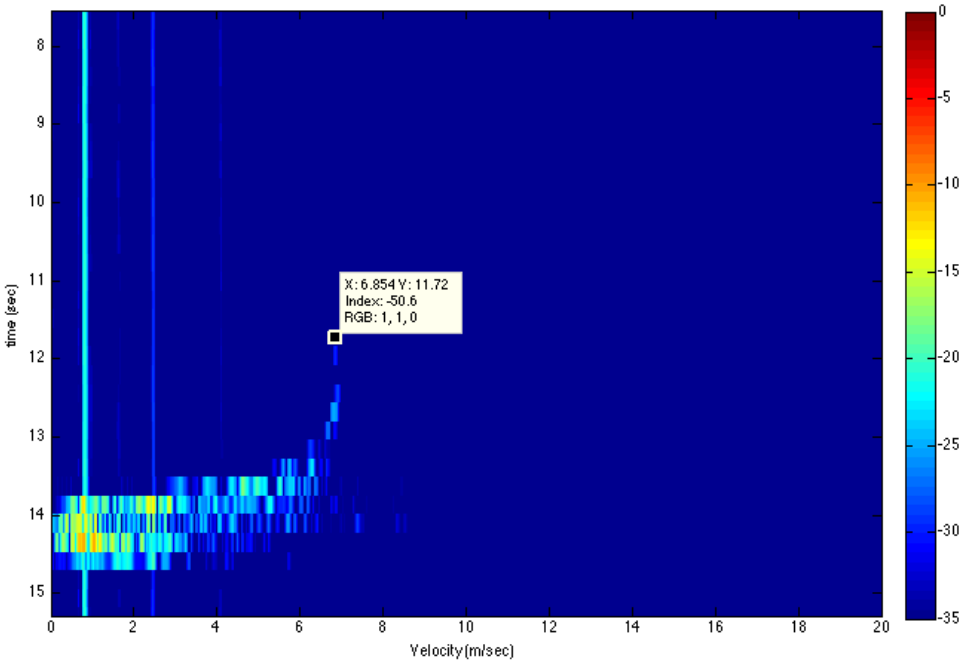

Figure 4.5 DTI plot of vehicle driving pass at 15mph

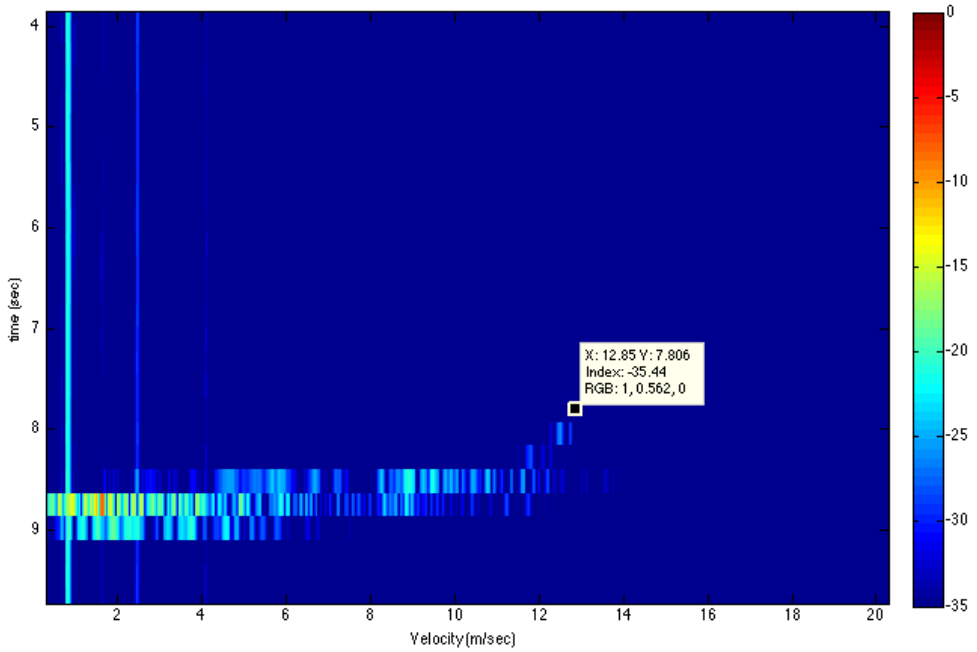

Figure 4.6 DTI plot of a vehicle driving pass at 30mph

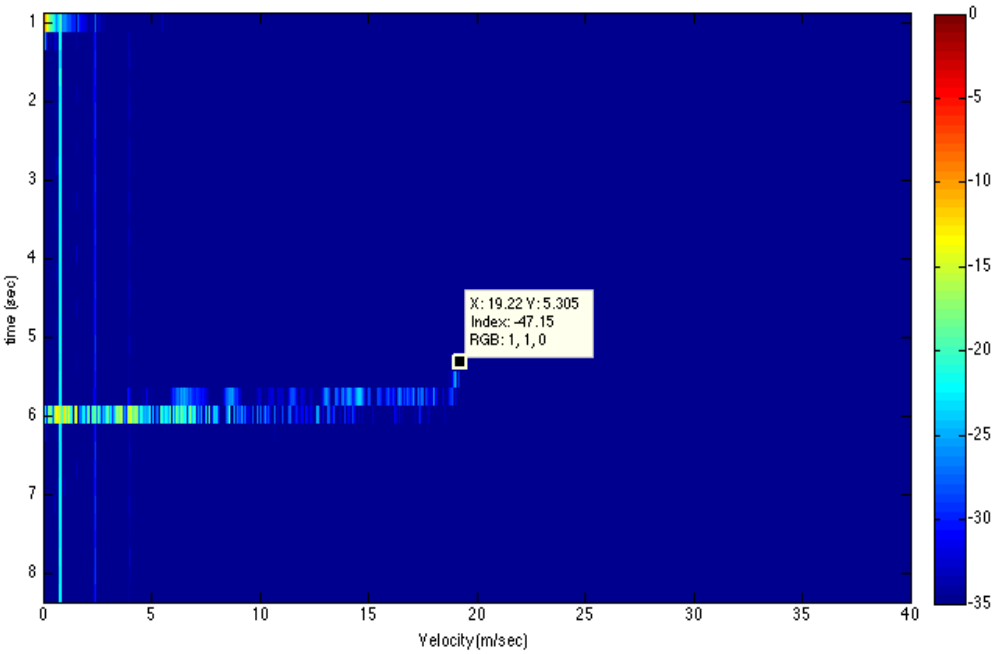

Figure 4.7 DTI plot of a vehicle driving pass at 45mph

4.3 Range Test Procedure

The range measurement procedure is conducted by measuring a known moving vehicle in an open area. Similar to Doppler testing, the radar system is placed 18 inches above the ground and pointing at the vehicle to measure the range and time as the vehicle moves toward and away from ten meters to a hundred meters. Vehicles typically have a higher reflection coefficient, which allows for a stronger signal to be received by the radar. To improve the accuracy of the range measurement, a flag is placed at every ten meters for indication (Figure 4.8). The driver is asked to drive the vehicle slowly and stop at every ten meters for five seconds and record the time when stopping. The experiment is repeated three times for each trip to record audio files for data analysis.

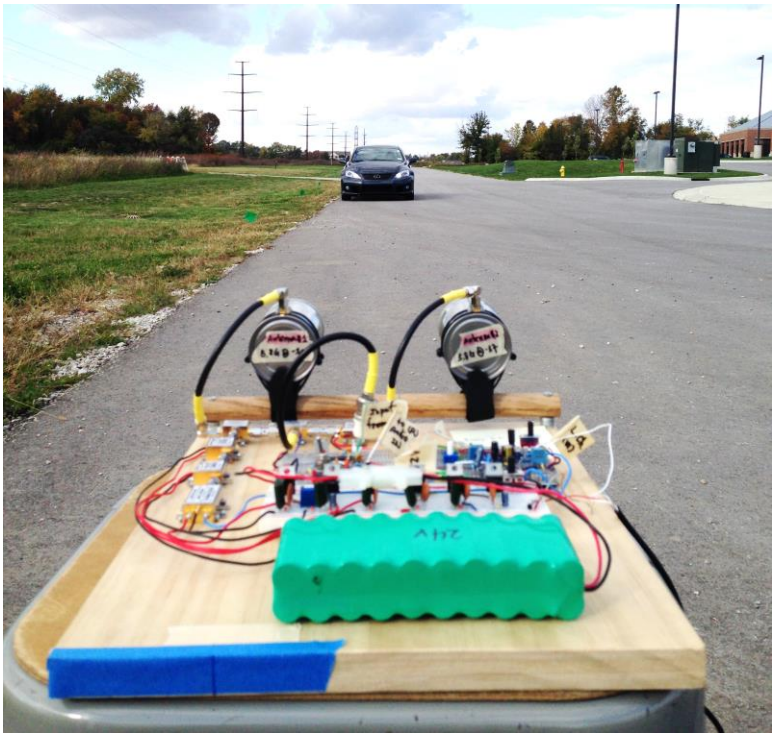

Figure 4.8 Range measurement setup

4.3.1 Range Test Results

The range test results were measured on the RTI output plots to compare with the actual distance (range) with respect to time. The maximum range that the radar can detect the vehicle position is 70 meters as shown in Figure 4.9 RTI plot. Using the RTI plot, the data points of range (m) and time (s) were measured from the signal's the left and right side boundaries and plotted in excel with expected data sets in Figure 4.10 for comparison.

Table 4.4 to 4.10 shows the average distance measurement for the vehicle driving away from the radar system every 10 meters. This data was taken from the right side boundaries of the signal consistently throughout the data collection and measurements. Similarly, Figure 4.11 RTI plot shows a vehicle driving toward the radar from 100 meters with the maximum detecting range at 80 meters. Figure 4.12 shows the data comparison and the average measured distance in Table 4.11 to Table 4.11.

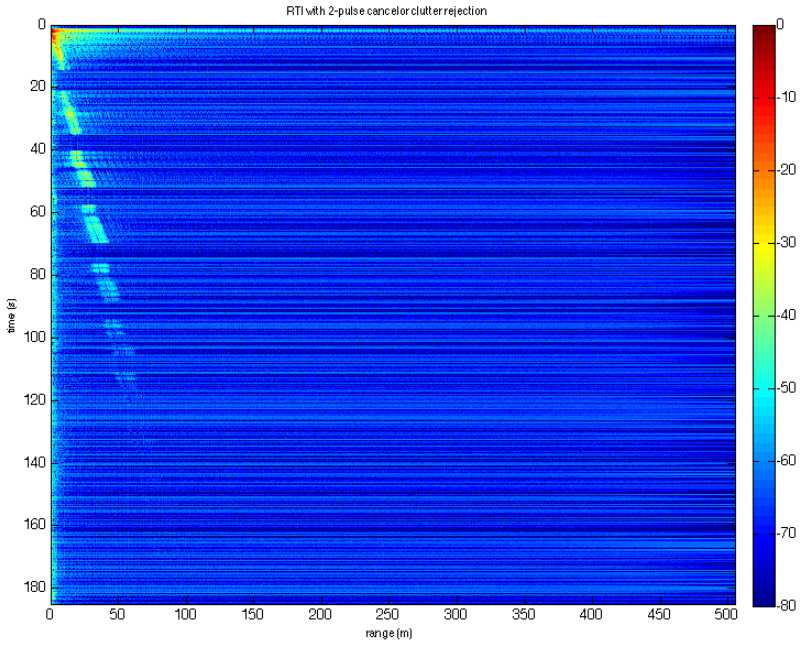

Figure 4.9 RTI output plot of a vehicle moving away from radar

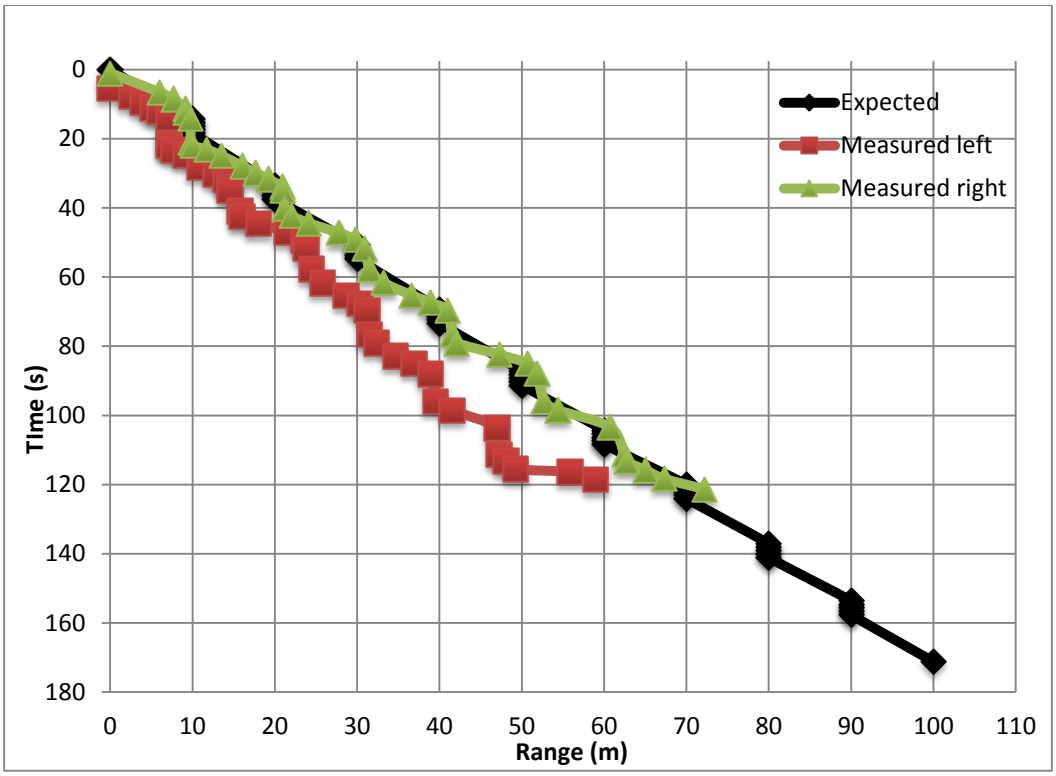

Figure 4.10 Range measurements comparison for a vehicle moving away from radar

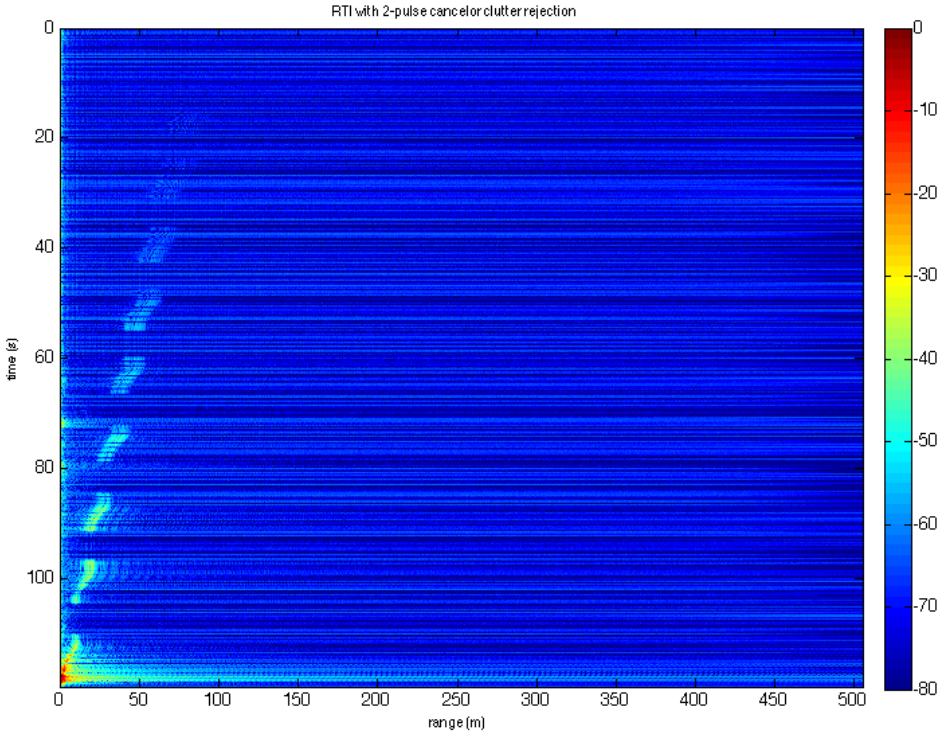

Figure 4.11 RTI output plot of a vehicle moving toward to radar

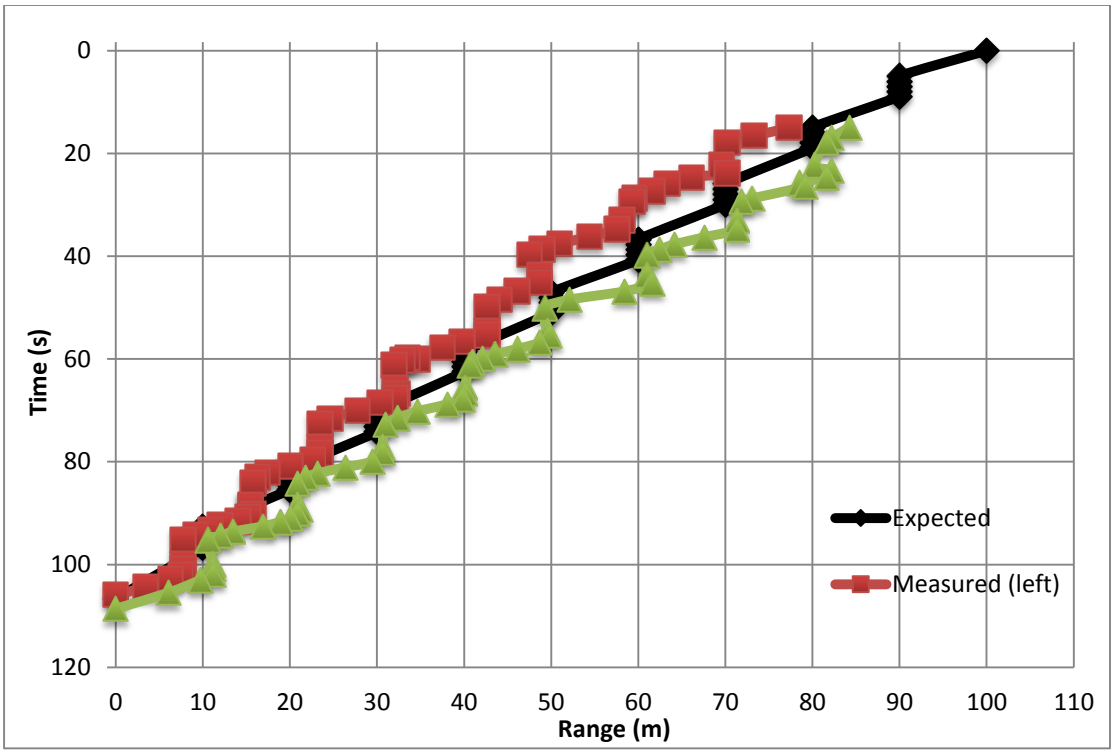

Figure 4.12 Range measurements comparison for a vehicle moving toward from radar

Table 4.4 *Vehicle driving away from radar at 10 meters*

Attempt	Actual distance(m)	Measured distance (m)	Average distance (m)	% Error
1	10	9.57	10.54	5.40
2	10	11.55		
3	10	10.50		

Table 4.5 *Vehicle driving away from radar at 20 meters*

Attempt	Actual distance(m)	Measured distance (m)	Average distance (m)	% Error
1	20	20.55	20.41	2.03
2	20	20.62		
3	20	20.05		

Table 4.6 *Vehicle driving away from radar at 30 meters*

Attempt	Actual distance(m)	Measured distance (m)	Average distance (m)	% Error
1	30	30.74	30.48	1.59
2	30	30.55		
3	30	30.14		

Table 4.7 *Vehicle driving away from radar at 40 meters*

Attempt	Actual distance(m)	Measured distance (m)	Average distance (m)	% Error
1	40	41.25	40.74	1.84
2	40	40.29		
3	40	40.67		

Table 4.8 *Vehicle driving away from radar at 50 meters*

Attempt	Actual distance(m)	Measured distance (m)	Average distance (m)	% Error
1	50	51.27	50.65	1.30
2	50	50.27		
3	50	50.41		

Table 4.9 *Vehicle driving away from radar at 60 meters*

Attempt	Actual distance(m)	Measured distance (m)	Average distance (m)	% Error
1	60	60.72	60.66	1.09
2	60	61.10		
3	60	60.15		

Table 4.10 *Vehicle driving away from radar at 70 meters*

Attempt	Actual distance(m)	Measured distance (m)	Average distance (m)	% Error
1	70	72.18	71.03	1.48
2	70	70.46		
3	70	70.46		

Table 4.11 *Vehicle driving toward to radar at 80 meters*

Attempt	Actual distance(m)	Measured distance (m)	Average distance (m)	% Error
1	80	80.16	80.19	0.23
2	80	80.20		
3	80	80.20		

Table 4.12 *Vehicle driving toward to radar at 70 meters*

Attempt	Actual distance(m)	Measured distance (m)	Average distance (m)	% Error
1	70	71.03	70.83	1.19
2	70	71.51		
3	70	69.96		

Table 4.13 *Vehicle driving toward to radar at 60 meters*

Attempt	Actual distance(m)	Measured distance (m)	Average distance (m)	% Error
1	60	59.86	59.91	0.15
2	60	60.00		
3	60	59.87		

Table 4.14 *Vehicle driving toward to radar at 50 meters*

Attempt	Actual distance(m)	Measured distance (m)	Average distance (m)	% Error
1	50	49.55	49.73	0.53
2	50	49.55		
3	50	50.10		

Table 4.15 *Vehicle driving toward to radar at 40 meters*

Attempt	Actual distance(m)	Measured distance (m)	Average distance (m)	% Error
1	40	40.82	40.46	1.15
2	40	40.46		
3	40	40.10		

Table 4.16 *Vehicle driving toward to radar at 30 meters*

Attempt	Actual distance(m)	Measured distance (m)	Average distance (m)	% Error
1	30	29.50	30.13	0.42
2	30	30.43		
3	30	30.45		

Table 4.17 *Vehicle driving toward to radar at 20 meters*

Attempt	Actual distance(m)	Measured distance (m)	Average distance (m)	% Error
1	20	21.58	21.13	5.67
2	20	20.91		
3	20	20.91		

Table 4.18 *Vehicle driving toward to radar at 10 meters*

Attempt	Actual distance(m)	Measured distance (m)	Average distance (m)	% Error
1	10	11.17	10.73	7.27
2	10	10.60		
3	10	10.41		

4.3.1.1 Troubleshooting Process

Before making the final set of range test measurements, the distance measured from the output RTI plot had a large percent error compared to the expected data (Figure 4.13 and 4.14). After a series of troubleshooting steps including increasing the sampling rate to 88.2 KHz and replacing 15 KHz low pass filter with 25 KHz filter, the results did not show any improvements. The radar was then taken back to the lab to perform bench test measurements on the chirp signal's up ramp sweep time, start frequency and stop frequency for verification. After collecting the actual values from the system and inputting to MATLAB to re-generate RTI plots, the results showed the improvements as

seen in Figure 4.9 and 4.11. Table 4.19 includes the assumed and actual values of the modulation signal.

Table 4.19 *Assumed value vs. Actual value of the system*

Parameters	**Assumed Value**	**Actual Value**
Chirp signal up ramp time (mS)	20	19
Start Frequency (MHz)	5800	5783
Stop Frequency (MHz)	5900	5910

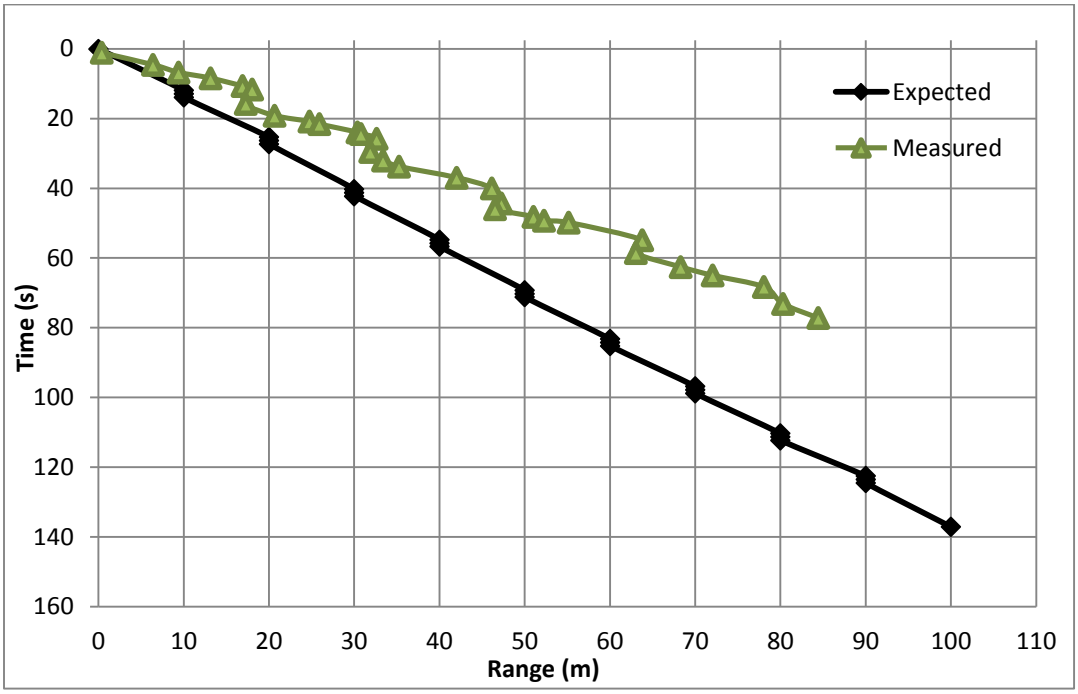

Figure 4.13 Un-calibrated range measurement of a vehicle driving away from radar

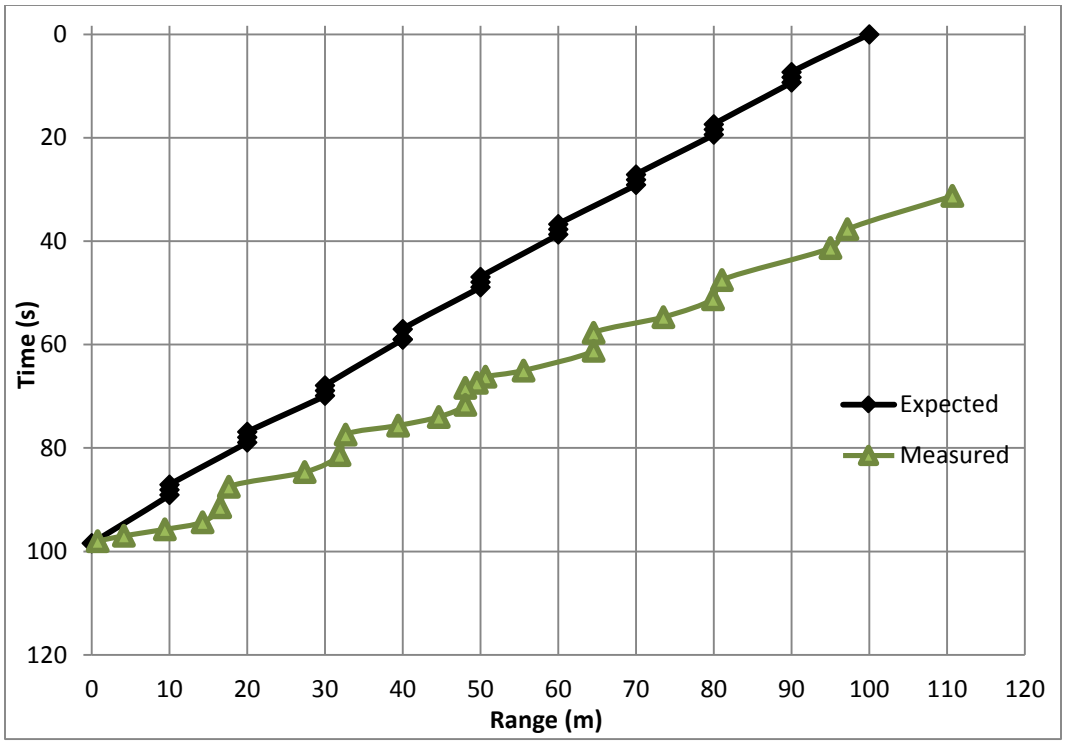

Figure 4.14 Un-calibrated range measurement of a vehicle driving towards radar

4.4 Synthetic Aperture Radar (SAR) Test Procedure

The SAR test procedure is conducted similar to range experiment by using the radar in FMCW mode. For SAR imaging, the radar requires range profiles for two inch increments along a three meter linear path to capture the image of stationary objects. Using the toggle switch to control the sync pulse to give the indication of every new position moved by the radar. The radar's cantenna are four inches apart and the system is placed on a three meter long wood board and 20 inches above the ground pointing at stationary objects (Figure 4.15 and 4.16). Objects chosen for this SAR experiment are two buildings on Purdue campus and a Car in an open area for greater reflections.

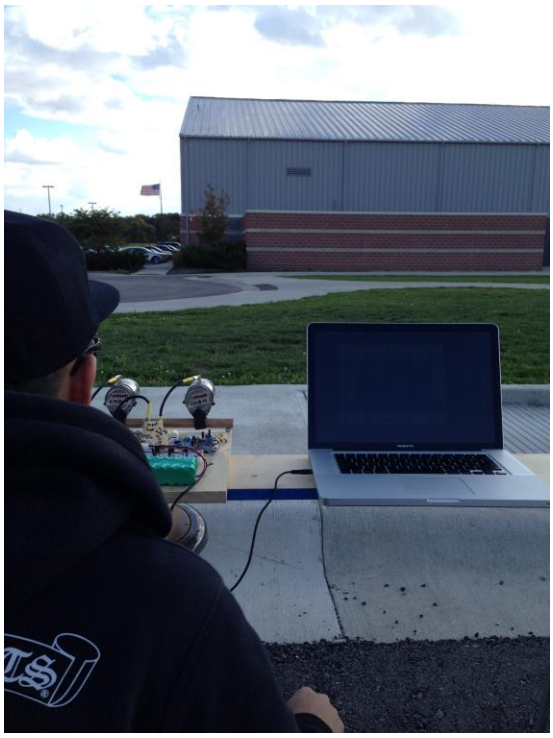

Figure 4.15 SAR measurement setup

Figure 4.16 SAR measurement process

4.4.1 SAR Test Results

First experiment was to image an indoor tennis building on Purdue campus. The radar is paced at 60 meters away from the side of the building to start the measurement from left to right consistently (Figure 4.17). The total recording time for one complete scan is about seven minutes with 59 stopping positions. Each position is recorded for three seconds on the right channel and position indication on the left (Figure 4.18).

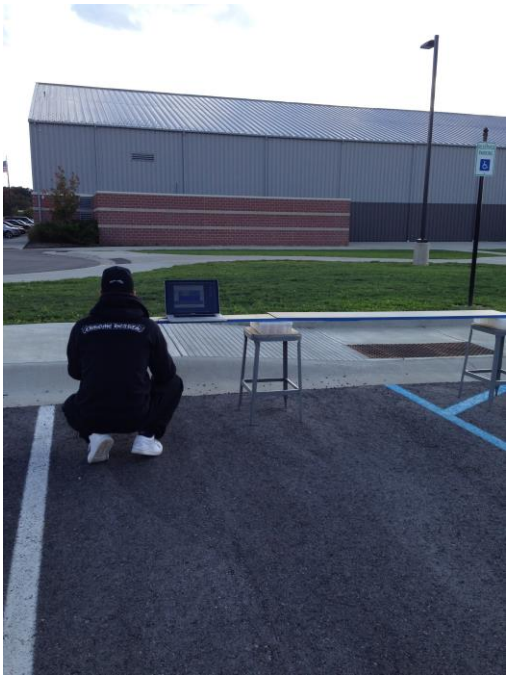

Figure 4.17 Tennis building SAR imaging

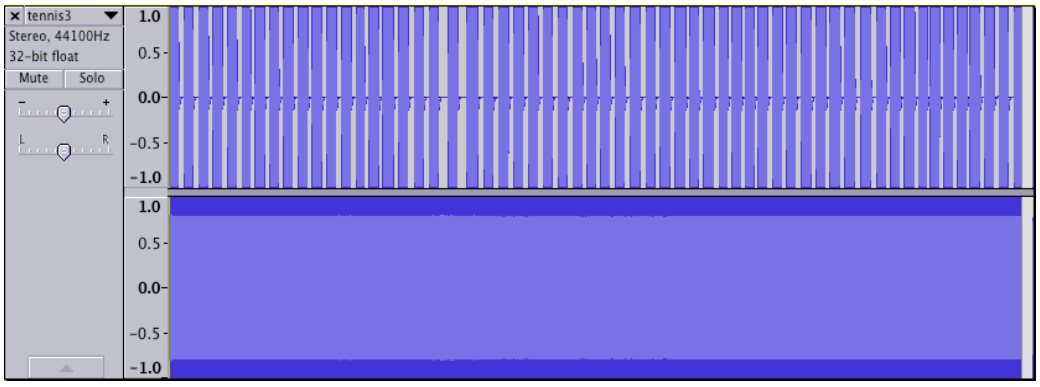

Figure 4.18 Recorded wave file in audacity for Tennis building

The output SAR image of the tennis building is shown in Figure 4.19. Since the building's side wall is not a flat surface which shows two strong reflections off the building at 60 meters (200ft) and at 90 meters (300ft). Figure 4.20 shows the SAR images plotted on the actual image of the building.

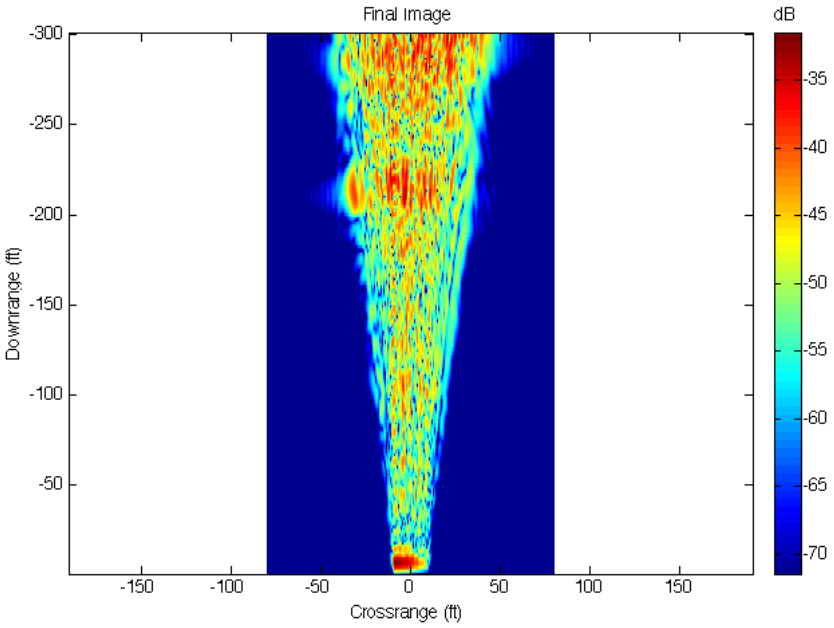

Figure 4.19 SAR image of the tennis building

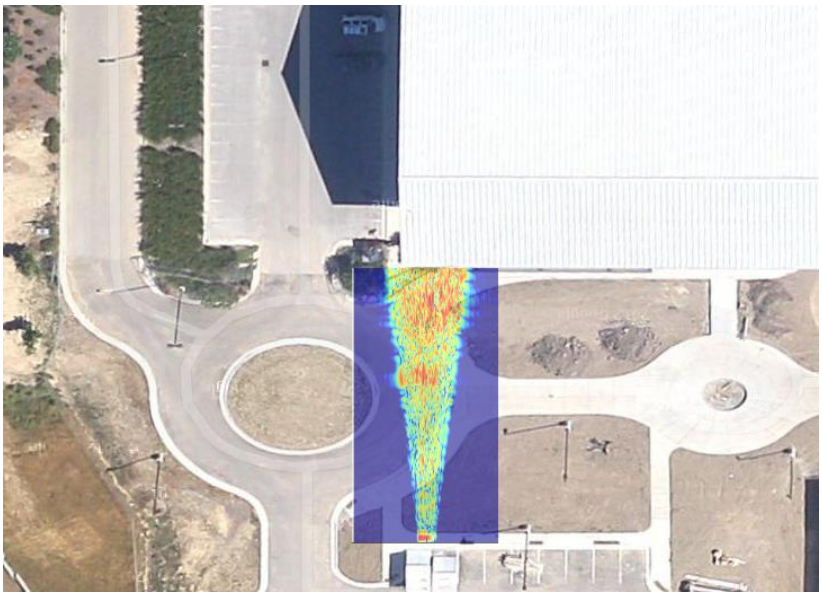

Figure 4.20 SAR image plotted on the tennis building image

Second SAR experiment is to image MGL laboratory building on Purdue campus. The same experiment procedure repeated showing the building's wall reflections at 80ft (24 meters) to 100ft (30 meters) in Figure 4.21 and 4.22.

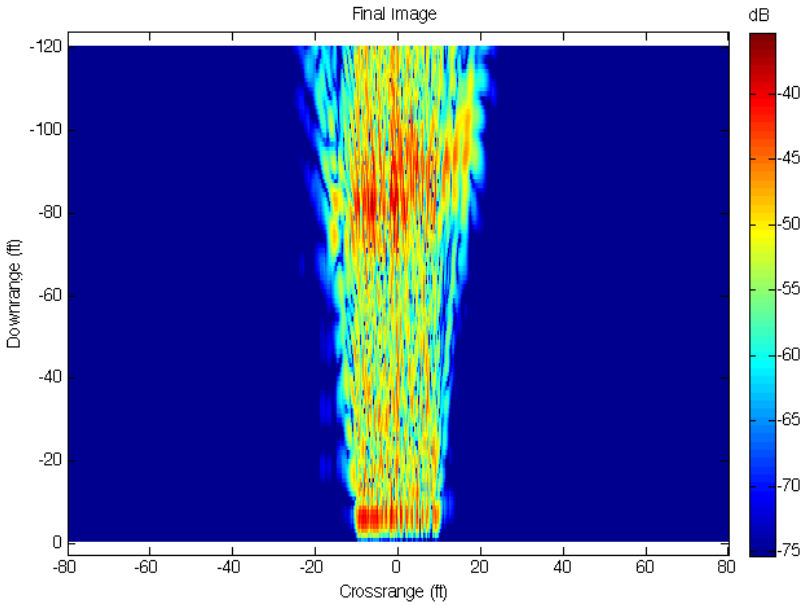

Figure 4.21 SAR image of the MGL building

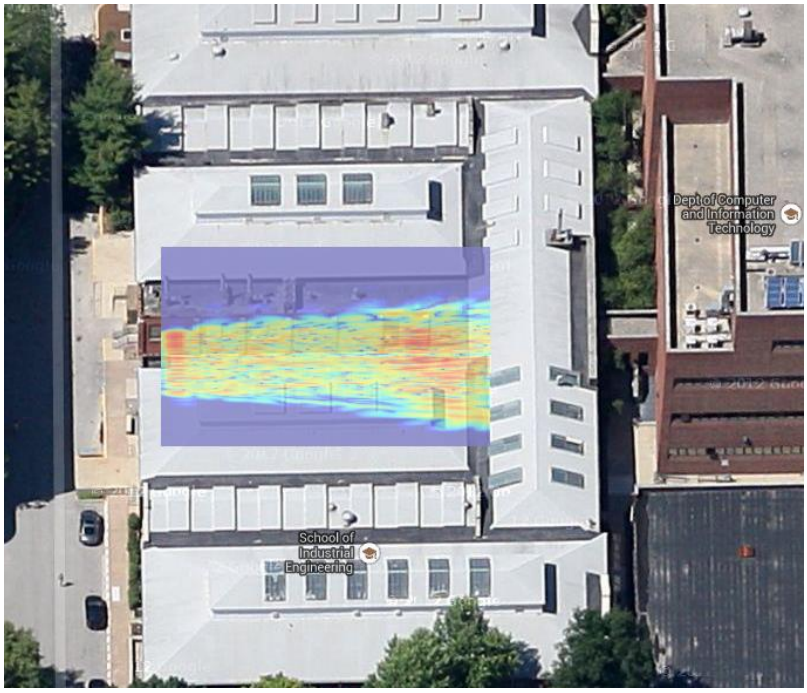

Figure 4.22 SAR image plotted on the MGL building image

The last SAR experiment is to capture the image of a vehicle 20 meters away from the radar in an open area. The purpose to image a vehicle is to demonstrate that the radar is capable of image a smaller object and shows strong reflection in Figure 4.23. In Figure 4.24 shows SAR image result with the strong reflection off the entire vehicle at 70ft (21 meters) and less reflection signal return when vehicle is out of the radar's path on the far left and far right of the SAR image.

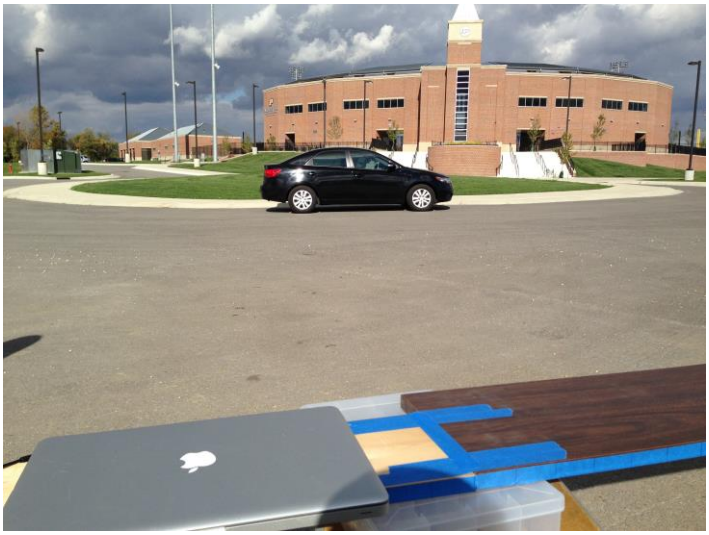

Figure 4.23 Vehicle SAR imaging

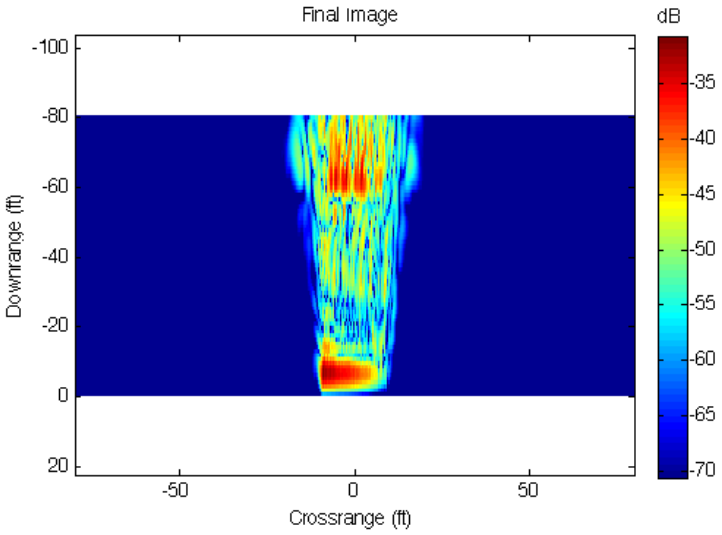

Figure 4.24 SAR image of the vehicle

The results of the three SAR images show the object's reflections at the corresponding distances, but it was not sufficient to distinguish the shape of buildings and the vehicle from the reflection signals and intensity level. From the observations, the radar received a lot of noise reflections which disrupted the signal reflected back from the object to the radar and the effect is clearly seen in the result image. Another possible reason affecting the outcome is due to the mechanisms of the experiment procedure, meaning the errors caused during the physical movement of the radar at each position.

4.4.1.1 Troubleshooting Process

The SAR troubleshooting process consisted of many different experiment trials on imaging two cans both indoor and outdoor. The first experiment was to place two cans three inches apart and one meter away from the radar. The down-range was measured at one meter and radar scan of ten centimeters per step to cover the cross-range of the image. The output SAR image in Figure 4.25 shows that there are many reflection signals received to the radar but had no obvious return signals from the two cans.

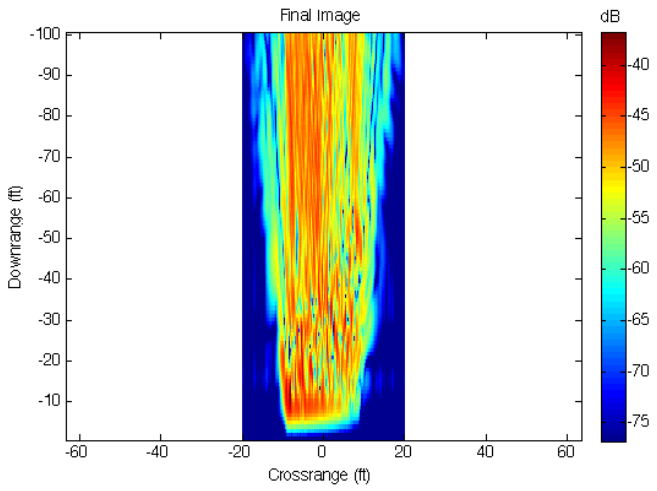

Figure 4.25 First SAR image of two cans

The second experiment was to adjust the down-range to three meters from the cans to the radar to see if there are any improvement. Figure 4.26 shows that there are no improvements by adjusting the distance between the object and the radar.

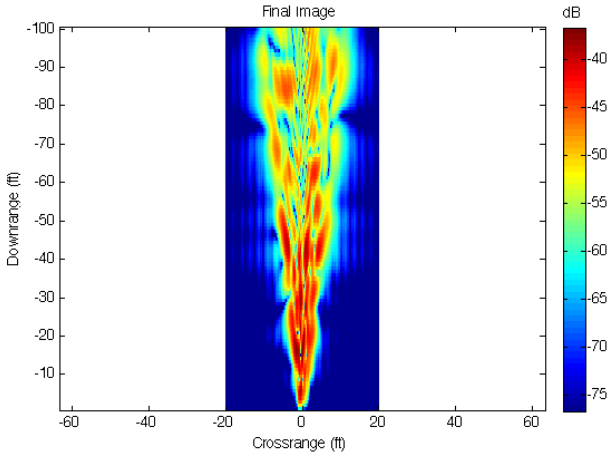

Figure 4.26 Second SAR image of two cans

The third experiment was to adjust the down-range back to one meter and vary the radar scan from ten centimeters to two centimeters per step over one meter (total of 25 scans). The output SAR image in Figure 4.27 shows no obvious improvement on increasing the radar scan per step.

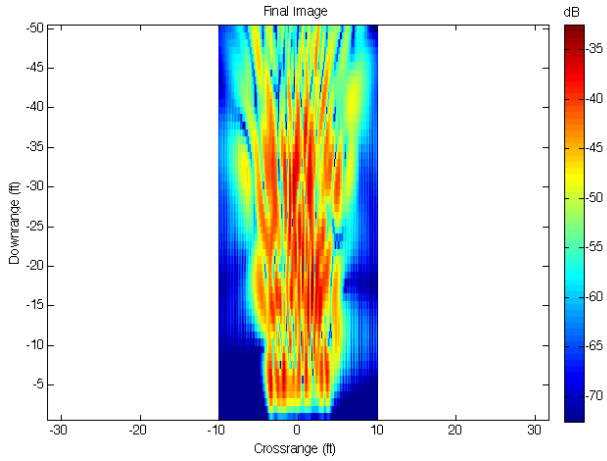

Figure 4.27 Third SAR image of two cans

The fourth experiment trial is to vary the transmit and receive cantenna spacing from four inches to two inches with radar scan of two inches per step to match the cantenna spacing (total of 17 scans). The down-range and cross-range was the same as the previous experiment at meter. Figure 4.28 shows less signal reflections but still has no improvements on imaging two cans.

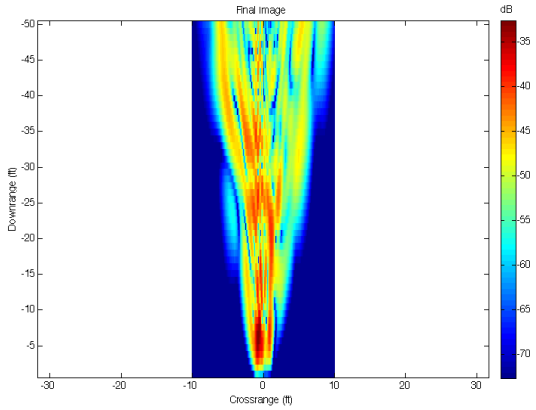

Figure 4.28 Fourth SAR image of two cans

The last experiment trial was to repeat the same setup as the second experiment outdoors to see if there are any improvements on noise and interference received by the radar. Figure 4.29 shows improvement on noise and interference reduction but still no improvement on imaging the two cans.

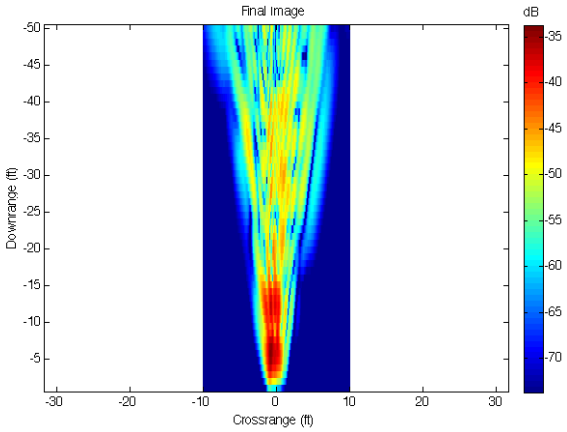

Figure 4.29 Fifth SAR image of two cans

After series of experiment trials on imaging two cans at both indoor and outdoor, the results shows that the radar's resolution is not sufficient to distinguish two small objects at short distance from one to three meters. The noise and interference received by the radar was reduced by imaging objects at out-door. Based on the experiment trial results, the current SAR setup requires the imaging of large objects in outdoor open areas with the increase of down-range distance in between 20 to 60 meters and a radar scan of 3 meters or greater. Improvements of imaging large objects can be observed in the previous section.

4.5 Conclusion

This chapter demonstrated that 5.8 GHz radar is capable of measurement Doppler shift, ranging and to form SAR images. The radar was able to measure a moving vehicle speed at 15, 30 and 45 mph with ±5% error. Radar ranging experiment was performed to determine the accuracy of distance measurement from ten meters up to 100 meters with ±2% error. The maximum detecting range by the radar is at 80 meters with ±0.2% error. Lastly, the radar was able to form SAR images of large objects including building and a vehicle with strong signal reflections at the corresponding distances at 20, 30 and 60 meters.

CHAPTER 5. SUMMARY AND RECOMMENDED FUTURE WORK

5.1 Summary

This study demonstrated the process of design, fabrication, and testing of a 5.8 GHz laptop-based radar system. The radar has the ability to operate in CW and FMCW mode to perform radar measurements including Doppler, ranging and SAR images. Due to the decrease in wavelength of electromagnetic radiation, the radar was able to carry more energy in radio waves and expected to be more effective in detecting an object's Doppler frequency, distance, and image. The experiments demonstrated the radar's overall functionality to operate at high frequency and provide accurate data results, which brought a new perspective to the existing radar project by increasing the ISM band frequency.

5.2 Recommended Future Work for Doppler and Ranging

Future work on measuring the Doppler and ranging should include an improved mechanism on data acquisition. Data acquisition can be improved by using real time data processing, which involves a continual input from the radar, process and display output data simultaneously. Using a high resolution Analog-to Digital converter along with microcontroller or field-programmable gate array (FPGA) integrated circuit could increase the speed of data processing and accuracy of measurement. PCB design for

analog circuitry including video amplifier, modulator and power supply could reduce noise interference, physical project size and immunity to movement.

5.3 Recommended Future Work for SAR

Future work on forming SAR images should include an analysis on performing background subtraction on final SAR images. Background subtraction could improve the resolution of the final image by filtering out background noises received from the radar. SAR measurement procedure can also be improved by setting up linear rail along with rail control system and stepper motor to control the movement of the radar. This allows the radar to have more stability and consistency when performing for both background subtraction and final image measurement.

LIST OF REFERENCES

LIST OF REFERENCES

Accuracy Weather. (Producer). (2013, 7 9). Weather Radar [Web Photo]. Retrieved from www.accuweather.com

AIAA (American Institute of Aeronautics and Astronautics).Airborne Early Warning Association, (2012). *Radar frequency bands*. Retrieved from website: http://www.aewa.org/Library/rf_bands.html

Antenna Theory. (Designer). (2009). Horn Antenna [Web Drawing]. Retrieved from http://www.antenna-theory.com/antennas/aperture/horn.php

Australian Government.Burea of Metrology, (2013). *Radar images*. Retrieved from website: http://www.bom.gov.au/australia/radar/about/what_is_radar.shtml

Bacon, F. W. (1965).An introduction to radar sensors.*Naval Engineers Journal*, *77*(3), 437-447.doi: 10.1111/j.1559-3584.1965.tb04962.x

Chang, K. (2004). *RF and microwave wireless systems.* New Jersey: John Wiley & Sons

Charvat, G. L., & Kempel, L. C. (2008, 05 06). *A unique approach to frequency-modulated continuous-wave radar design*. Retrieved from http://glcharvat.com/websitepdfs/AMT04_unique_approach_FMCW.pdf

Charvat, Gregory, Jonathan Williams, Alan Fenn, Steve Kogon, and Jeffrey Herd. *RES.LL-003 Build a Small Radar System Capable of Sensing Range, Doppler, and Synthetic Aperture Radar Imaging, January IAP 2011*. (MIT OpenCourseWare: Massachusetts Institute of Technology), http://ocw.mit.edu/resources/res-ll-003-build-a-small-radar-system-capable-of-sensing-range-doppler-and-synthetic-aperture-radar-imaging-january-iap-2011 (Accessed 21 Nov, 2013). License: Creative Commons BY-NC-SA

Connor , M., Haas, K., &Volfson, A. (2008). *Multiple target tracking*. Unpublished manuscript, WORCESTER POLYTECHNIC INSTITUTE, Retrieved from http://www.wpi.edu/Pubs/E-project/Available/E-project-101608-152650/unrestricted/Group31Final.pdf

Curry, G. R. (2012). *Radar essentials: A concise handbook for radar design and performance anaylsis*. Raleigh, NC : SciTech Publishing.

Daniels, D. J. (2009). *Em detection of concealed targets*.Hoboken,NJ: John Wiley & Sons

Devine, P. (2000). *Radar level measurement*. Sussex: VIP Print. Retrieved from http://www.level-know-how.com/downloads/VEGA-Radar_book.pdf

EOSNAP.(2009, 04 03). *Asar image orthorectification*. Retrieved from http://www.eosnap.com/earth-observation/asar-image-orthorectification/

Fabry, F., Austin, G. L., & Tees, D. (1992). The accuracy of rainfall estimates by radar as a function of range.*Quarterly Journal of the Royal Meteorological Society, 118*(505), 435-453. doi: 10.1002/qj.49711850503

Gilmour, A. S. (2011). *Principles of klystrons, traveling wave tubes, magnetrons, cross-field amplifiers, and gyrotrons*. Norwood, MA: Artech House

Global Security.(2012). *Types of radars*. Retrieved from http://www.globalsecurity.org/military/systems/aircraft/systems/radar-types.htm.

Golio, M. (2003). *Microwave and RF product applications*. (1 ed.). Boca Raton, FL: CRC Press.

Hocking, W. K. (2012). Recent advances in radar instrumentation and techniques for studies of the mesosphere, stratosphere, and troposphere. *Radio Science, 32*(6), 2241-2270.doi: 10.1029/97RS02781

James, P. K. (1980). A review of radar observations of the troposphere in clear air conditions. *Radio Science,15*(2), 151-175. doi: 10.1029/RS015i002p00151

Kingsley, S., &Quegan, S. (1999). *Understanding radar systems*. (1 ed.). Raleigh, NC: SciTech Publishing.

Krishnan, S. (2000).*Modeling and simulation analysis of an FMCW radar for measuring snow thickness*. (Unpublished master's thesis)Retrieved from http://printcouncil.org/research/thesis/documents/sudarsan_krishnan_thesis.pdf

Kurtz, S. R. (1978, 02).Mixers as phase detectors.*WJ Tech Notes*, *5*(1), Retrieved from http://rfcafe-com.secure38.ezhostingserver.com/references/articles/wj-tech-notes/Mixers_phase_detectors.pdf

Leberl, F. W., Kobrick, M., &Domik, G. (2006).Mapping with aircraft and satellite radar images. *The Photogrammetric Record*, *11*(66), 647-665.doi: 10.1111/j.1477-9730.1985.tb01315.x

Levanon, N., &Mozeson, E. (2004). *Radar signals*. New Jersey, NY: John Wiley & Sons.

Loekken, S. European Space Agency (ESA), Earth Observation Ground Segment Department. (2013).*The applications of sardata* . Retrieved from website: http://earth.esa.int/applications/data_util/SARDOCS/

Lopez, M. R. Sandia National Laboratories, (2012).*Synthetic aperture radar applications* (SAND99-0018). Retrieved from Sandia Corporation website: http://www.sandia.gov/radar/sarapps.html

Massonnet, D., &Feigl, K. L. (1998). Radar interferometry and its application to changes in the earth's surface.*Reviews of Geophysics*, *36*(4), 441-500.doi: 10.1029/97RG03139

M/A-COM, T. S. (2001, 6 04). Using microwave mixers as phase detectors. *Application Note M506*. Retrieved from http://www.eetasia.com/ARTICLES/2001JUN/2001JUN04_AMD_RFD_AN.PDF?SOURCES=DOWNLOAD

National Research Council.(2008). *Evaluation of the multifunction phased array radar planning process*. Washington, DC: National Academies Press.

Nessmith , J. T., &Trebits, R. N. (2003). Radar technology. *Encyclopedia of Applied Physics*, doi: 10.1002/3527600434.eap372

Nicolaescu, L., & Oroian, T. (2001). *Radar cross section*. In *International Conference on Telecommunication* (pp. 65-68). doi: 10.1109/TELSKS.2001.954850

Noorizadeh, S. (2010). *An introduction to synthetic aperture radar resolution*. Unpublished manuscript, Electrical Computer Engineering, Georgia Institute of Technology, Atlanta, Georgia, Retrieved from http://www.123seminarsonly.com/Seminar-Reports/014/30937362-An-Introduction-to-Synthetic-Aperture-Radar-Resolution.pdf

Peebles, P. (1998). *Radar principles*. (1 ed.). New York: Wiley.

Renato, C. (2002, 10 06). *Radar basic*. Retrieved from http://www.alphalpha.org/radar/intro_e.html

Rennie, S. J., Illingworth, A. J., Dance, S. L., & Ballard, S. P. (2010). The accuracy of doppler radar wind retrievals using insects as targets. *Meteorological Applications*, *17*(4), 419-432.doi: 10.1002/met.174

Royrvik, O. (1985). Radar comparison of 2.66-mhz and 40.92-mhz signals scattered from the mesosphere.*Radio Science*, *20*(6), 1423-1434. doi: 10.1029/RS020i006p01423

Scheer, J. A. (2010). The radar range equations.In*Principles of Modern Radar* (2 ed.). Raleigh, NC: SciTech Publishing.

Seed, A. W., Nicol, J., Austin, G. L., & Stow, C. D. (1996). The impact of radar and raingauge sampling errors when calibrating a weather radar.*Meteorological Applications*, *3*(1), 43-52.doi: 10.1002/met.5060030105

Siversia. (2011, 06). *FMCW radar sensors application notes*. Retrieved from https://docs.google.com/viewer?url=http://www.siversima.com/wpcontent/uploads/2012/03/FMCW-Radar-App-Note.pdf&chrome=true

Skolnik, M. I. (2003). *Introduction to radar systems*.(3 ed.). New York: McGraw-Hill Education.

Skolnik, M. I. (2006). *Introduction to radar systems (sie)*.(2 ed.). New York: McGraw-Hill Education.

Stimson, G. (1998). *Introduction to airborne radar*.(2 ed.). Raleigh, NC: SciTech Publishing.

Suvllivan , R. (2004). *Radar foundations for imaging and advanced concepts*. Raleigh, NC: SciTech Publishing.

United States Government, (2001).*Radar navigation and maneuvering board manual* (Pub 1310). Retrieved from National Imagery and Mapping Agency website: http://msi.nga.mil/NGAPortal/MSI.portal?_nfpb=true&_pageLabel=msi_portal_page_62&pubCode=0008

Varshney, L. (2002). Radar System Components and System Design.*Syracuse Research Corporation*. Retrieved from http://www.mit.edu/~lrv/cornell/publications/radar%20system%20components%20and%20system%20design.pdf

Wolff, C. (1996). *Doppler- effect*. Retrieved from http://www.radartutorial.eu/11.coherent/co06.en.html

Wolff, C. (2009, 12 20). *Radartutorial book 2 "radar sets"*. Retrieved from http://www.radartutorial.eu/druck/Book1.pdf

Zyl, J. J. (2011). *Synthetic aperture radar polarimetry*. New Jersey: John Wiley & Sons.

APPENDICES

Appendix A MATLAB code for Doppler

```
%MIT IAP Radar Course 2011
%Resource: Build a Small Radar System Capable of Sensing Range, Doppler,
%and Synthetic Aperture Radar Imaging
%
%Gregory L. Charvat

%Process Doppler vs. Time Intensity (DTI) plot

%NOTE: set Vtune to 3.2V to stay within ISM band and change fc to frequency
%below

clear all;
close all;

%read the raw data .wave file here
%[Y,FS,NBITS] = wavread('151.wav'); %About 6.8m/s = 15.2mph
%[Y,FS,NBITS] = wavread('152.wav');
%[Y,FS,NBITS] = wavread('153.wav');
%[Y,FS,NBITS] = wavread('301.wav'); %About 12.83m/s = 28.69mph
%[Y,FS,NBITS] = wavread('302.wav');
%[Y,FS,NBITS] = wavread('303.wav');
%[Y,FS,NBITS] = wavread('451.wav'); %About 20.07m/s = 44.89 mph
%[Y,FS,NBITS] = wavread('452.wav');
%[Y,FS,NBITS] = wavread('453.wav');

%constants
c = 3E8; %(m/s) speed of light

%radar parameters
Tp = 0.250; %(s) pulse time
N = Tp*FS; %# of samples per pulse
fc = 5800E6;  %(Hz) Center frequency (Connted VCO Vtune to +3.39V)

%the input appears to be inverted
s = -1*Y(:,2);
clear Y;

%creat doppler vs. time plot data set here
for ii = 1:round(size(s,1)/N)-1
   sif(ii,:) = s(1+(ii-1)*N:ii*N);
end
```

```
%subtract the average DC term here
sif = sif - mean(s);

zpad = 8*N/2;

%doppler vs. time plot:
v = dbv(ifft(sif,zpad,2));
v = v(:,1:size(v,2)/2);
mmax = max(max(v));
%calculate velocity
delta_f = linspace(0, FS/2, size(v,2)); %(Hz)
lambda=c/fc;
velocity = delta_f*lambda/2;
%calculate time
time = linspace(1,Tp*size(v,1),size(v,1)); %(sec)
%plot
imagesc(velocity,time,v-mmax,[-35, 0]);
colorbar;
xlim([0 40]); %limit velocity axis
xlabel('Velocity (m/sec)');
ylabel('time (sec)');
```

Appendix B MATLAB code for Ranging

```
%MIT IAP Radar Course 2011
%Resource: Build a Small Radar System Capable of Sensing Range, Doppler,
%and Synthetic Aperture Radar Imaging
%
%Gregory L. Charvat

%Process Range vs. Time Intensity (RTI) plot

%NOTE: set up-ramp sweep from 2-3.2V to stay within ISM band
%change fstart and fstop bellow when in ISM band

clear all;
close all;

%read the raw data .wave file here
%[Y,FS,NBITS] = wavread('final_test1_away.wav');
%[Y,FS,NBITS] = wavread('final_test1_toward.wav');
%[Y,FS,NBITS] = wavread('final_test2_away.wav');
%[Y,FS,NBITS] = wavread('final_test2_toward.wav');
%[Y,FS,NBITS] = wavread('final_test3_away.wav');
%[Y,FS,NBITS] = wavread('final_test3_toward.wav');

%Wavread microsoft .wav sound file.
%Y reads the file specficed by the string file, retunred the sample data
%store in Y. Values from in the range [-1,+1]
%FS - returns the sample rate (FS) in Hz
%NBITS - number of bits per sample used to encode the data in the file.

%constants
c = 3E8; %(m/s) speed of light

%radar parameters
Tp = 20E-3; %(s) pulse time
N = Tp*FS; %# of samples per pulse
fstart = 5771E6; %(Hz) LFM start frequency for ISM band
fstop = 5902E6; %(Hz) LFM stop frequency for ISM band
BW = fstop-fstart; %(Hz) transmit bandwidth
f = linspace(fstart, fstop, N/2); %instantaneous transmit frequency

%range resolution
rr = c/(2*BW);
```

```
max_range = rr*N/2;

%the input appears to be inverted
trig = -1*Y(:,1);
s = -1*Y(:,2);
clear Y;

%parse the data here by triggering off rising edge of sync pulse
count = 0;
thresh = 0;
start = (trig > thresh);
for ii = 100:(size(start,1)-N)
   if start(ii) == 1 & mean(start(ii-11:ii-1)) == 0
      %start2(ii) = 1;
      count = count + 1;
      sif(count,:) = s(ii:ii+N-1);
      time(count) = ii*1/FS;
   end
end
%check to see if triggering works
% plot(trig,'.b');
% hold on;si
% plot(start2,'.r');
% hold off;
% grid on;

%subtract the average
ave = mean(sif,1);
for ii = 1:size(sif,1);
   sif(ii,:) = sif(ii,:) - ave;
end

zpad = 8*N/2;

%RTI plot
figure(10);
v = dbv(ifft(sif,zpad,2));
S = v(:,1:size(v,2)/2);
m = max(max(v));
imagesc(linspace(0,max_range,zpad),time,S-m,[-80, 0]);
colorbar;
ylabel('time (s)');
xlabel('range (m)');
title('RTI without clutter rejection');
```

```
%2 pulse cancelor RTI plot
figure(20);
sif2 = sif(2:size(sif,1),:)-sif(1:size(sif,1)-1,:);
v = ifft(sif2,zpad,2);
S=v;
R = linspace(0,max_range,zpad);
for ii = 1:size(S,1)
   %S(ii,:) = S(ii,:).*R.^(3/2); %Optional: magnitude scale to range
end
S = dbv(S(:,1:size(v,2)/2));
m = max(max(S));
imagesc(R,time,S-m,[-80, 0]);
colorbar;
ylabel('time (s)');
xlabel('range (m)');
title('RTI with 2-pulse cancelor clutter rejection');

% %2 pulse mag only cancelor
% figure(30);
% clear v;
% for ii = 1:size(sif,1)-1
%     v1 = abs(ifft(sif(ii,:),zpad));
%     v2 = abs(ifft(sif(ii+1,:),zpad));
%     v(ii,:) = v2-v1;
% end
% S=v;
% R = linspace(0,max_range,zpad);
% for ii = 1:size(S,1)
%     S(ii,:) = S(ii,:).*R.^(3/2); %Optional: magnitude scale to range
% end
% S = dbv(S(:,1:size(v,2)/2));
% m = max(max(S));
% imagesc(R,time,S-m,[-20, 0]);
% colorbar;
% ylabel('time (s)');
% xlabel('range (m)');
% title('RTI with 2-pulse mag only cancelor clutter rejection');
```

Appendix C MATLAB code for SAR

```
%MIT IAP Radar Course 2011
%Resource: Build a Small Radar System Capable of Sensing Range, Doppler,
%and Synthetic Aperture Radar Imaging
%
%Gregory L. Charvat

%SAR algorithm from:
%Range Migration Algorithm from ch 10 of Spotlight Synthetic Aperture Radar
%Signal Processing Algorithms, Carrara, Goodman, and Majewski

%NOTE: set up-ramp sweep from 2-3.2V to stay within ISM band
%change fstart and fstop bellow when in ISM band

%------------------------------------------%
%Process raw data here
clear all;
close all;

%read the raw data .wave file here
%[Y,FS,NBITS] = wavread('Tennis_building.wav');
%[Y,FS,NBITS] = wavread('MGL_building.wav');
[Y,FS,NBITS] = wavread('Car.wav');

%constants
c = 3E8; %(m/s) speed of light

%radar parameters
Tp = 20E-3; %(s) pulse time
Trp = 0.25; %(s) min range profile time duration
N = Tp*FS; %# of samples per pulse
fstart = 5801E6; %(Hz) LFM start frequency
fstop = 5912E6; %(Hz) LFM stop frequency
BW = fstop-fstart; %(Hz) transmti bandwidth
f = linspace(fstart, fstop, N/2); %instantaneous transmit frequency

%the input appears to be inverted
trig = -1*Y(:,1);
s = -1*Y(:,2);
clear Y;

%parse data here by position (silence between recorded data)
```

```
rpstart = abs(trig)>mean(abs(trig));
count = 0;
Nrp = Trp*FS; %min # samples between range profiles

for ii = Nrp+1:size(rpstart,1)-Nrp
   if rpstart(ii) == 1 & sum(rpstart(ii-Nrp:ii-1)) == 0
      count = count + 1;
      RP(count,:) = s(ii:ii+Nrp-1);
      RPtrig(count,:) = trig(ii:ii+Nrp-1);
   end
end

%parse data by pulse
count = 0;
thresh = 0.08;
clear ii;
for jj = 1:size(RP,1)
   %clear SIF;
   SIF = zeros(N,1);
   start = (RPtrig(jj,:)> thresh);
   count = 0;
   jj
   for ii = 12:(size(start,2)-2*N)
      [Y I] =  max(RPtrig(jj,ii:ii+2*N));
      if mean(start(ii-10:ii-2)) == 0 & I == 1
         count = count + 1;
         SIF = RP(jj,ii:ii+N-1)' + SIF;
      end
   end
   %hilbert transform
   q = ifft(SIF/count);
   sif(jj,:) = fft(q(size(q,1)/2+1:size(q,1)));
end
sif(find(isnan(sif))) = 1E-30; %set all Nan values to 0

%SAR data should be ready here
clear s;
s = sif;
save routsidewarehouse2 s; %for image data

%-----------------------------------------%
%load additional varaibles and setup constants for radar here
clear all;
c = 3E8; %(m/s) speed of light
```

```
%load IQ converted data here
load routsidewarehouse2 s; %load variable sif %for image data

for ii = 1:size(s,1)
   s(ii,:) = s(ii,:) - mean(s,1);
end

%sif = s-sif_sub; %perform coherent background subtraction
%sif = sif_sub; %image just the background
sif = s; %image without background subtraction
clear s;
clear sif_sub;

%**************************************************************************
*
%radar parameters
fc = (5912E6 - 5801E6)/2 + 5801E6; %(Hz) center radar frequency
B = (5912E6 - 5801E6); %(hz) bandwidth
cr = B/20E-3; %(Hz/sec) chirp rate
Tp = 20E-3; %(sec) pulse width
%VERY IMPORTANT, change Rs to distance to cal target
%Rs = (12+9/12)*.3048; %(m) y coordinate to scene center (down range), make this
value equal to distance to cal target
Rs = 0;
%Xa = 0; %(m) beginning of new aperture length
Xa = 0;
delta_x = 4*(1/12)*0.3048; %(m) 4 inch antenna spacing
L = delta_x*(size(sif,1)); %(m) aperture length
Xa = linspace(-L/2, L/2, (L/delta_x)); %(m) cross range position of radar on aperture L
Za = 0;
Ya = Rs; %THIS IS VERY IMPORTANT, SEE GEOMETRY FIGURE 10.6
t = linspace(0, Tp, size(sif,2)); %(s) fast time, CHECK SAMPLE RATE
Kr = linspace(((4*pi/c)*(fc - B/2)), ((4*pi/c)*(fc + B/2)), (size(t,2)));

%Save background subtracted and callibrated data
save sif sif delta_x Rs Kr Xa;
%clear all;

%run IFP
SBAND_RMA_IFP;
```